

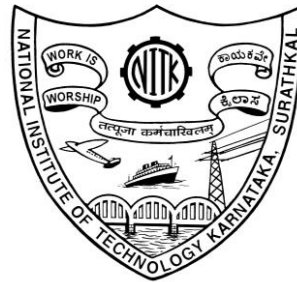
**SHORT-TERM OFFSHORE WIND SPEED FORECASTING  
USING BUOY OBSERVATIONS  
AND  
REGIONAL SCALE WIND RESOURCE ASSESSMENT  
BASED ON SCATTEROMETER DATA**

**Thesis**

**Submitted in partial fulfillment of the requirement for degree of  
DOCTOR OF PHILOSOPHY**

**By**

**SANJEEV GADAD**



**DEPARTMENT OF APPLIED MECHANICS AND HYDRAULICS  
NATIONAL INSTITUTE OF TECHNOLOGY KARNATAKA  
SURATHKAL-575 025**

**SEPTEMBER – 2016**

**SHORT-TERM OFFSHORE WIND SPEED FORECASTING  
USING BUOY OBSERVATIONS  
AND  
REGIONAL SCALE WIND RESOURCE ASSESSMENT  
BASED ON SCATTEROMETER DATA**

**Thesis**

**Submitted in partial fulfillment of the requirement for degree of  
DOCTOR OF PHILOSOPHY**

**By**

**SANJEEV GADAD**

**AM12F05**

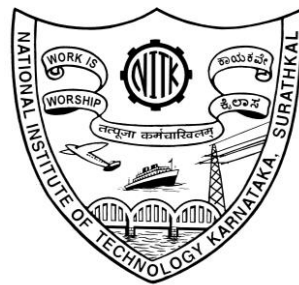
Under the guidance of

**Dr. PARESH CHANDRA DEKA**

Associate Professor

Dept. of Applied Mechanics & Hydraulics

NITK Surathkal



**DEPARTMENT OF APPLIED MECHANICS AND HYDRAULICS  
NATIONAL INSTITUTE OF TECHNOLOGY KARNATAKA  
SURATHKAL-575 025**

**SEPTEMBER – 2016**

## **D E C L A R A T I O N**

*By the Ph.D. Research Scholar*

I hereby *declare* that the Research Thesis entitled **Short-term Offshore Wind Speed Forecasting using Buoy Observations and Regional scale Wind Resource Assessment based on Scatterometer Data**, which is being submitted to the **National Institute of Technology Karnataka, Surathkal** in partial fulfilment of the requirements for the award of the Degree of **Doctor of Philosophy in Applied Mechanics and Hydraulics Department** is a *bonafide report of the research work* carried out by me. The material contained in this Research Thesis has not been submitted to any University or Institution for the award of any degree.

121157AM12F05, SANJEEV GADAD

(Register Number, Name & Signature of the Research Scholar)

Department of Applied Mechanics and Hydraulics

Place: NITK-Surathkal

Date:

## C E R T I F I C A T E

This is to *certify* that the Research Thesis entitled **Short-term Offshore Wind Speed Forecasting using Buoy Observations and Regional scale Wind Resource Assessment based on Scatterometer Data** submitted by SANJEEV GADAD (Register Number: 121157AM12F05) as the record of the research work carried out by him, is *accepted as the Research Thesis submission* in partial fulfilment of the requirements for the award of degree of **Doctor of Philosophy**.

Dr. Paresh Chandra Deka  
Associate Professor  
Research Guide  
(Name and Signature with Date and Seal)

Chairman - DRPC  
(Signature with Date and Seal)

## **Acknowledgements**

I feel it is a great privilege to express my deepest and most sincere gratitude to my supervisor, Prof. Paresh Chandra Deka for his suggestions, constant encouragement and support during the course of the work. With deepest gratitude, I like to express sincere thanks to my supervisor for guidance, background knowledge, patience and editing skills in the completion of this document. Many of the ideas in the thesis originally came from my discussions with the professor. I have whole heartedly enjoyed the challenge of examining and researching a prominent issue that could greatly impact society and public education instead of just performing another educational study. I am also grateful to the other members of my doctoral committee, namely Prof. Arkal Vittal Hegde and Dr. Sam Johnson for their valuable comments on my work. I take this opportunity to thank Prof. Subba Rao and Prof. G.S. Dwardish, the former head and the present Head of Department of Applied Mechanics & Hydraulics for their kindness and continuous support. I would like to express sincere thanks to Prof. Lakshman Nandagiri for his help and suggestion in keeping myself motivated. I would like to extend my deepest gratitude towards all the other faculty members of the department for their never-ending support, encouragement and help.

I extend my sincere thanks to Mr. Jagadish, Mr. Balakrishna and all other non-teaching staff for their extended support and unrelenting efforts in structuring this research. I thank all my fellow research scholars and M.Tech students for their cooperation. My thanks also go out to all my friends who have rendered their help at different times which made my stay in this institute a memorable period of my life.

Finally, special recognition goes out to my parents, brother and family for their unbounded love, encouragement and patience during my pursuit of Doctorate in Applied Mechanics & Hydraulics Engineering. I am deeply indebted to them for their countless sacrifices and support without which my research work would not have finished.

*- Sanjeev Gadad*

## **Dedication**

**Every challenging work needs self effort as well as  
guidance of elders especially those who were very  
close to our heart.**

**My humble effort I dedicate to my sweet and loving**

*Father and Mother,*

**Whose affection, love, encouragement and prays of day  
and night make me able to get such success and honor,**

**Along with all hard working and respected**

*Teachers*

If we knew what we were doing, it wouldn't be called  
research, would it?

— *Albert Einstein*

## ABSTRACT

Offshore winds are valuable source of renewable energy. To recognize the potential of area it is essential to assess the available resource and understand the sporadic nature of winds. Wind Resource Assessment (WRA) coupled with short-term forecast of winds will aid in establishing the confidence for undertaking offshore wind farm development.

Wind speed forecasting is important for estimating power generation capacity of turbines. The knowledge of availability of the winds in future time steps will be pivotal in planning and improving the efficiency of energy production. Buoys are the fundamental source of in situ atmospheric parameter observations. One of the primary objectives of the present research is to determine suitable technique for short-term forecasting of offshore winds. So, the present study focuses on assessing accuracy of the ANFIS hybrid model for short-term wind speed forecasting. In addition, the Arabian Sea belongs to tropical humid climate zone and therefore the influence of Relative Humidity (RH) on the ANFIS model to estimate offshore wind speed was investigated. In the study, two buoys with id- AD07 and CB02 apart approximately by 500 km were selected. Two models (model 1: 5 inputs, 1 output and model 2: 4 inputs, 1 output) and two scenarios (scenario 1: estimate wind speeds and scenario 2: forecasting wind speeds) were developed for the study. From scenario 1, it was found that at both the buoy locations the model 1 outperformed model 2 in estimating observed wind speeds and RH had noticeable influence on the model performance.

Persistence Method (PM) was chosen as base method for comparing the wind speed forecasts. From scenario 2, at AD07, model 1 forecasts were accurate than other two models and at CB02, the PM forecasts were most accurate. However, it was found that the model 1 forecasts at CB02 were closer to PM. Altogether, the model 1 performance was higher than model 2 indicating the error in forecasts due to absence of RH observations. The study concludes that the model performance was enhanced by incorporating RH observations as an input to the ANFIS model. The RMSE of forecasted wind speeds up to three time steps, at AD07 and CB02 would be approximately lower by 37% and 14% respectively.



Further, the study examines the performance of ANFIS and Wavelet-ANFIS (WT+ANFIS) hybrid techniques to forecast wind speeds for multiple time steps at the same buoy locations (AD07 and CB02) in the Arabian Sea. The forecast accuracy of ANFIS and WT+ANFIS were compared with PM. The RMSE for the testing dataset at AD07 and CB02 using ANFIS model was found to be  $1.3 \text{ m s}^{-1}$  and  $1.26 \text{ m s}^{-1}$  for 1<sup>st</sup> (t+1) time step respectively. The RMSE for WT+ANFIS model at AD07 and CB02 was obtained as  $1.5 \text{ m s}^{-1}$  and  $1.20 \text{ m s}^{-1}$  for 1<sup>st</sup> (t+1) time step respectively. It was observed at CB02, the WT+ANFIS model forecast was closest to PM. At AD07, an ANFIS and WT+ANFIS model performance was almost similar and found to be better than PM. In general, the WT+ANFIS model outperformed ANFIS and PM for multiple time steps. Thus, the analysis establishes that WT+ANFIS hybrid method has the potential to be a complementary tool in obtaining short-term offshore wind speed forecasts.

In the offshore region the scarcity of in situ wind data in space proves to be a major setback for wind power potential assessments. Satellite data effectively overcomes this setback by providing continuous and total spatial coverage. The satellite data needs to be validated at the study area before conducting WRA study. Hence the work centers on estimating the performance of Oceansat-2 scatterometer (OSCAT)-derived wind vector using in situ data from buoys (id- AD02 and CB02) at different locations in the Arabian Sea. For the validation of OSCAT winds, the buoy winds are required to be extrapolated to height of 10 m and are known as *Equivalent Neutral Winds (ENW)*.

A comparative study among three methods- power law, logarithmic and Liu-Katsaros-Businger (LKB) method for estimating the ENW for buoys is carried out. OSCAT winds were closest to ENW estimated by the Liu-Katsaros-Businger (LKB) method. The spatial and temporal windows for comparison were  $0.5^\circ$  and  $\pm 60$  minutes, respectively. The monsoon months (June-September) of 2011 were selected for the study. The root mean square deviation for wind speed is less than  $2.5 \text{ m s}^{-1}$  and wind direction is less than  $20^\circ$ , and a small positive bias is observed in the OSCAT wind values. From the analysis, the OSCAT wind values were found to be consistent with in situ-observed values. Furthermore, wind atlas maps were developed

with OSCAT winds, representing the spatial distribution of winds at a height of 10 m over the Arabian Sea.

Satellite-based regional scale offshore wind power resource assessment was carried out for the Karnataka state, which is located on the west coast of India. OSCAT wind data and GIS based methodology were adopted in the study. The real time ship based observations is considered in the present work, to assess the accuracy of OSCAT wind data. The INCOIS Realtime All Weather Station (IRAWS) data provides greater spatial coverage than conventional buoy setup. Probably, this is the first attempt to validate OSCAT data using IRAWS dataset, which offered greater number of collocated observation points and hence provided better assessment.

Wind speed maps at 10 m, 90 m and wind power density maps using OSCAT data were developed to understand the spatial distribution of winds over the study area. Bathymetric map was developed based on the available foundation types and demarking various exclusion zones to help in minimizing conflicts. The wind power generation capacity estimation performed using REpower 5 MW turbine, based on the water depth classes was found to be 9,091 MW in Monopile (0-35 m), 11,709 MW in Jacket (35-50 m), 23,689 MW in Advanced Jacket (50-100 m) and 117,681 MW in Floating (100-1000 m) foundation technology.

In Indian scenario, major thrust may be given for wind farm development in Monopile region. Therefore, as first phase of development for 10% of the estimated potential in this region, 116% of energy deficit for FY 2011-12 could be met. Also, up to 79% of the anticipated energy deficit for the FY 2014-15 of the Karnataka state of India could be achieved.

*Keywords – ANFIS, Buoy winds, Equivalent Neutral Winds, GIS, Hybrid techniques, IRAWS, LKB method, Oceansat-2 Scatterometer, Offshore Wind Resource Assessment, Relative Humidity, Renewable Energy, Short-term forecast, Offshore Wind Energy, Wavelets, Wavelet+ANFIS.*

## TABLE OF CONTENTS

SI No.		Page No.
<b>CHAPTER 1 INTRODUCTION AND LITERATURE REVIEW</b>		
1.0	General	01
1.1	Satellite based Global Ocean Wind Observations	05
1.2	Extrapolation Approaches	14
1.3	Offshore Wind Energy Assessment	16
1.4	Forecasting Methods	24
1.5	Relative Humidity (RH) and Influence on Wind Speed	29
1.6	Summary	31
1.7	Problem Formulation	34
1.8	Objectives	35
1.9	Organization of Thesis	35
<b>CHAPTER 2 DATA AND METHODOLOGY</b>		
2.0	General	37
2.1	Buoy Observations	37
2.2	Ship based Observations	40
2.3	Oceansat-2 Scatterometer Observations	41
2.4	Methods Adopted and Developed for the Study	44
2.4.1	Persistence Method	44
2.4.2	Adaptive Neuro-Fuzzy Inference System (ANFIS)	44
2.4.3	Combination of Wavelet Transform and ANFIS (WT+ANFIS)	46
2.4.4	Power Law Method	47
2.4.5	Logarithmic (log) Method	48
2.4.6	Liu-Katsaros-Businger (LKB) Method	48
2.4.7	Wind Power Density (WPD)	49
2.4.8	Capacitance Factor (CF)	50
2.5	Short-term Offshore wind speed Forecasting and Relative Humidity Influence on the accuracy of ANFIS	52

2.6	Short-term Offshore wind speed Forecasting by ANFIS and WT+ANFIS hybrid techniques	55
2.7	Estimation of ENW and Performance evaluation of Oceansat-2 scatterometer winds	56
2.8	Regional scale Offshore wind power resource assessment using Oceansat-2 scatterometer winds	60
<b>CHAPTER 3 RESULTS AND DISCUSSIONS</b>		
3.0	General	67
3.1	Short-term Offshore wind speed Forecasting and Relative Humidity Influence on the accuracy of ANFIS	67
3.1.1	Scenario 1: Evaluate the accuracy of models to estimate the offshore wind speeds	67
3.1.2	Scenario 2: Wind speed forecasting at different ahead time steps and comparison with Persistence Method	71
3.2	Short-term Forecasting by ANFIS and WT+ANFIS hybrid techniques	75
3.2.1	Adaptive Neuro-Fuzzy System (ANFIS)	75
3.2.2	Combination of Wavelet Transform and ANFIS (WT+ANFIS)	80
3.2.3	Comparison of ANFIS, WT+ANFIS with Persistence Method	88
3.3	Estimation of ENW and Performance evaluation of Oceansat-2 Scatterometer winds	89
3.3.1	Equivalent Neutral Winds (ENW) estimation	89
3.3.1.1	Scenario 1: Daily averaged buoy winds compared to OSCAT winds	91
3.3.2	Scenario 2: $\pm 60$ minutes of buoy measurements and filtered data	93
3.3.3	Wind maps	100

3.4	Regional scale Offshore wind power resource assessment using Oceansat-2 scatterometer winds	103
3.4.1	OSCAT data comparison with IRAWs ship data	103
3.4.2	Mapping Available Area	105
3.4.3	Calculating Capacitance Factor (CF) for Turbine	106
3.4.4	Mapping wind potential	106
<b>CHAPTER 4 CONCLUSIONS</b>		
4.0	General	117
4.1	Short-term Offshore wind speed Forecasting and Relative Humidity Influence on the accuracy of ANFIS	117
4.2	Short-term Forecasting by ANFIS and WT+ANFIS hybrid techniques	118
4.3	Estimation of ENW and Performance evaluation of Oceansat-2 Scatterometer winds	120
4.4	Regional scale Offshore wind power resource assessment using Oceansat-2 scatterometer winds	121
4.5	Limitations of the Study	122
4.6	Scope for Future Work	123
<b>REFERENCES</b>		125
<b>PUBLICATIONS</b>		
<b>RESUME</b>		

## LIST OF FIGURES

Fig. 1.1	Global atmospheric circulation	02
Fig. 1.2	INCOIS moored buoy network	04
Fig. 1.3	Source-wise purchase by utilities in FY13 (in Million units)	19
Fig. 2.1	Buoys in the Arabian Sea deployed by INCOIS	38
Fig. 2.2	IRAWS observations along Karnataka coast	42
Fig. 2.3	Satellite missions Coordination Group for Meteorological Satellites (CGMS), CEOS Ocean Surface Vector Winds Virtual Constellation, April 2014	43
Fig. 2.4	Architecture of ANFIS for present study	45
Fig. 2.5	Architecture of 1D wavelet transform	47
Fig. 2.6	Turbine power curves for Siemens- SWT 2.3 (blue), Vestas-V90 (brown), REpower 5M (black). Dotted lines represent max theoretical $P_t$ (Betz limit, $C_p = 59.3\%$ ) for three-turbine manufacturers	51
Fig. 2.7	Flowchart of scheme developed for short-term forecasting with multiple input combinations	53
Fig. 2.8	Time series plot of observed wind speeds at a) AD07 and b) CB02	54
Fig. 2.9	Flowchart of scheme developed for short-term forecasting by hybrid techniques	55
Fig. 2.10	Flowchart of scheme developed for estimation of ENW and comparison with OSCAT	57
Fig. 2.11	Buoy location and bathymetry map of study area	58
Fig. 2.12	Monthly mean wind speeds for 2011 at buoys (a) AD02 and (b) CB02	59
Fig. 2.13	Methodology modified after Sheridan et al., (2012)	61
Fig. 2.14	Bathymetry of study area based on offshore foundation technologies	63

Fig. 3.1	Observed versus model 1 estimated wind speed at a) AD07 and b) CB02	69
Fig. 3.2	Observed versus model 2 estimated wind speed at a) AD07 and b) CB02	70
Fig. 3.3	Scatter plot of observed and ANFIS wind speeds at buoy a) AD07 and b) CB02	78
Fig. 3.4	Observed versus ANFIS forecasted wind speeds at buoy a) AD07 and b) CB02	80
Fig. 3.5	Observed versus WT+ANFIS forecasted wind speeds at buoy a) AD07 and b) CB02	84
Fig. 3.6	Comparison of observed and forecasted wind speeds a) ANFIS and b) WT+ANFIS at AD07, observed wind speed $> 7 \text{ m s}^{-1}$	84
Fig. 3.7	Comparison of observed and forecasted wind speeds a) ANFIS and b) WT+ANFIS at AD07, observed wind speed between $4\text{-}7 \text{ m s}^{-1}$	86
Fig. 3.8	Comparison of observed and forecasted wind speeds a) ANFIS and b) WT+ANFIS at CB02, observed wind speed $> 7 \text{ m s}^{-1}$	86
Fig. 3.9	Comparison of observed and forecasted wind speeds a) ANFIS and b) WT+ANFIS at CB02, observed wind speed between $4\text{-}7 \text{ m s}^{-1}$	87
Fig. 3.10	Comparison of observed and ENW winds at buoy (a) AD02 and (b) CB02	90
Fig. 3.11	Daily wind speed profile, buoy winds at (a) AD02 and (b) CB02 versus time of the day, and OSCAT wind (local time)	90
Fig. 3.12	Scatter plot of buoy (a) AD02 (b) CB02 against OSCAT wind speeds	95
Fig. 3.13	Scatter plot of buoy (a) AD02 (b) CB02 against OSCAT wind direction	96

Fig. 3.14	Scatter plot of residual versus buoy (a) AD02 and (b) CB02 wind speeds	98
Fig. 3.15	Scatter plot of residual versus buoy (a) AD02 and (b) CB02 wind direction	99
Fig. 3.16	Spatial wind map at 10 m for June 2011	101
Fig. 3.17	Spatial wind map at 10 m for July 2011	101
Fig. 3.18	Spatial wind map at 10 m for August 2011	102
Fig. 3.19	Spatial wind map at 10 m for September 2011	102
Fig. 3.20	Comparison of OSCAT and IRAWS (a) wind speeds and (b) wind directions	104
Fig. 3.21	Exclusion zones and shipping exclusion area for study area	105
Fig. 3.22	Histograms of monthly averaged OSCAT winds for the study area	108
Fig. 3.23	OSCAT Winds at (a) 10 m and (b) 90 m over the study area	108
Fig. 3.24	(a) WPD at 90 m over the study area. (b) Classification of WPD (at 10m) based on foundation technology depths	109
Fig. 3.25	Wind power output based on REpower 5 MW turbine	111
Fig. 3.26	Seasonal rose plots of OSCAT wind direction: (a) Pre- monsoon (b) Monsoon (c) Post-monsoon	113



## LIST OF TABLES

Table 1.1	List of global scatterometer missions	06
Table 1.2	Advantages and limitation of different space based sensors for offshore wind observations	09
Table 1.3	List of extrapolation methods available to obtain ENW	15
Table 1.4	Classification of forecast horizons (Soman, et al. 2010; Jung and Broadwater, 2014)	25
Table 2.1	Sensors used in moored buoy system (Venkatesan et al., 2013)	39
Table 2.2	Friction Coefficient ( $\alpha$ ) of different terrain types (Patel, 2012)	48
Table 2.3	Statistics of wind speed dataset at both buoys	54
Table 2.4	Offshore wind turbine foundation technologies based on operational water depths	61
Table 2.5	Details of PFZ locations off-coast of Karnataka (source: INCOIS)	65
Table 3.1	Error analysis of model 1 and 2 estimated wind speeds at AD07 and CB02	68
Table 3.2	RMSE and MAPE of PM, model 1 and 2 for multiple forecast at AD07	73
Table 3.3	RMSE and MAPE of PM, model 1 and 2 for multiple forecast at CB02	74
Table 3.4	Percentage error in model 2 forecasted wind speed at both the buoy locations	75
Table 3.5	Performance indices of ANFIS model estimates at both the buoys	76
Table 3.6	Performance of ANFIS, forecast up to 3 time steps at buoy AD07	77
Table 3.7	Performance of ANFIS, forecast up to 3 time steps at buoy CB02	77

Table 3.8	Performance indices for WT+ANFIS model estimates at both the buoys	81
Table 3.9	Performance of WT+ANFIS for forecast up to 3 time steps at buoy AD07	82
Table 3.10	Performance of WT+ANFIS, forecast up to 3 time steps at buoy CB02	83
Table 3.11	Comparison of PM, ANFIS and WT+ANFIS forecasts at both buoys	88
Table 3.12	RMSD and Correlation between methods	89
Table 3.13	Correlation, RMSD and MAPE for different methods with OSCAT winds (scenario 1)	91
Table 3.14	RMSD and Bias for OSCAT winds against buoy winds (scenario 2)	94
Table 3.15	Monsoon period maximum and minimum OSCAT and buoy wind speeds	101
Table 3.16	Classes of wind power density at 10 m and 50 m (source: <a href="http://www.nrel.gov/gis/wind_detail.html">http://www.nrel.gov/gis/wind_detail.html</a> )	110
Table 3.17	Depth wise available area, power potential and annual output	114
Table 3.18	Wind Power potential for Karnataka coast before and after subtracting shipping conflict areas	115

## LIST OF ABBREVIATIONS AND SYMBOLS

Abbreviations	Description
ADEOS	Advanced Earth Observing Satellite
ARIMA	Auto-Regressive Integrated Moving Average
ASCAT	Advanced Scatterometer
AWS	Automated Weather Station
BVW	Bourassa-Vincent-Wood
ECMWF	European Centre for Medium-Range Weather Forecasts
ENW	Equivalent Neutral Winds
IMD	India Meteorological Department
INCOIS	Indian National Centre for Ocean Information System
INSAT	Indian National Satellite System
IRAWS	INCOIS Real Time Automated Weather Station
IRS	Indian Remote Sensing Satellites
ISRO	Indian Space Research Organization
LiDAR	Light Detection And Ranging
LKB	Liu- Katsaros-Businger
MAPE	Mean Absolute Percentage Error
MetOp	Meteorological Operational Satellite Program of Europe

NCEP	National Centers for Environmental Prediction
NCMRWF	National Centre for Medium Range Weather Forecasts
NIOT	National Institute of Ocean Technology
NRCS	Normalized Radar Cross Section
NRSC	National Remote Sensing Center
NSCAT	NASA Scatterometer
NWP	Numerical Weather Prediction
OOIS	Ocean Observation Information System
OSCAT	Oceansat-2 Scatterometer
PSLV	Polar Satellite Launch Vehicle
QSCAT	Quik Scatterometer Satellite
RAMA	Research Moored Array for African–Asian–Australian Monsoon Analysis and Prediction
RMSD	Root Mean Square Deviation
RMSE	Root Mean Square Error
SAR	Synthetic Aperture Radar
SASS	SEASAT-A Scatterometer System
SODAR	Sound Detection And Ranging
SSM/I	Special Sensor Microwave Imagers
WAsP	Wind atlas analysis and Application Program
WRF	Weather Research and Forecasting

<b>Symbol</b>	<b>Description</b>
$Z_o$	ocean surface roughness length
$U_*$	Friction Velocity
$\alpha$	Friction coefficient
$g$	Gravitational Force
$Z_{ch}$	Charnock constant
$\kappa$	von Kármán constant
$(c_p/ U_*)$	Wave age
$Z_{ot}$	Roughness length for temperature
$Z_{oq}$	Roughness length for humidity
$\psi\left(\frac{z}{L}\right)$	Atmospheric Stability
$L$	Monin-Obukhov Length
$G$	Gustiness Factor
$P$	Wind Power Density
$P_t$	Theoretical Power
$\rho$	Air Density
$C_p$	Power coefficient
$AP$	Atmospheric Pressure

AT	Atmospheric Temperature
RH	Relative Humidity
SST	Sea Surface Temperature
WS	Wind Speed
WD	Wind Direction

## CHAPTER 1

### INTRODUCTION AND LITERATURE REVIEW

#### 1.0. GENERAL

Wind movement is in response to difference in the pressure, uneven solar heating of earth's surface and earth's rotation. Due to the pressure difference in different parts of the earth, the air tends to move from low pressure to high-pressure region. The pressure gradients are result of non-uniform heating of earth surface by the solar radiation. As the surface gets heated, the energy is transferred to surrounding air leading to expansion and rising of air and there occurs a drop in pressure. The reverse process is seen when the surface cools down and the pressure rises. Therefore, it can be concluded that solar radiation is inevitably the fundamental driving force for wind, variations in temperature and pressure. In addition, the earth's rotation also plays a vital role in circulation patterns. The Coriolis effect (which is a property of observing motions from a rotating reference frame) causes air moving toward the poles to bend towards east. Likewise, the air moving towards equator to bend towards west. In other words, the earth's surface moves faster around the axis at the equator than it does closer to poles. As a result, an object freely moving towards equator and surface underneath towards east. However, to an observer on the surface it would appear to turn towards west.

Also, the temperature gradient along with Coriolis effect is responsible for global wind patterns between equator and poles, most importantly for equatorial winds and midlatitude westerlies (Brower and Bernadett, 2012). Hot air from equator rises up and moves towards higher latitudes through convection process and cooler air replaces it. Such a circulation is known as *Hadley cell*.

At poles, circulation between poles and high latitudes is known as *polar cell*. In between Hadley and Polar cells are *Ferrel cells* located. The circulation in Ferrel cells is opposite direction to other cells. The circulation in *Ferrel cells* occurs due to rising and sinking of hot and cold air from neighboring cells is shown in Fig. 1.1. The circulation patterns are also significantly influenced by the land masses, since the land mass heats and cools much faster than the oceans. Further, in the land masses there

are different factors that impact the surface heating like – topography, land cover, vegetation and anthropogenic elements, which collectively impact global and local circulation patterns. In general, surface roughness parameter plays important role in classification of winds as high and low. For example on land, high roughness leads to high drag and winds near ground tend to be low, whereas relative low roughness over oceans is responsible for high winds.

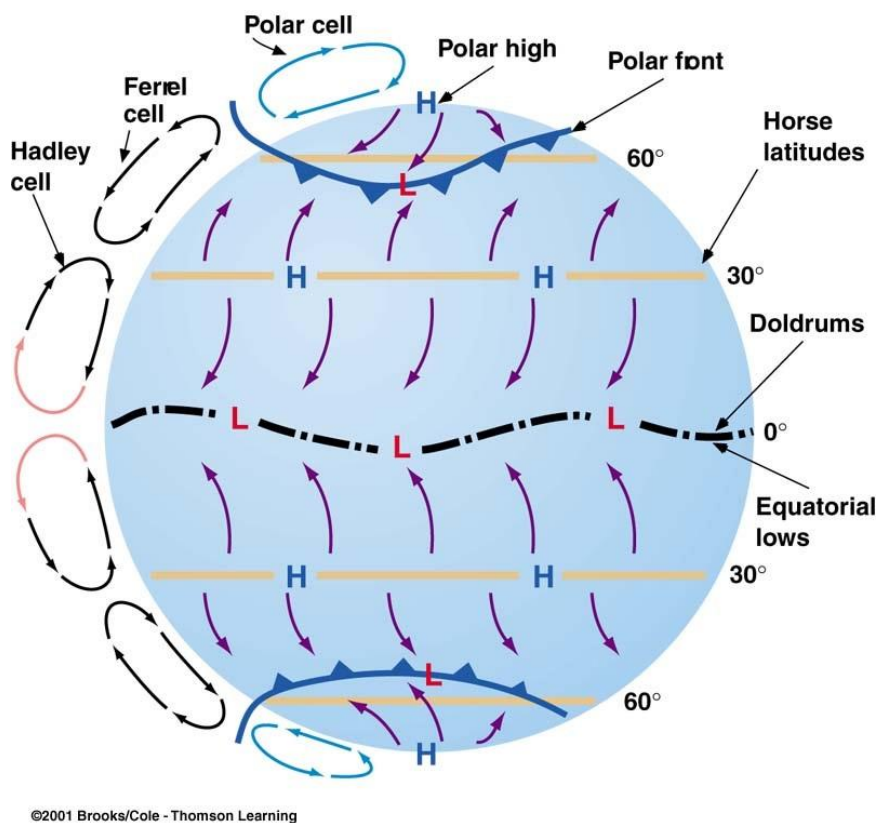


Fig. 1.1: Global atmospheric circulation (Newman, 2007)

Measurements of winds are conducted at both global and regional scale. The wind vector data are an important parameter for wide range of studies from meteorological (weather and climate) studies, understanding the circulation patterns to wind resource assessment studies. Winds observations can be obtained from different types of platforms and different heights (on land and offshore) like fixed structures, masts, balloon based or space-borne. There are diverse types of instruments, which can be employed to measure wind speeds like anemometers – cup or sonic, remote sensing instruments like – radars (LiDAR, SODAR, Scatterometer, SAR). So, wind observations can be broadly categorized as in situ and satellite based remotely sensed



observations. In case of offshore wind observations, principal source of in situ observations are meteorological buoys, masts and ships. The sensors mounted on buoy and masts record and transmit meteorological data in real time via satellites to the onshore stations. The advantages of such data are high temporal resolution and continuous real time data transmissions. The data are relatively accurate and provide us with a continuous time series data. The major limitations of buoy and mast observations is that they are point measurements, leading to low spatial coverage (Gadad and Deka, 2015). However ship based observations were the only source of ocean observations prior to buoys. Ship based observations provide greater spatial coverage than the buoys and masts.

*Indian scenario -*

In India, National Institute of Ocean Technology (NIOT) and Indian National Center for Ocean Information Services (INCOIS) are the government organizations that are responsible for observation and recording of the metocean parameters using buoys, masts and ships. In addition, National Remote Sensing Center (NRSC) and Indian Space Research Organization (ISRO) are responsible for satellite based observations of ocean winds and distribution of data. The network of moored buoys deployed under National Data Buoy Programme of India for in situ measurements around Arabian Sea and Bay of Bengal can be seen in Fig. 1.2. The satellite data can be accessed from NRSC web link ([www.nrsc.gov.in](http://www.nrsc.gov.in)). The IRAWS program was initiated in 2009 under Ocean Observations and Information Services (OOIS). Automated Weather Station (AWS) sensors are mounted on ships at height of 13 m above sea level. Meteorological parameters that are measured include- atmospheric pressure, atmospheric temperature, relative humidity, wind speed, wind direction, sea surface temperature, long wave radiation and short wave radiation. There are 9 research vessels operating in the Arabian Sea, a graphical representation of ships can be seen at the INCOIS website (<http://www.incois.gov.in/portal/datainfo/aws.jsp>). The data is transmitted in real time to INCOIS station through Indian geosynchronous satellites INSAT 3A and 3C (Harikumar, et al. 2013). The major limitations associated with in situ data are their sparsity in both in space and time, the establishment, operation, and maintenance of instruments, and the associated economic factors.

Advancements in satellite-based measurements of wind vector and retrieval techniques have resulted in improved observation of global ocean surface winds (Mathew, et al. 2012). Indian organizations have made progress in employing satellite-based remote sensing for oceanographic research and applications. Focus has been given on measuring various ocean parameters and processes such as ocean surface waves, wind, sea surface temperature, chlorophyll pigments, oceanic eddies, heat budget, mixed layer depth and latent heat studies. Series of the ocean satellites, first of them IRS-P4 (Oceansat-1), was launched successfully on 26 May 1999 using the indigenous Polar Satellite Launch Vehicle (PSLV) from Sriharikota (Desai, et al. 2000) and many more satellite missions have been launched for earth observation as listed in the link (<http://www.isro.gov.in/spacecraft/list-of-earth-observation-satellites>).

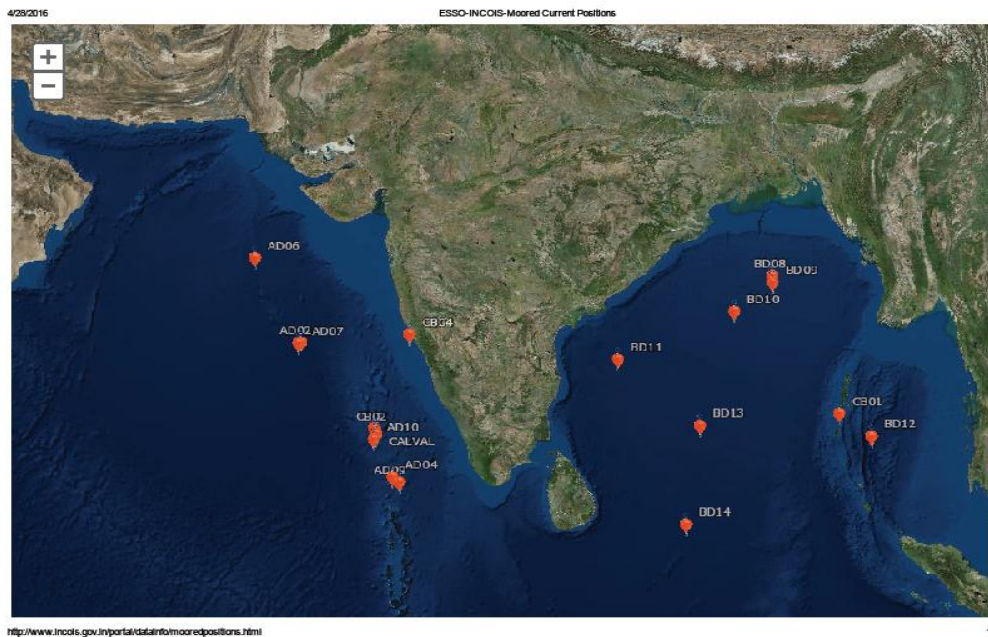


Fig. 1.2: INCOIS moored buoy network

(source: <http://www.incois.gov.in/portal/datainfo/mooredpositions.html>)

## **1.1. SATELLITE BASED GLOBAL OCEAN WIND OBSERVATIONS**

The significant advantages of space borne observations are their vast spatial coverage and low data cost. Bragg scattering would prove to be the key to understanding how to measure winds over the ocean from space. The first space-borne active radar for earth remote sensing was RADSCAT. The combined 13.9 GHz radiometer and scatterometer measured the ocean, demonstrated the fundamental ability to make both wind and wave measurements. Scatterometers were first flown in space on board the Skylab missions in 1973 and 1974. In 1978, the Seasat-A satellite was flown, however the mission lasted around four months. Seasat had on board radar altimeter to measure sea surface height, wind speed and significant wave height; a microwave radiometer and scatterometer (SASS) for wind speed measurements (NCEP, 2002). Additionally, a L-band synthetic aperture radar (SAR) for ocean surface wave spectra, with imagery of sub-kilometer resolution (Eoportal, 2015).

The European Space Agency flew a Scatterometer (SCAT) onboard its European Remote Sensing Satellite (ERS) -1 in 1991. The NASA Scatterometer (NSCAT) was launched onboard the Advanced Earth Observing Satellite (ADEOS-I) and provided 90% coverage of the ocean areas within a 2-day period until the satellite lost power in 1997. The Quick Scatterometer Satellite (QuikSCAT) carrying the SeaWinds Scatterometer was launched in 1999 to fill the gap created when NSCAT data was no longer available. Table 1.1 presents the list of satellite missions with scatterometer on board and their intended applications. QSCAT at 700–850 km altitude, has a swath of 1800 km thus provides complete coverage of the world's ocean surface every two days. It has ku-band pencil beam scatterometer providing wind data at 25 km resolution. Due to the success of NSCAT and QSCAT, another SeaWinds Scatterometer on the ADEOS-II Satellite was launched in December 2002. The Metop-A satellite was launched in 2006, operated by the European Organisation for the Exploitation of Meteorological Satellites. It has on board the Advanced Scatterometer (ASCAT), a C-band scatterometer, which provides wind vector data at a spatial resolution of 25 km. The Oceansat-2 satellite was launched by ISRO, India, in 2009, with a ku-band pencil beam scatterometer (OSCAT). The scatterometer is active radar and the wind observations obtained are function of backscatter power,

which depends on the ocean surface roughness. Also, the radiation of Ku-band is subjected to attenuation by the atmosphere. Climatological values of this attenuation were found to be function of location and time of year (Manual, 2013). Thus the scatterometer data are indirect measurements of offshore winds and requires validation by the in situ observations. The spatial resolution of global wind vector data provided by NRSC, is 50 km and 25 km (since July 2013). QSCAT and OSCAT have a revisit time of 2 days. The OSCAT mission goals were to provide wind data between 4 and 24 m s<sup>-1</sup>, with an accuracy of 2 m s<sup>-1</sup> and directional accuracy of 20° (Gadad and Deka, 2015).

Table 1.1: List of global scatterometer missions

Operational years	Satellite	Instrument	Facts
1973-1974	Skylab	<ul style="list-style-type: none"> <li>• Simple scatterometer</li> <li>• Single measurements at one location at any given time</li> </ul>	<ul style="list-style-type: none"> <li>• First time a scatterometer was flown in space</li> <li>• Wind direction had to be calculated from another source.</li> </ul>
1978	Seasat-A	<ul style="list-style-type: none"> <li>• Ku-band scatterometer (14GHz)</li> <li>• Four fanned beamed antennas</li> <li>• 2 swaths (600Km each)</li> </ul>	<ul style="list-style-type: none"> <li>• Operational for 4 months</li> <li>• Proved that accurate wind speed and direction measurements could be made from space.</li> </ul>
1991-2000	ERS-1	<ul style="list-style-type: none"> <li>• Scatterometer (SCAT)</li> <li>• C-band (5 GHz)</li> <li>• Single swath (500 km)</li> </ul>	<ul style="list-style-type: none"> <li>• Provided the longest record of global scatterometer data yet obtained.</li> </ul>
1995-2011	ERS-2	<ul style="list-style-type: none"> <li>• Scatterometer (SCAT)</li> <li>• C-band (5 GHz)</li> <li>• Revisiting interval of 8 days</li> </ul>	

1996-97	ADEOS-I	<ul style="list-style-type: none"> <li>• NASA Scatterometer (NSCAT)</li> <li>• Ku-band (14GHz)</li> <li>• Two swaths, 600 km wide</li> </ul>	<ul style="list-style-type: none"> <li>• Provided measurements of ocean surface winds in all weather and cloud conditions.</li> <li>• Operated for 10 months until the solar panel failed.</li> <li>• Obtained 190,000 measurements per day mapped 90% earth's oceans every 2 days.</li> </ul>
1999-2009	QuikSCAT	<ul style="list-style-type: none"> <li>• SeaWinds scatterometer</li> <li>• Ku-band, (13.4GHz)</li> <li>• Rotating dish antenna</li> <li>• One swath, 1800 km wide</li> </ul>	<ul style="list-style-type: none"> <li>• Quick fix for the loss of NSCAT data 400,000 measurements in one day</li> <li>• Provides measurements of ocean surface winds in all weather and cloud conditions.</li> <li>• Maps 90% earth's oceans every 2 days.</li> </ul>
2002-03	ADEOS-II	<ul style="list-style-type: none"> <li>• SeaWinds scatterometer</li> <li>• Ku-band, (13.4GHz)</li> <li>• Rotating dish antenna</li> <li>• One swath, 1800 km wide</li> </ul>	<ul style="list-style-type: none"> <li>• Launched in December 2002</li> <li>• Will provide measurements of ocean surface winds in all weather and cloud conditions.</li> <li>• Will map 90% earth's oceans every 2 days.</li> </ul>

2006-2014	MetOp	<ul style="list-style-type: none"> <li>• Advanced Scatterometer (ASCAT)</li> <li>• Design life of 5 years</li> <li>• Real aperture C-band (5.255 GHz)</li> <li>• Dual-swath and three-look radar instrument</li> </ul>	<ul style="list-style-type: none"> <li>• Cloud imagery for forecasting applications</li> <li>• Measurement range of 4-24 m s<sup>-1</sup> with an accuracy of 2 m s<sup>-1</sup> and a direction accuracy of ±20°</li> <li>• Two- 550 km wide, swaths.</li> </ul>
2009-14	ISRO Ocean sat-2	<ul style="list-style-type: none"> <li>• Ku-band Scatterometer</li> <li>• One swath, 1800 km wide</li> <li>• Design period of 5 years</li> </ul>	<ul style="list-style-type: none"> <li>• Sea-state forecast-waves, circulation</li> <li>• Monsoon and cyclone forecast</li> <li>• Observation of Antarctic sea ice</li> <li>• Study of sediment dynamics</li> </ul>

SSM/I on satellites in the U.S Defense Meteorological Satellite Program provided surface wind speed as early as from 1987, along with ERS-1's altimeter and scatterometer. The wind speeds were estimated using empirical models separately for each type of instrument. The accuracy of wind speed estimates was aimed to better than 2 m s<sup>-1</sup>. The comparison between scatterometer, altimeter and SSM/I wind speed measurements, for Atlantic tropic area was carried out by Bentamy, et al. (1994). In the study, RMSE was found to be less than 2 m s<sup>-1</sup> and it was inferred that, the difference between measurements by scatterometer and altimeter may depend on the significant wave height and the difference between scatterometer and SSM/I may be dependent of the integrated water vapor content. Kent, E. C (1998) made an early attempt to compare and validate scatterometer winds using ship observations and the RMSE was found to be less than 2 m s<sup>-1</sup>. A regression expression was proposed to compute ship based wind speeds from scatterometer wind speeds. Table 1.2 presents

the pros and cons of different instruments on board satellites for ocean surface wind observation.

Table 1.2: Advantages and limitation of different space based sensors for offshore wind observations

Instrument	Advantages	Limitations
Anemometer	Turbulent wind stress can be measured. Very high frequency of measurements	Air-sea interface can be harsh layer for anemometers; hence measurements are fixed heights (at least 3 m above sea level). Point locations
Scatterometer	Global coverage, large swath. Spatial Resolution of wind data: 25 km or 50 km. Efficient in open waters.	In accurate nearer to the coast. Coarse frequency of data in comparison to anemometer.
Altimeters and Radiometers	Measures the power of the returned signal, which is related to the wind induced roughness of the sea surface. Accurate localized measurements of winds.	Only wind speed can be inferred. Measurement can be obtained for small area (limited to 10 km radius from satellite nadir). Less accurate than scatterometer for high wind speed conditions.
Synthetic Aperture Radar	High-resolution patterns of wind speed and direction variations. Efficient in measuring surface winds from space in coastal regions. SAR derived winds are equivalent to buoy anemometer winds and are capable to substitute the anemometer observations	Linear features in SAR images are not available for wind direction estimates. Wind direction information from numerical weather models can be used to initiate SAR wind speed retrieval. The SAR directly measures only backscattered power from which NRCS is to be determined.

A comparison of ERS-2 SAR and ERS-1 scatterometer wind speeds was performed by Korsbakken and Furevik, (1998) for latitudes greater than about 63°. The study demonstrated the high resolution of SAR winds over scatterometer in coastal regions, however the SAR wind retrievals required inputs of wind direction. Stiles and Yueh, (2002) demonstrated the influence of rain on the accuracy of Ku-band scatterometer (NSCAT and QSCAT). The work was aimed at determining the rain-contaminated wind vector cells and then flag corresponding cells. In the study, collocated SSM/I rain rate measurements, NCEP wind fields, and QuikSCAT backscatter measurements were used, to empirically fit a simple theoretical model of the effect of rain. From the work, it was determined that horizontal polarization measurements are more sensitive to rain than vertical polarization. It was inferred that the sensitivity to rain varies intensely with wind speed and the additional backscatter due to rain overshadows the rain-related attenuation.

Ebuchi, et al. (2002) using buoy data on a global scale validated the QSCAT wind vectors and found that the wind satellite winds were in good agreement with the buoy winds. The study also assessed the effects of oceanographic and atmospheric environment on scatterometer measurements. It was concluded that, there was a weak positive correlation of the wind speed residuals with the significant wave height, and the dependencies on the sea surface temperature or atmospheric stability were not physically significant. Goswami and Rajagopal, (2003) examined the quality of the surface wind analysis at National Center for Medium Range Weather Forecast (NCMRWF), New Delhi over the tropical Indian Ocean and its improvement in 2001 by comparing it with in situ buoy measurements and QSCAT during 1999, 2000 and 2001. It was found that, the NCMRWF surface winds during 2001 were significantly improved with bias of the mean analyzed winds reduced everywhere considerably and within  $0.5 \text{ m s}^{-1}$  of QSCAT winds.

Barthelmie and Pryor, (2003) highlighted the necessity of remote sensing application for ocean surface wind observations and the uncertainties inherent in application of current methodologies required to be quantified. Overestimation of wind resource can be due to number of biases inherent in remote retrieval of wind speeds using satellite-borne instrumentation. As an interim measure, error bounds were proposed for the



wind speed probability distribution parameters, which may be applied to sparse (satellite wind) datasets to obtain better accurate wind estimates. Using ERS-2 SAR images, wind maps were developed for Horns Rev site in the North Sea and compared to meteorological in situ observations from a mast located 14 km offshore by Hasager, et al. (2006). In the study, in situ wind directions were used as input to the CMODIFR2 and CMOD4 model functions to obtain wind speed from SAR images. It was found that CMOD4 yielded better linear regression results. It was suggested that, SAR wind maps could be useful for mapping of future offshore wind resources. Monaldo, et al. (2004) performed systematic comparison of wind speed measurements from QSCAT and SAR (from RADARSAT-1). The study was carried out in the Gulf of Alaska for duration of two-year (2000 and 2001). The SAR wind speed estimates were found to better when QSCAT wind direction were used in comparison to wind direction input from the Navy Operational Global Atmospheric Prediction System (NOGAPS) model. SAR–scatterometer comparisons were then used to generate a new C-band horizontal polarization model function. With this new model function, the wind speed inversion improved. Thus it was demonstrated that SAR and QSCAT measurements could be combined to make better high-resolution wind measurements than either instrument could alone in coastal areas.

Wind measurements from NSCAT and QSCAT were compared with buoy measurements by Chelton and Freilich, (2005) to establish the accuracies of both scatterometers. In this study, it was established that after QSCAT winds were assimilated in to models of European Center for Medium Weather Forecast (ECMWF) and NCEP’s NWP models, large improvement in the accuracies of wind analysis was observed. Furevik, et al. (2011) considered eight years of QSCAT wind observations in order to demonstrate the capability of scatterometer to provide long-term statistics (like annual and monthly wind indexes), as available from buoy data. In the study, QSCAT data was compared with in situ data from 11 locations in the Mediterranean. The study revealed that the correlation between QSCAT and in situ observations was found to degrade closer to the coast. Singh, et al. (2011) used QSCAT winds in combination with SSM/I’s total precipitable water and Meteosat-7-derived atmospheric motion vectors in WRF-3DVAR model to investigate the impact on tracking and intensity prediction of tropical cyclones over the North Indian Ocean.

It was found that the tracking and prediction of cyclone tracks improved significantly with the assimilation of QSCAT winds. Also, the assimilation resulted in positive impact on the intensity (maximum surface level winds) prediction particularly for those cyclones, which are at their initial stages of the developments at the time of data assimilation. Stoffelen and Verhoef, (2011) evaluated the Oceansat-2 scatterometer backscatter and wind data, by comparing with ECMWF model and buoy winds. It was reported that the wind data quality is reasonably good. Also, it was found that the backscatter data appeared to be of good quality but small calibration issues remained. The study concluded that correction of the backscatter processing at low backscatter values is expected to further improve low wind processing. Singh, et al. (2012) assessed the quality of OSCAT winds using NCEP analyzed winds, ASCAT and buoy measured winds. After the quality assessment, the OSCAT winds were assimilated in to WRF-3DVAR model to investigate the impact of OSCAT winds on short-term forecasts, forecast of midtropospheric moisture, temperature, and upper tropospheric winds. From the study, it was concluded that the assimilation improved the forecast accuracy of model. Ebuchi, (2012 and 2013) compared OSCAT wind data against ECMWF reanalysis wind data over globe to assess the systematic errors. It was found that, wind speed histograms calculated from OSCAT wind data clearly showed excess concentration at very low wind speed ranges. From the frequency distribution of the wind directions (relative to the flight direction) it was revealed that wind vectors of the OSCAT wind exhibit systematic directional preference. This artificial directivity was considered to be caused by imperfections in the instrument calibration, wind retrieval algorithm, and geophysical model function.

The calibration of OSCAT winds by the ocean calibration method yielded high quality data when compared with NWP wind data (Yun, et al. 2012). Mathew, et al. (2012) used global ocean surface wind speeds from QSCAT for 5 years (2005–2009) and OSCAT for 1 year (2010), to compare with wind speeds estimates from JASON Altimeters for representative months. The investigation was focused to assess the consistency in wind speeds between these sensors. The results of the inter-comparison suggested that OSCAT wind speeds are almost as consistent with JASON as QSCAT wind speeds. Validation of OSCAT was performed using buoy observations; ASCAT and QSCAT surface winds by Kumar, et al. (2013). The analysis for duration of 9

months, revealed RMSE of around  $1.5 \text{ m s}^{-1}$  for the wind speed and around  $20^\circ$  for the direction. High correlation was observed between OSCAT and ASCAT data and RMSE was found to be  $1.2 \text{ m s}^{-1}$  for the range of 4 to  $24 \text{ m s}^{-1}$ . Rani and Gupta (2013) validated OSCAT winds against the Research Moored Array for African– Asian– Australian Monsoon Analysis and Prediction (RAMA) buoy winds for a period of one year to establish the accuracy of OSCAT winds. The monthly mean RMSE in the wind speed and wind direction were found to be around  $2.5 \text{ m s}^{-1}$  and around  $20^\circ$  respectively. During monsoon period (June–September) of 2011, better match between the OSCAT and RAMA buoy wind was observed. The root RMSE was found to be less than  $1.9 \text{ m s}^{-1}$  and  $11^\circ$  for wind speed and direction respectively. Also, ASCAT and OSCAT winds statistics were found to be similar to RAMA buoy winds during monsoon 2011 over the Indian Ocean, thus establishing the accuracy of scatterometers. Jayaram, et al. (2014) attempted to generate daily composites of OSCAT Level-3 (L3) wind vectors using Data-Interpolating Variational Analysis (DIVA) method from ascending and descending passes over the Indian Ocean region. The daily composite wind vectors were validated, by comparing with ASCAT and observations from in situ buoys for the year 2012. Wind composites thus generated were found to be in good agreement with in situ and ASCAT wind products. Minor deviations in L3 wind vectors were observed with respect to ASCAT wind, which could be attributed to the difference in interpolation techniques used for the two-scatterometer products. OSCAT has a revisit period of 2 days, it was suggested that the wind products could be conveniently used for real-time met-ocean studies.

The satellite (scatterometer) winds are referenced to height of 10 m above sea level. The height of 10 m above sea level is considered as neutral atmospheric region. The observations from buoy are generally obtained at height of 3 to 5 m (may vary subject to instrument set up). The ship observations are obtained by instruments mounted at different locations on the vessel and generally may range from 10 to 30 m. In order to assess the quality and validate the satellite winds, it is required to extrapolate the in situ observed winds to 10 m height. In the following section, methods employed for obtaining 10 m winds is discussed with supporting literature.

## 1.2. EXTRAPOLATION APPROACHES

The near-surface winds measured by scatterometer are referenced to a height of 10 m above sea level. The buoys deployed by NIOT measure meteorological parameters at 3 m above sea level. Those winds transferred from 3 to 10 m height are known as equivalent neutral winds (ENW). Hsu, et al. (1994) established the mean and standard deviation for the friction coefficient of the power-law wind profile over the oceans, under near-neutral atmospheric stability conditions as to be  $0.11 \pm 0.03$ . The study was based on anemometers located at different heights in the Gulf of Mexico and off the Chesapeake Bay, Virginia. Since the mean value was obtained from both deep and shallow water environments, it was recommended for use at sea, to adjust the wind speed measurements at different heights to height of 10 m above the sea surface. Lange, et al. (2001) worked on Charnock relation, which is employed to compute  $z_0$ .  $z_0$  is function of  $U^*$ ,  $g$  and  $z_{ch}$ - a constant, but was found to be site specific (for sites with coastal influence). In the study, wave age ( $c_p/U^*$ ) a dimensionless parameter was used to estimate  $z_0$  and it was found that, only a small improvement was observed in prediction of 10 m winds. Thus, it was inferred that, there was insignificant improvement in 10 m predicted winds in comparison to Charnock equation.

Further, Lange, et al. (2004) using LKB method computed winds at 50 m height from in situ observations at 10 m. Ebuchi, (2002) adopted Liu-Katsaros-Businger (LKB) method to convert wind speed measured by the buoys at various heights above the sea surface was converted to ENW. The converted winds were then used to validate QSCAT winds over the globe. QSCAT winds were compared to moored buoys in the Indian Ocean by Satheesan, et al. (2007). It was an early attempt at using the LKB method for estimating ENW in the Indian Ocean. Kara, et al. (2008) examined the spatial and temporal variability of the impact of air-sea stratification on the differences between satellite-derived 10 m wind speeds and in situ derived 10 m (ENW) wind speeds, over the global ocean. The study compared COARE3.0, Bourassa-Vincent-Wood (BVW) and LKB methods at many buoy locations. The results demonstrated that, the ENW estimated by methods were relatively similar and difference between ENW and satellite winds was insignificant. Various methods available to estimate ENW were described by Peng, et al. (2013). It was suggested

that the Logarithmic (Log) method would be more appropriate approach to estimate ENW. Singh, et al. (2013) compared logarithmic and LKB methods with the focus on buoy data, measured over the northern Indian Ocean. These are well established methods for neutral wind estimation from buoy measurements. Scatterometer calibration is designed to account for the assumption of neutral stability. However, the assumption of a particular sea state and negligible currents, often introduces an error in wind stress estimations. Ali, et al. (2013) developed a method to estimate wind stress directly from the scatterometer measurements of sigma-0 and their associated azimuth angle and incidence angle using a neural network approach. Since the fundamental scatterometer measurement is of the surface radar backscatter (sigma-0), which is related to surface roughness and hence the stress. Comparison was carried out with conventional in situ estimations and it was found that, the proposed method's 10 m wind estimates were more accurate. Table 1.3 presents most widely used approaches to obtain ENW for in situ observations from any height to 10 m above sea level.

Table 1.3: List of extrapolation methods available to obtain ENW

Method	Equation	Parameters
Power Law	$\frac{U_1}{U_2} = \left( \frac{z_2}{z_1} \right)^\alpha$	wind speed, height and friction co-efficient
Logarithmic	$U_z = U_{\text{ref}} \left( \ln \frac{z}{z_o} / \ln \frac{z_{\text{ref}}}{z_o} \right)$	wind speed, height and ocean roughness length.
Liu–Katsaros–Businger (LKB)	$U_z = U_s + \frac{U_*}{\kappa} \left[ \left( \ln \frac{z}{z_o} - \psi \left( \frac{z}{L} \right) \right) \right]$	extrapolation height, surface wind speed, friction velocity, von-Kármán constant, ocean roughness length, atmospheric stability and Monin Obukhov Length

<p>Coupled Ocean– Atmosphere Response Experiment, version 3.0 (COARE3.0)</p>	$U_{10n} = \frac{U_*}{\left(G^{\frac{1}{2}}k\right) \left[\ln\left(\frac{10}{z_o}\right)\right]}$	<p>friction velocity, gustiness factor, von- Kármán constant, and ocean roughness length</p>
<p>Bourassa– Vincent–Wood (BVW)</p>	$[U_z - U_s] \times \hat{e}_i = \frac{U_* \times \hat{e}_i}{k} \left[ \ln\left(\frac{z}{z_o} + 1\right) + \varphi(z, z_o, L) \right]$	<p>friction velocity, orthogonal horizontal basis vectors, von- Kármán constant, ocean roughness length, atmospheric stability and Monin Obukhov Length</p>

The estimation of ENW can be generally associated with quality assessment of satellite-derived winds and in the present study, accuracy of scatterometer winds has been considered. The current work focuses on exploring the capability of scatterometer wind data to be assimilated in to regional scale offshore wind resource assessment and corresponding wind power generation potential.

### 1.3. OFFSHORE WIND ENERGY ASSESSMENT

Wind turbines depend on winds as fuel for power generation. Vast oceans, high winds due to low surface roughness and continuous availability of winds offshore have made it a key source of renewable energy. Renewable energy sources offer to bridge supply shortages, reduce carbon emissions and enhance energy security. About 5 GW offshore wind capacity has already been installed around the world and approximately an equal capacity is under construction. There are a large number of offshore wind farms in Belgium, Denmark, Finland, Germany, Ireland, the Netherlands, Norway, Sweden, and the United Kingdom. The European Union has established aggressive targets to install 40 GW of offshore wind by 2020 and 150 GW by 2030 (Govt. of

India, 2013). Esteban and Leary, (2012) highlighted the developments in offshore wind and ocean energy in the Asian-Pacific countries. Based on historical trends in the offshore wind industry and future prediction of growth, it was estimated that the world's electricity production from ocean based devices to be around 7% by 2050, and this would lead significant amount of employment opportunities.

#### *Indian Scenario –*

India, with a long coastline spanning over 7500 km and positioned in the central part of the Indian Ocean, is one of the important regions for many developments. Oceans play an important part in the social and economic life of people in the region and hence there is growing interest to study about them. Much about the marine resources still remains to be understood, largely due to lack of detailed and accurate observations. Satellite based observations have demonstrated to be reliable in providing global and long-term observations. Data from such observations can be used together with point-based in situ data for sustainable exploration and exploitation of these resources; and for improving the accuracy of forecast of weather conditions, ocean state and longer-term climatic changes (Desai, et al. 2000).

India's 136 GW of power generation capacity is based on conventional sources that exert a huge demand on the natural resources. There is a need for exploring the alternate sources of energy to address the demand-supply mismatch and ever increasing fuel security concerns. The Indian government, in order to harness and promote renewable energy, has a dedicated section called Ministry of New and Renewable Energy (MNRE) and also has established the Indian Renewable Energy Development Agency (IREDA), which promotes, develops and extends financial assistance for renewable energy projects (CII Karnataka, 2012). In India, the installed wind energy capacity is over 19 GW (MNRE, 2015) and the country ranks fifth in the world. Kota, et al. (2015) highlighted the scenario as to how UK, USA and India, respectively are enabling offshore wind, to make a vital and sizeable contribution to the low carbon economy. India is still in its infancy stage where the policy frame works are framed by MNRE and getting ready with the tools to enter in to the offshore market. A draft policy has been laid out by MNRE to help develop and guide in offshore wind energy development. The objectives of Draft National Offshore

Wind Energy policy are aimed towards developing Offshore Wind Farm that will enable optimum exploitation of Offshore Wind energy. To mention a few-

- To Achieve Energy Security
- To Reduce Carbon Emissions
- To Promote Research and Development in the Offshore Wind Energy Sector
- To Promote Spatial Planning and Management of Maritime Renewable

Energy Resources in the Exclusive Economic Zone of the Country.

The cost of electricity produced from wind farms in India is at par with the cost of grid electricity. According to the MNRE guidelines, the buyback rate for electricity from wind farms is in the range Rs. 3.39/kWh– Rs. 5.31/kWh depending on each state, compared to Rs. 3.90/kWh–Rs. 5.90/kWh for grid electricity. More importantly, using wind to generate electricity emits much less harmful greenhouse gases than during the combustion of fossil fuels that are generously used for electricity generation. It was estimated that there could be saving of 300–500 tones of CO emission from a wind farm of 4 MWh, 24 electricity generation capacity in India. (Ramasesha and Chakraborty, 2013). However, very little offshore wind generation capacity has been explored and developed, which needs to be reviewed and quantified. With such a huge coastline, there is an enormous opportunity to carry resource assessment studies also, the energy requirement differs from state to state. Thus as a pilot study, it is required to study and develop models for states part-wise that can spearhead in potential site identification for harnessing offshore wind potential. In this work, focus has been on Karnataka State. However, the application of study can be adopted for other coastal states, which provide safe and sustainable environment for development of offshore wind farms.

*Karnataka State –*

Karnataka is 8<sup>th</sup> largest state in India with a population of 61 million (Census, 2011). Karnataka has an installed capacity of 13 GW (by, 30 June 2012) and accounts for 6.64% of the total installed capacity in India. It has been observed that energy demand during 2006-2012 grew at a rate of 8% while the supply grew only by 6%, leading to constantly increasing energy deficits. The energy deficit has increased from 2.1% in 2006-07 to as high as 11.2% in 2011-12 registering a growth rate of 52% for the period. During one-year period, the demand for energy shot up by almost 21%, while



supply grew only by 16%. As on 31<sup>st</sup> March 2012, the state has a demand of 60,830MU against a supply of 54,023MU, resulting in a shortage of 6,807MU. (CII Karnataka Conference on Power, 2012). Fig. 1.3 represents the source-wise contribution of power purchased by all utilities in the State. Major contribution is by thermal and hydro plants (40%) and renewable sources contribute to 10% during financial year 2013. The State is increasingly relying on short-term purchases, often at expensive rates, to meet the growing energy demand (CSTEP & Govt. of Karnataka, 2013). The renewable sources do not consider offshore potential. Karnataka state has 320 km long coastline and a huge potential that needs to be explored.

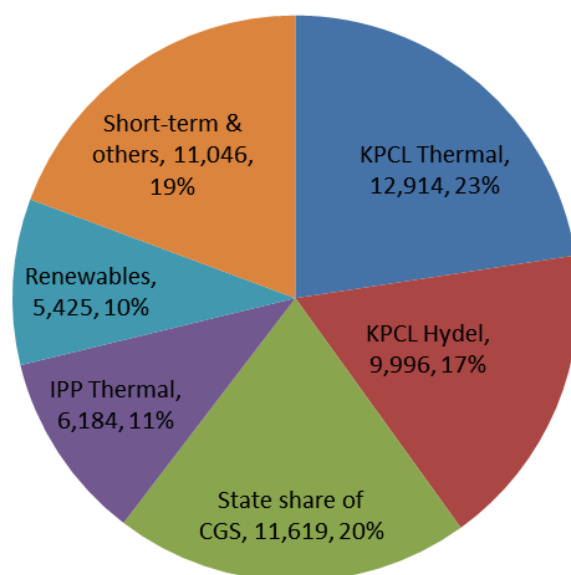


Fig. 1.3: Source-wise purchase by utilities in FY13 (in Million units)  
(source: CSTEP & Govt. of Karnataka, 2013)

The amount of energy a wind turbine can generate is directly affected by wind resource at site. Wind Resource Assessment (WRA) studies are required to quantify and realize the wind resource available at the site. Resource planning and evaluation in advance are essential as they help in understanding the distribution of wind energy resources (Zheng, et al. 2016). To represent the local wind conditions, it is essential to conduct a minimum of one-year wind measurements at the sites (Bailey, et al. 1997). In situ data plays a vital role in WRA studies and the validation of assessments. Major sources of in situ offshore wind data are ships, meteorological buoys and masts. The

buoy data are relatively accurate and provide us with a continuous time series data. Lange, et al. (2004) computed wind speeds (using LKB method) and wind power at 50 m using in situ measurements from Rødsand, located in the Danish Baltic Sea. On comparison with measured wind speeds and power output (estimated using measured wind speed), a small deviation was observed in computed winds. The power output estimation was also compared with Wind Atlas Analysis and Application Program (WAsP) program computed power output. A correction was proposed to the LKB method to reduce the error between estimated winds and measured winds. Also, it was suggested that a constant surface roughness could be used for wind resource assessment.

Kempton, et al, (2007) and Dhanju, et al. (2008) developed a simple methodology to assess available offshore wind power potential using in situ buoy measurements, bathymetric maps. The studies were aimed at mapping the potential area for Mid-Atlantic Bight and Delaware waters, USA respectively at 80 m height. The depth wise classification for turbine installation and optimized layout for sustainable development were emphasized. It was pioneer study that established the need for consideration of exclusion zones, which may hinder the offshore wind farm development. The offshore wind farm development is significantly governed by the bathymetry of the area. It is necessary to consider the depth details for large-scale offshore wind farm development. The type of foundation necessary for offshore wind turbines at the site can be one of the major costs of offshore wind turbine installations (Krohn, et al. 2009). Thus, detail information regarding the water depth can be useful to designers and planners, to assist in deciding suitable foundation technology for the wind turbines. Similar approach was applied by Sheridan, et al. (2012) to estimate power resource at 90 m, off the coast of Maryland, USA. The study was improved by incorporating availability and wake losses in turbine power output. It was found that, the offshore power resource was capable of addressing the energy requirement of the coastal state and recommendation for effective policy was suggested.

Bagiorgas, et al. (2012) quantified wind power resource considering 5 MW wind turbine in Ionian and Aegean Seas using buoy data at 3 and 10 m. It was reported that, around 15–16% higher winds were observed at 10 m compared to that at 3 m. Wind

speed distributions were found to be well represented by Weibull parameters when compared to WAsP and Method of Moments.

The major limitation of buoy observations is that they are point measurements, leading to low spatial coverage (Zheng, et al. 2016). Since the cost of installation and maintenance of buoys can be high, the number of buoys deployed for surface observation is constrained (Peng, et al. 2013).

Ship based wind observations are capable of providing greater spatial coverage than buoys and have advanced with time and now it is possible to obtain offshore meteorological data in real time (like IRAWS) (Harikumar, et al. 2013). Hayashi, et al. (2006) demonstrated the ability of wind characteristics measured using a small ship for decision of suitable site for offshore wind power. The anemometer wind measurement on ship was corrected for rolling and pitching of the ship using differential GPS (DGPS) and the inertial measurement unit. However, the low temporal resolution has been the major limitation of ship data.

Meteorological masts are the alternative source for in situ observations along with buoy and ship observations. The high cost of installation and maintenance limits the use of masts for long-term observations (Carvalho, et al. 2014a). The need for continuous, greater spatial coverage and low cost data was addressed by the satellite based observations of global ocean winds. Scatterometer sensor has proved to be of greater advantage, due to its wide swath of 1800 km and both wind speed and direction data can be retrieved. Pimenta, et al. (2008) used QSCAT data, validated against in situ buoy data, for evaluation of oceanic wind power for southern coast of Brazil. Based on the QSCAT data and bathymetry of the area, maps of wind speed, wind power density were developed and practical turbine output in power units was estimated. The analysis established that, shallow waters of south Brazil, the most favorable conditions for offshore wind farm development. Yan, et al. (2012) estimated offshore wind energy resources of Chinese coastal seas using QSCAT wind data at 10 and 80 m.

Stability dependent wind (SDW) speeds were estimated based on Monin-Obukhov similarity theory using QSCAT data and NCEP Final Analysis data. It was observed that SDW was  $0.5 \text{ m s}^{-1}$  smaller than QSCAT winds. Further, the energy density

distribution map based on Weibull's shape and scale parameters was developed to characterize the offshore wind energy resources. Similar analysis was performed by Jiang, et al. (2013) for China, the offshore wind power potential (at 10 m) was assessed using QSCAT data. Oh, et al. (2012) performed a feasibility study of offshore wind farm using a combination of buoys and QSCAT data assessed wind resources and economical efficiency considering expected capacity factor. The study lead to identification of location of the first offshore wind farm in Korea.

Offshore WRA using SAR and corresponding estimation of wind energy production capacity with special focus on coastal areas has been explored early by Furevik et al. (2003). The high spatial resolution of SAR data in coastal regions has demonstrated the ability to provide accurate wind speeds and energy densities. Kozai, et al. (2010) compared different SAR wind speed algorithm and inferred that CMOD5N in combination with SDW produced more accurate energy density than others. Chang, et al. (2014) used SAR data for mapping offshore wind resources at a small area, reported that there was high correlation between SAR winds and in situ observations. However, the frequency and area coverage of SAR data limits its usage for large scale WRA. Further, Doubrawa, et al. (2015) proposed a methodology to combine in situ and multiple satellite wind observations for offshore wind resource assessment. The study used QSCAT, SAR and in situ observations to develop wind atlases (at 90 m) for the Great Lakes. The analysis represented an uncertainty reduction in wind speeds of about 50% relative to using only SAR, and about 40% to using only SAR and QuikSCAT without in situ observations.

Recent change in trend of WRA is marked by application of NWP models (mesoscale models) that use Global Circulation Model (GCM) as one of the inputs. Multiple datasets from different sources can be incorporated in to NWP models to obtain accurate estimates of offshore wind speeds and power density (Dvorak, et al. 2010). In general, the analysis and reanalysis datasets provided by different organizations are used as inputs to model (example- WRF). The Carvalho, et al. (2014 and 2014a) demonstrated the accuracy of reanalysis data to simulate observed wind data, for both onshore and offshore scenarios. Chang et al. (2015) developed a methodology to incorporate QSCAT, SAR and in situ observations and using WRF model estimated

wind resources at 100 m for South China Sea. This established that mesoscale models (WRF) could produce accurate estimate of winds and corresponding power potential. The advantage of WRF simulated winds over satellite observations can be higher temporal and spatial resolutions. Nevertheless, the application of mesoscale models to regional scale assessments continues to be a challenge. The mesoscale models are generally limited by the accuracy of the observations in the reanalysis dataset and therefore, reliability of the models. Also, the biases in the observations and model can reduce the accuracy of reanalysis output. It was also reported that higher the resolution of model the bigger size outputs are generated and requires enormous computation power to carry out such simulations (Draxl, et al. 2015). WRA, identification of suitable sites for harnessing energy potential and efficiency of wind energy developments depend on the energy distribution, which is a function of regional and seasonal variations. Therefore, in-advance resource planning and management is must for sustainable development. However, on the other hand for optimal use of wind farms (after constructing) it is vital to have comprehensive knowledge of availability of winds over wide range of future time steps. Thus, forecasting of wind speeds plays a prominent role in increasing the efficiency of power production. Short-term forecasting of wind energy can provide reference for wind farm operators, which can then improve the collection and conversion efficiency of wind energy and provide an accurate basis for regulating short-term electricity generation (Zheng, et al. 2016). The standard methods for predicting wind speed/wind energy include numerical weather prediction and wind forecasting, ensemble forecasting, physical methods, statistical and learning approach methods, and hybrid methods.

#### 1.4. FORECASTING METHODS

Winds as discussed earlier, are generated mainly due to pressure, temperature, rotation of earth and difference in global environment. These complex phenomenon and their interactions that drive winds make it highly unpredictable, intermittent and stochastic in nature, which affects corresponding wind power generation. Accurate forecasting of wind speed and power is important for the safety of renewable energy utilization (Liu, et al. 2010). Wind speed is converted into power through characteristic curve of turbine (Lei, et al. 2009; Foley, et al. 2012).

Wind power (P) can be expressed as: 
$$P = \frac{1}{2}(\rho \times A \times V^3) \quad (1.1)$$

where,  $\rho$  : air density ( $\text{kg m}^{-3}$ ), depends on temperature and air pressure.

A: swept area ( $\text{m}^2$ ) and V: wind speed ( $\text{m s}^{-1}$ ) (Soman, et al. 2010)

Wind power forecasts are often met with limitations, which can be generalized as -

- Limitations of machine design and
- Wind speed forecasting tools.

The turbine manufacturing industry with advanced technology is now capable in limiting the losses due to design constraints. In the equation 1.1, considering constant  $\rho$  and A, wind power (P) is directly proportional to the cube of wind speed (V). The wind power fluctuation depends on the volatility of wind speeds. The forecasts provide knowledge about the operating costs of wind farm (Sideratos and Hatziargyriou, 2007) and help in improving the reliability of wind as energy resource. The increase in the lead-time leads to increase in the forecast error. Therefore, the wind speed forecast models are clearly more accurate than wind power prediction models. The forecasting intervals can be classified into different horizons as presented in Table 1.4.

The availability of powerful winds and vast ocean surface makes the offshore winds an important source of energy generation (Jung and Broadwater, 2014). There exists demand for advances in the wind forecasting techniques to keep up with the rapid growth of offshore wind energy. In general, accurate wind forecasts can reduce the risk of financial and technical risk of uncertainty in power generation.

Table 1.4: Classification of forecast horizons (Soman, et al. 2010; Jung and Broadwater, 2014)

Time interval	Class	Application
Few seconds to 30 minutes	Very short term	Turbine control and load tracking
30 minutes to 6 hours	Short term	Pre-load sharing
6 to 24 hours	Medium term	Power management and energy trading
1 to 7 days	Long term	Maintenance scheduling of turbines

The following section discusses the available methods for forecasting wind speed and power. Due to high costs involved in obtaining offshore wind data, the methods that are developed for onshore wind forecasting are generally extended to offshore wind forecasting. There exists little literature on the available methods for offshore wind speed and power forecasting (Foley, et al. 2012) and the advancement in the offshore wind forecasting tools will improve the wind penetration in grid supply (Jung and Broadwater, 2014).

There are various techniques available and being developed for wind speed and power forecasting. Soman, et al. (2010) provided a detail description of the foremost forecasting methods and forecasting horizons with the application of each forecasting intervals. Lei, et al. (2009) discussed existing methods for forecasting of wind speed and generated power. The classification of long-term and short-term forecasts, their application in wind energy industry and techniques adopted were discussed. Long-term wind forecasts help in identification of potential sites and are important for accurate power assessments.

Short-term forecasts are vital for understanding variations in wind speeds and improve the efficiency of wind power generation systems. With accurate wind power forecasts risk of uncertainty can be reduced, leading to better grid planning and integration (Foley, et al. 2012). There are accounts of multiple types of classification of wind forecasting methods that can be found in Sideratos and Hatziaragyriou, (2007); Lei, et al. (2009); Liu, et al. (2010); Foley, et al. (2012); Jung and Broadwater,

(2014). The generalized classification presented here may be considered as widely accepted classification, which is –

- Numerical Weather Prediction (NWP) method and
- Persistence, Statistical and Artificial Neural Network (ANN) methods

The NWP are mesoscale models that are dominant methods applied for forecasting domains ranging from short-term to long-term intervals. NWP can predict smaller scale wind patterns (like on land or sea breeze) (Potter, et al. 2004). NWP uses current weather conditions as input to four dimensional (longitude, latitude, elevation and time) grid model of the area of interest and by applying conservation equations at various places, predict the changes in the winds. For large-scale weather pattern simulation and forecasting, NWP are most suited method. They are highly accurate method for long term forecasting. However such models performance is affected when they are employed for regional scale forecasting (Castellanos and James, 2009). NWP methods require high computational power and are time consuming. For smaller area applications, the NWP models cannot be assumed to be hydrostatic, require continuous remodeling, which is laborious and also is a costly process but the forecast by NWP are accurate (Negnevitsky and Potter, 2006).

Persistence method (PM) is referred to as benchmark method for wind speed forecasting (Lei, et al. 2009). This tool can be considered as supplementary to NWP and is widely used by meteorologists. The working principle of PM is based on the assumption that there exists high correlation between current and future wind speed. At times PM can be more effective than NWP (Negnevitsky and Potter, 2006; Castellanos and James, 2009; Foley, et al. 2012). Time series analysis is also an effective statistical modeling tool widely used for wind speed forecasting. There are two types of models depending on the number of inputs, Univariate model which uses only current and past wind speed data and Multivariate model which uses wind speed and variables that are correlated with wind speeds. Auto-Regressive Integrated Moving Average (ARIMA) method is most widely used method for short-term wind forecasting. Statistical methods use auto-recursive mathematical algorithm to calculate the difference between predicted and actual wind speed in the immediate past to tune the model parameters. Major limitation of these methods was that, the



changes in the model required attention of the expert for retuning and technique could be impractical to implement at times (Negnevitsky and Potter, 2006).

Artificial neural networks are low level computational network that perform well dealing with raw data. ANN is most widely used for wind forecast studies. It has input, output and hidden layers with lot of neurons in each of the layer (Lei, et al. 2009). The ANN method looks for patterns in the historical input and output data over a long period of time. This mechanism is the major difference between statistical and ANN methods.

Sfetsos, (2000) provided a detail account of various forecasting approaches using time series analysis and compared with neural network approaches. It was observed that Artificial Intelligence (AI) based models outperformed linear and non-linear time series models. The combination of Neural Logic Network and Linear Regression (NLN+LR) was superior model when compared to PM. More and Deo, (2003) employed Neural Networks (NN) to forecast multi time step wind speeds in Indian coastal locations. The NN was compared with ARIMA and the NN was found to capture the trend much better than ARIMA, hence NN was more accurate. Detailed analysis on the pros and cons of NWP, AI and statistical methods can be found in Potter, et al. (2004). Cao, et al. (2012) investigated the performance of Recurrent NN and ARIMA for short-term wind forecasts.

*Hybrid methods-* combines the superiority of different approaches and by overcoming the limitations of each provide a unique method. Combination can be a mix of NWP, statistical and or AI approaches. With the advancements in the hybrid methods and from the literature it is expected that these models can performer better than the conventional methods. Hunt and Nason, (2001) presented multiscale wavelet decomposition of time series data collected from meteorological stations and compared it to linear regression method to assess the accuracy of proposed hybrid method. The study inferred that the hybrid method performed significantly better than the regression method. Damousis, et al. (2004) using spatial correlation and genetic algorithm developed a method to obtain wind speed and power forecasts in a wind farm. The method performed better than the PM for forecasts ranging from 30 minutes to 2 hours lead-time. Siddiqi, et al. (2005) employed wavelets to study hourly

mean wind speed measured over land and presented the procedure for working with different wavelets and decomposition levels. Sideratos and Hatzigryriou, (2007) developed a hybrid method combining ANN and Fuzzy Logic (FL) techniques to predict wind power generated at a offshore farm and then compared was carried out with the actual wind farm power output. They found that the proposed hybrid method performed well due to RBF, FL and NWP predicted winds as input to the model for lead-time  $> 4$  hours in comparison to PM. Cadenas, et al. (2010) developed Single Exponential Smoothing (SES) method to perform short-term wind forecasts for onshore wind data. The method employed the moving average centered technique to identify the tendency and the trend-cycle in the wind speed time series data. The developed method was robust and produced accurate forecasts when compared to ANN. Liu, et al. (2010) proposed a new method called, Improvised Time Series Method (ITSM), which was combination of wavelet and classical time series analysis to obtain short-term onshore wind forecasts. Forecasts up to lead-time of 10 hours was carried out. They found that the proposed method was suitable for both wind speed and power forecasts. The study concluded that the proposed method was robust and better performer than ANN method.

ANFIS is a hybrid technique that combines the low computational skill of neural network and high level reasoning by applying FL (if-then rules). The outputs are drawn based on the rules and known facts leading to reasonable decisions (Negnevitsky and Potter, 2006; Catellanos and James, 2009). Mohandes, et al. (2011) applied ANFIS to estimate and predict wind speeds at higher heights from lower height ground based measurements. The study established ANFIS as an effective tool for extrapolation of wind to higher height. Yao, et al. (2013) carried out a comparative study of combination of wavelet, NN and ANN. They proposed a hybrid method that consisted of the individual models and on comparison with PM and Back Propagation Neural Network (BPNN) they found that the proposed method outperformed the PM and BPNN methods for wind speed forecasting. However the hybrid method required high computation time, which was the only limitation.

Genetic Programming (GP) technique was applied for real-time prediction of offshore wind, using buoy observations by Charhate, et al. (2009). The developed method was

compared with PM and ANN. It was concluded that GP produced attractive results and performance was satisfactory. Zeng and Qiao, (2012) worked with wavelet and support vector machine (SVM) to develop an effective short-term wind power prediction tool. The study highlighted the importance of knowledge of power at a given point to achieve grid stability and integration. The developed hybrid model was superior in performance to ANN, Radial Basis Function (RBF)-SVM and PM.

From the previous works it can be inferred that, the hybrid methods have proven to perform well, by combining the advantages of consisting methods. There is a need to investigate the performance of ANFIS and wavelet combined with ANFIS (WT+ANFIS) for offshore wind speed forecasting, such a study has not been carried out as per authors knowledge. It is understood that WRA and accurate wind speed forecasting tool are necessary for establishing the potential available at a offshore site and installing the confidence in the government to take up development of offshore wind energy.

### **1.5. RELATIVE HUMIDITY AND INFLUENCE ON WIND SPEED**

Humidity is the presence of water vapor in air. It affects many properties of air. Water vapor is key agent in both weather and climate. Humidity is expressed as Relative Humidity (RH) in %. The relative aspect is effectively relative to temperature (Stephanie Bell, 2012). The air temperature variation brings about a change in water evaporation and air saturation, leading to the change in air humidity. Furthermore, the air temperature differences between different locations will also cause air pressure differences, which in turn would produce air movement thereby, wind. This variation in humidity and wind speed and direction affects rainfall. Thus, all atmospheric variables on the earth are more or less affected by each other (Valsson and Bharat, 2011).

The process of water vapor removal depends mainly on the wind and air turbulence, which transfers large quantities of air over the evaporating surface, thus responsible for movement of air (Allen, et al. 1998). In the event of evaporation over the water

surface, there is absorption of heat energy from surrounding air. The quantification of water vapor content is therefore some measurement of the latent heat available to the air, which, if released, can strongly affect the atmospheric stability to vertical motions (Ramis, et al. 2005). Air-Sea exchange of momentum, heat and moisture over the oceanic surface plays an important role in understanding several processes related with atmospheric circulations. Subrahmanyam and Ramachandran, (2003) estimated air-sea exchange parameters for large area in Indian Ocean. The study provided better understanding of the wind speed dependence of air-sea interaction parameters, such as roughness lengths for wind ( $z_0$ ), temperature ( $z_{0t}$ ) and humidity ( $z_{0q}$ ), which play a key role in the determination of the air-sea exchange coefficients and interface fluxes across the tropical oceans.

Barthelmie, et al. (2010) showed the effect of humidity fluxes on wind speed profiles was found to be important in stable conditions. It was observed that averaged predicted winds using Monin-Obukhov theory at 150 m from 10 m were 4% higher when humidity fluxes were not considered. Verburg and Antenucci, (2010) examined the effect of atmospheric stability on the heat fluxes on seasonal time scales at Lake Tanganyika, East Africa. It was found that because of higher water surface temperature than air temperature, there was unstable atmosphere condition, which is generally found in tropical climate. Further, low humidity further enhanced the frequency of unstable conditions and enhanced the exchange of heat and vapor from the lake to the atmosphere. Kumar, et al. (2009) demonstrated that the momentum and energy exchange at air-sea interface through wind stress is very important for air-sea interaction studies, ocean modeling, and climate studies. The accurate representation of wind stress, in terms of drag coefficient, is a key factor in estimating the momentum transfer at the interface. Humidity observations are generally in situ, satellite based and reanalysis datasets. The confidence in reanalysis-based estimates of specific humidity over the ocean was less than over land. However, the in situ based humidity analyses have suffered in recent years with a reduction in observation numbers and lack of information on observation methods and heights. Consequently near surface humidity remains relatively poorly known over the oceans (Kent, et al. 2014).

The influence of atmospheric temperature, RH and wind speed has been focused on weather and climate analysis or forecasting. Such studies are conducted at global scale, along with monitoring the atmospheric circulation over oceans. These studies are generally based on physical models and complex computations. However, there is need for investigating the influence of RH on offshore winds in non-physical methods, which can be applied for regional scale wind speed and direction analysis. The focus of investigation should be directed towards performance evaluation of hybrid methods, to be applied for short-term wind speed forecasting.

## **1.6. SUMMARY**

The literature survey carried out under each section presented earlier helped in gathering vital information on the existing and current research on offshore wind resource assessment and forecasting techniques. The major driving forces for research in the domain of offshore wind energy are the benefits of the vast oceans and high potential winds. Further, the need for reducing dependency on the non-renewable sources of energy and thus reducing the carbon footprint of country in reaching energy security. Energy resources are assessed based on the in situ and or remotely sensed data. It was established that buoy observations are most accurate measurements and economical than other sources of in situ instrument setup. However, immense focus has been on application of space-born ocean surface observations due to its global coverage, which addresses the limitation associated with the in situ observations. Satellite data also have limitations, but they are subsided by the advantages like - global coverage, low/free of cost data and real-time data. A detail account of satellite missions by various countries has been presented, which emphasizes the importance of reliable and continuous data on offshore winds. Scatterometer and SAR are the most widely used sensors for ocean surface wind observations. The advantages and disadvantages of these sensors were discussed and it can be inferred that combination of these two sensor data can lead to higher resolution data (but such data can be site specific).

The satellite data requires validation against in situ observations before they are assimilated in resource assessment studies. Generally, buoy observations are used for validation of satellite data. The process involves estimation of ENW, since buoy observations are around 3 to 5 m above sea level and satellite data are referenced at 10 m. There are various approaches available for computing ENW where LKB method is most widely adopted. However, Log method is normally adopted due to the assumption that wind profile varies logarithmically when extrapolated and also because of ease of computation. Hence, there is a need to investigate the performance of these methods to estimate ENW and establish best method for validation of scatterometer data.

One of the major limitation observed in the offshore wind resource assessment studies was based on the assumption that a single buoy (nearer to the coast) represents the wind regime over entire area and the power potential estimate was conducted on this basis. Scatterometer winds based WRA studies were small in number (globally) and existing studies provided incomplete information on the necessities for development of offshore wind farm. While, WRA studies are site specific in nature, it is necessary to address these limitations with satellite-based data and a methodology, a framework to assess wind energy resource that can be applied to other sites.

Along with the identification of potential sites, it is very important to have knowledge of wind characteristics at a particular site. WRA and information of winds in future time steps can form a comprehensive assessment of wind resource that can be quantized. Thus, forecasting of wind speed is a significant task that will assist in development of wind farms. The existing literature provided detail information of the tools and techniques that have been developed for forecasting winds over different time horizons. Short-term forecasting domain is of significant importance in operation of wind farm and scheduling the power generation. Statistical and Artificial Intelligence methods are meticulously adopted for forecasting wind speeds. Combination of multiple approaches known as *hybrid methods* has been recently applied for obtaining short-term forecast. The forecast accuracy of hybrid methods was found to be better than other approaches. However, from the literature it was observed that most of the developed methods are applicable to onshore conditions.

The combination of time series analysis with fuzzy-neural network and with wavelet transformation combined with other approaches were found to be competent hybrid techniques that can be applied for offshore wind speed forecasts. An investigation of these approaches on different locations and multiple forecast time steps need to be carried out to enhance forecasting accuracy.

The mechanisms involved in the generation and movement of winds are interdependent in nature. Based on the literature, it was also found that in tropical regions, relative humidity (RH) can be a major influencing factor on the circulation of winds. There are no specific studies that discussed the effect of RH on short-term offshore wind speed forecasting techniques. Hence, the influence of RH on wind speed may be investigated on performance of short-term forecasting methods at sites, where there may be limited or unavailability of RH observations.

## **1.7. PROBLEM FORMULATION**

The wind as a energy resource is observed to be associated with various limitations like- intermittency, huge cost of instrument installations and maintenance. In addition to multiple ocean water users and unfavorable offshore weather conditions, they should be systematically and carefully addressed. Such an attempt ought to incorporate techniques to ensure reliable and identification of potential sites for sustainable energy development based on locally available resources. To ensure the economically best sites for installations of in situ instruments and ecologically sound wind energy growth, it is therefore necessary to conduct a preliminary regional-scale assessment. Along with assessment of resources, for development of offshore wind farms, the knowledge of availability of winds in future time steps plays vital role.

Accurate forecasts of wind speeds would help in better integration of wind energy in to grids, better planning. Hence, there is need for an efficient tool for forecasting offshore winds. Hybrid techniques have demonstrated the capability to handle the volatile nature of wind speeds better than other methods and higher performance in the domain of short-term forecasting can be expected. There is a need for investigation of application of hybrid techniques at multiple locations and influence of certain atmospheric parameter over the performance of hybrid techniques to establish it as complementary tool for short-term forecasting of offshore winds.

Furthermore, the application of regional planning instruments on energy issues would lead to a highly sustainable energy policy and to various benefits for government authorities as well as for individual developers. Thus, the focus of the present work is towards developing hybrid technique for short-term forecasts of offshore winds in the Arabian Sea and regional scale assessment of wind power potential in combination with GIS methodology, to quantize the resource available for the Karnataka state, India. The aim of work is towards emphasizing on the enormous energy potential to the authorities, to elaborate and develop energy plans that can regularize offshore wind-power based energy projects.



## **1.8. OBJECTIVES OF THE STUDY**

Based on the literature summary, the objectives of the present research have been designed to develop complementary short-term forecasting tool based on buoy observations in the Arabian Sea and perform comprehensive analysis of offshore power generation capacity using satellite data. To achieve the objectives, following tasks have been proposed,

- Short-term forecasts of offshore winds by ANFIS and Wavelet combined ANFIS techniques.
- To investigate the influence of humidity on the developed tools for the offshore wind speed forecasting based on in-situ Relative Humidity observations.
- Satellite-based regional scale WRA and to develop power potential maps.

## **1.9. ORGANIZATION OF THESIS**

The information congregated from the work is presented in four chapters followed by list of references.

Chapter 1 provides background of atmospheric circulation, factors responsible for wind generation, offshore wind observations with significance towards the evolution of satellite-based measurement of ocean surface winds. Established approaches for obtaining ENW necessary for validation of satellite winds are introduced. The application of various satellite data, for offshore WRA and assessment of power potential throughout globe is presented. Furthermore, the importance of short-term wind speed forecasting in offshore scenario for intended applications is introduced. Influence of RH (a atmospheric parameter) on the offshore winds is presented with focus on understanding its impact on forecasting model.

Also, in the chapter supporting literature is presented that helped in understanding the advantages and limitations of current methods that are applied for

aforementioned applications. The objectives are thus designed to develop new approach to address the limitations and enhance existing knowledge.

Methodology and Data that was developed and collected are described in Chapter 2. Detail information on the characteristics of Data are presented in this chapters.

Chapter 3 discusses the results obtained for short-term forecast of offshore winds, influence of RH on the model performance, efficient method for estimation of ENW and satellite-based regional scale WRA assisted by GIS based approach for better understanding of resources.

Finally, conclusions drawn from the study are presented in Chapter 4 along with limitations of study and future scope of work.

## CHAPTER 2

### DATA AND METHODOLOGY

#### 2.0. GENERAL

The open waters of seas and oceans are a huge resource of winds that can be source for clean and renewable energy generation. Measurement of offshore wind characteristics and atmospheric parameters can be challenging task when compared with onshore measurement. Buoys, ships, masts are the major source of in situ observations. Satellite based ocean surface wind observation have gained importance due to their global coverage capacity. There are limitations associated with each type of observation technique. Continuous advancements in techniques have been focused to address the limitations and enhance the resource assessment accuracy. On the other hand to quantize the energy potential of offshore winds, multi-platform measurements are required to be emphasized.

#### 2.1. BUOY OBSERVATIONS

Buoys are the major source for in situ meteorological observations in the oceans. The buoy data are relatively accurate data in comparison to other sources of in situ observations. Also, buoy data have better temporal resolutions. The network of moored buoys deployed by Indian National Center for Ocean Information Services (INCOIS), Hyderabad in the Arabian Sea can be seen in Fig. 2.1. Moored buoys are known to function from 20 m to full ocean depth, and meteorological observations are generally recorded at 3 m height. The buoys selected for the study are AD07 and CB02. All the met-ocean parameters, their sensors, resolutions, accuracies and ranges measured by moored buoys are presented in table 2.1. The parameters used in the study are Atmospheric Pressure (AP), Atmospheric Temperature (AT), Relative Humidity (RH), Sea Surface Temperature, Wind speed (WS) and Wind Direction (WD). Observations for the period of about one year have been considered for the study. The data at AD07 are averaged three hourly wind speeds and at CB02 the data are averaged hourly. The selection of buoys was based on the availability of continuous data for the duration of one year, different temporal resolutions and

geographical location. However there were few missing observations in the dataset (number of observations per day, at AD07 < 5% and at CB02 < 10%) and simple averaging of preceding and succeeding wind speeds were performed to obtain the missing data.

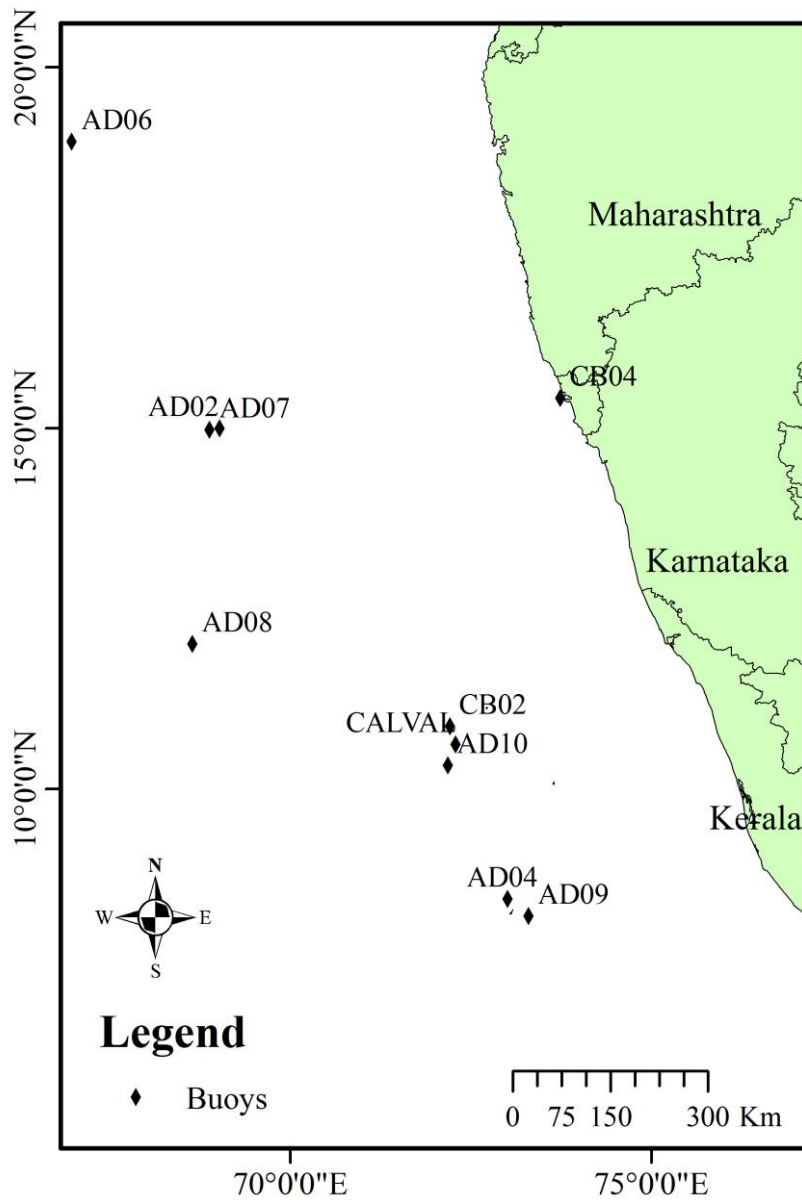


Fig. 2.1: Buoys in the Arabian Sea deployed by INCOIS

Table 2.1: Sensors used in moored buoy system (Venkatesan, et al. 2013)

Parameter	Sensor type	Resolution	Accuracy	Range
Wind speed	Cup anemometer	0.1 m s <sup>-1</sup>	± 2%	0–35 m s <sup>-1</sup>
Wind direction	Vane + fluxgate compass	0.1°	1.5– 4°	0-359
Air temperature	Pt/100 RTD	0.0015 °C	± 0.3 °C	–30–70 °C
Relative humidity	Capacitance	0.47	± 1%	0–100% RH
Air pressure	Pressure transducer	0.01 hPa	± 0.15 hPa	500–1100 hPa
Rainfall	Capacitance	0.058	± 1 mm	0–50 mm
Downwelling long- wave radiation	Pyrgeometer	1.27 W m <sup>-2</sup>	5%	0–700 W m <sup>-2</sup>
Downwelling short-wave radiation	Pyranometer	0.488 W m <sup>-2</sup>	3%	0–2800 W m <sup>-2</sup>
Water temperature	Thermistor	T: 0.0001 °C	0.002 °C	–5–35 °C
Conductivity	Conductivity cell	C: 0.0001 mS cm <sup>-1</sup>	0.003 mS cm <sup>-1</sup>	0–70 mS cm <sup>-1</sup>
Water pressure	Strain gauge	P: 0.002%	0.1%	0–100 bar
Directional wave spectra	Accelerometer, angular rate sensor, magnetometer	Pitch and roll: < 0.001°	Heave: 5 cm pitch and roll: 0.05° Heading: 1.2°	Heave: ± 50 m Heading: ± 180°
Ocean current profile	Acoustic Doppler current profiler	Velocity: 0.1 cm s <sup>-1</sup> Dir: 0.01°	Velocity: ± 5 mm s <sup>-1</sup> Dir: ± 2°	0–256 cm s <sup>-1</sup>
Single point	Doppler volume sampler	Velocity: 0.1 cm s <sup>-1</sup> Dir: 0.01°	Velocity: 1% Dir: ± 2°	0–600 cm s <sup>-1</sup>

## 2.2. SHIP BASED OBSERVATION

Major sources of in situ offshore meteorological data are buoys and ships. The advantages of buoy meteorological observations are the higher temporal resolution and continuous real time data transmissions. However, ship based observations were the only source of ocean observations prior to buoys.

IRAWS data was obtained from Indian National Centre for Ocean Information System (INCOIS). The program was initiated in 2009 under Ocean Observation Information System (OOIS). AWS sensors are mounted on the ships at height of 13 m above sea level. Meteorological parameters that are measured include- atmospheric pressure, atmospheric temperature, relative humidity, wind speed, wind direction, sea surface temperature, long wave radiation and short wave radiation. There are 9 research vessels operating in the Arabian Sea, a graphical representation of ships can be seen at the INCOIS website- <http://www.incois.gov.in/portal/datainfo/aws.jsp>. The data is transmitted in real time to INCOIS station through Indian geosynchronous satellites INSAT 3A and 3C. The wind data provided by INCOIS are average hourly observations. The major advantage of IRAWS data over conventional ship based meteorological observation are-

- High accuracy in surface variable measurements.
- Real time transmission and high temporal resolution.
- Greater spatial coverage than Voluntary Observation Fleet (VOF) and buoys.

The VOF is an understanding between ships operating in oceans and Indian Meteorological Department (IMD). The logged observations obtained from these ships are then provided to IMD. IMD is eminent organization in India responsible for meteorological data collection, dissemination and data analysis for various applications. Limitations of this data are low temporal resolution, human induced errors and data are passed to IMD in bulletin format when ships arrive at ports, which makes the data less accurate than the real time transmitted data. Also, obtaining ship based meteorological observations can be expensive. Fig. 2.2 shows the point of observations of IRAWS data during cruise in the study area. The data used in present study is a composite of all the ships operating in the Arabian Sea during 2011 to 2013. The sonic wind monitor used in IRAWS wind observations operates in range of 0-60

$\text{m s}^{-1}$ , has a resolution of  $0.01 \text{ m s}^{-1}$  with accuracy of  $\pm 2\%$ . The calibration of the sensors of IRAWS was carried using automated weather station (AWS) installed by the Indian Institute of Science (IISc), Bangalore on the same masts (1 m below the IRAWS sensors) onboard the ship. Wind speed and direction measured by both AWS were in a good agreement. Further the meteorological parameters obtained from IRAWS were validated against two models (Year of Tropical Convention (YOTC) data from ECMWF and NCMRWF model data). It was observed that bias in wind speeds was less than  $1 \text{ m s}^{-1}$  and RMSE for wind speeds was around  $3 \text{ m s}^{-1}$ , this high RMSE value was due to smaller number of ship observations when validation was carried out (Harikumar, et al. 2013). Perhaps the uniqueness and larger data set are valuable for validating model based surface parameter estimations (like the scatterometer winds, numerical weather prediction, etc.)

### **2.3. OCEANSAT-2 SCATTEROMETER OBSERVATIONS**

Advancements in satellite-based measurements of wind vector and retrieval techniques have resulted in improved observation of global ocean surface winds. Scatterometer sensor's global ocean data are most widely used among other sensors, due to wide swath of 1800 km, thus providing a greater field of view and wind vector (speed and direction) measurements can also be retrieved. Scatterometer is mounted onboard polar orbiting satellite, at 700–850 km altitude and is able to scan the globe in 2 days. The main limitation of satellite data is the frequency of data measurements. The Oceansat-2 satellite was launched by ISRO, India, in 2009, with a ku-band pencil beam scatterometer (OSCAT). The resolution of global wind vector data provided by the National Remote Sensing Centre (NRSC) is  $50 \times 50 \text{ km}$  and  $25 \times 25 \text{ km}$  (since July 2013). The Oceansat-2 has a revisit time of 2 days. The OSCAT mission goals were to provide wind data between  $4$  and  $24 \text{ m s}^{-1}$ , with an accuracy of  $\pm 2 \text{ m s}^{-1}$  and directional accuracy of  $\pm 20^\circ$ . The near-surface winds measured by scatterometer are referenced to a height of 10 m above sea level. The data can be downloaded from the NRSC website ([www.nrsc.gov.in](http://www.nrsc.gov.in)). The OSCAT was reported not functioning due to irreparable failure in its traveling wave tube amplifier (TWTA) toward the end of February 2014. It was functional for around 4.5 years as against its designed life of 5

years (Podaac, 2014). Following the loss of OSCAT, only ASCAT data from MetOp-A and -B of EUMETSAT are currently available in near real-time. Since both MetOp satellites are on the same orbit, there is now a lack of scatterometer data on a well separated orbital plane. In Fig. 2.3, a schematic representation of scatterometer missions launched, working and upcoming satellite launches, developed and presented by Coordination Group for Meteorological Satellites (CGMS, 2014).

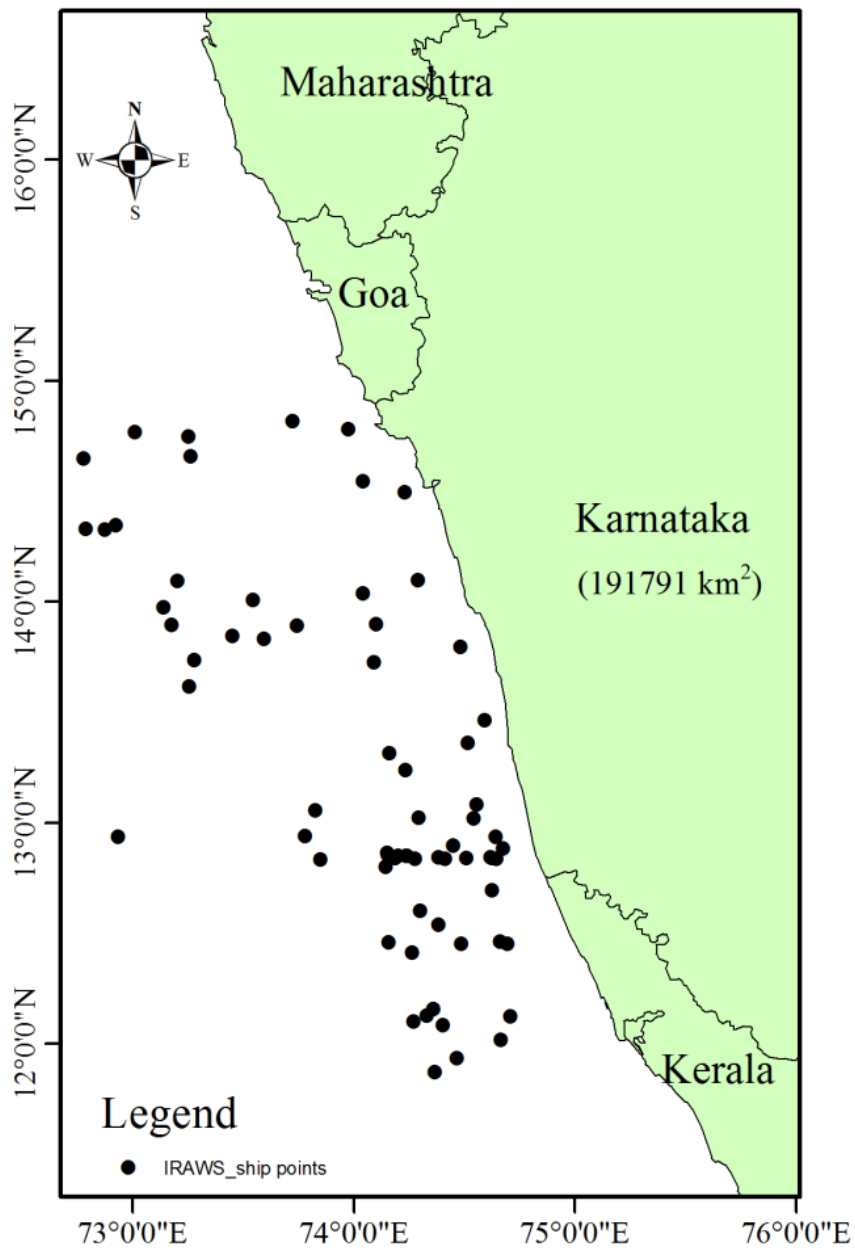


Fig. 2.2: IRAWS observations along Karnataka coast



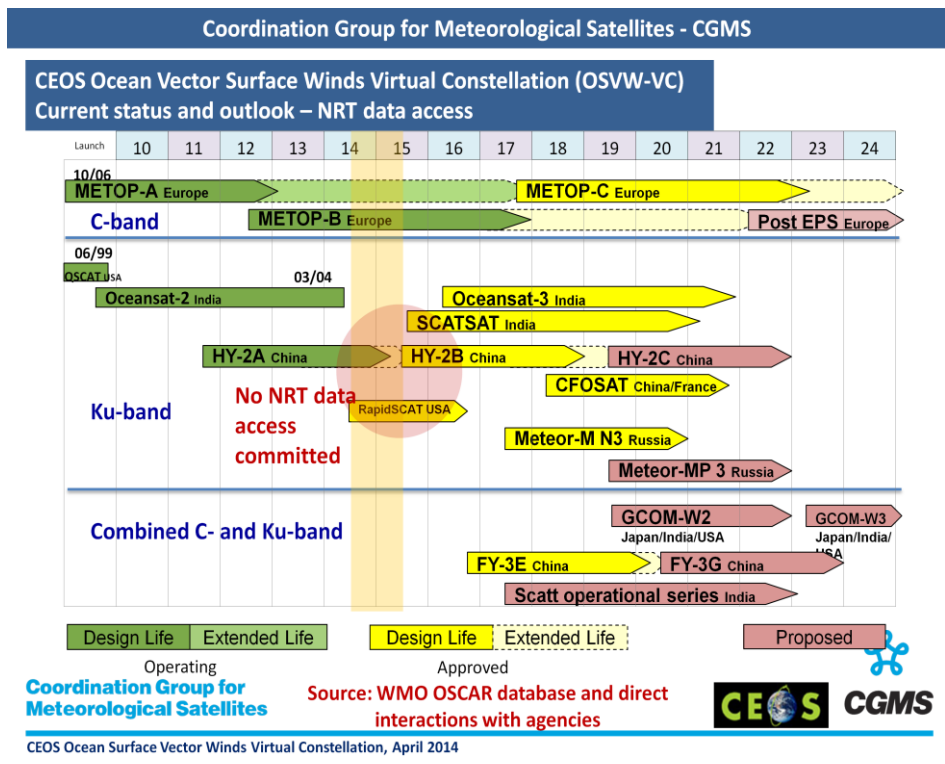


Fig. 2.3: Satellite missions Coordination Group for Meteorological Satellites (CGMS), CEOS Ocean Surface Vector Winds Virtual Constellation, April 2014

Limitations of Dataset

During the course of study the data for all the buoys in the west coast of India was collected along with Oceansat-2 scatterometer and IRAWS ship data. The availability of continuous time series buoy data for longer duration was itself a significant limitation. Hence, the dataset was constructed with minimum 1-year observations. The developed buoy dataset was to be employed to obtain short-term forecasts, which will be discussed in future sections of thesis. With the updated ship data being available after vessels traversed in the area of interest, the number of observation points during the year 2011-13 was of small quantity. However, for the validation of satellite data, it was a quality dataset compared to buoy data. Scatterometer data for all the months during year 2011-12 was available and the same was adopted for wind resource mapping and estimation, which are discussed in future sections of the thesis.

## 2.4. METHODS ADOPTED FOR THE STUDY

### 2.4.1. PERSISTENCE METHOD

Persistence method is the simplest method to obtain wind forecasts. It is referred to as benchmark method (Sfetsos, 2002) for hourly wind speed forecasting. The fundamental principle in this method is that there exists high correlation between current and future wind speed (Castellanos and James, 2009). PM is a robust method and very effective tool for forecasting in the range of minutes to hours. However the accuracy of this method decreases with increase in the lead-time. In this study PM method is considered as base method to compare the performances of other forecasting methods.

PM forecast can be expressed as - 
$$WS_{(t+k)} = WS_t \quad (2.1)$$

where,  $WS_{(t+k)}$  : is the forecasted wind speed ( $m s^{-1}$ ); 'k' : is the lead-time step and  $WS_t$  : is the wind speed ( $m s^{-1}$ ) at time 't'

### 2.4.2. ADAPTIVE NEURO-FUZZY INFERENCE SYSTEM (ANFIS)

ANFIS is a hybrid technique combining Artificial Neural Networks (ANN) and Fuzzy Inference System (FIS). ANN using historical data learns and mimics the system whereas FIS helps in human like reasoning through linguistic variables (like small, medium and large). ANFIS method brings out the advantages of both the approaches. Thus ANFIS output is drawn based on if-then rules and input time series dataset. ANFIS is capable of handling non-stationary and performs well when it is difficult to model system accurately. The architecture of ANFIS method can be seen in Fig. 2.4. The method can be explained in five layers and each layer carries out specific task.

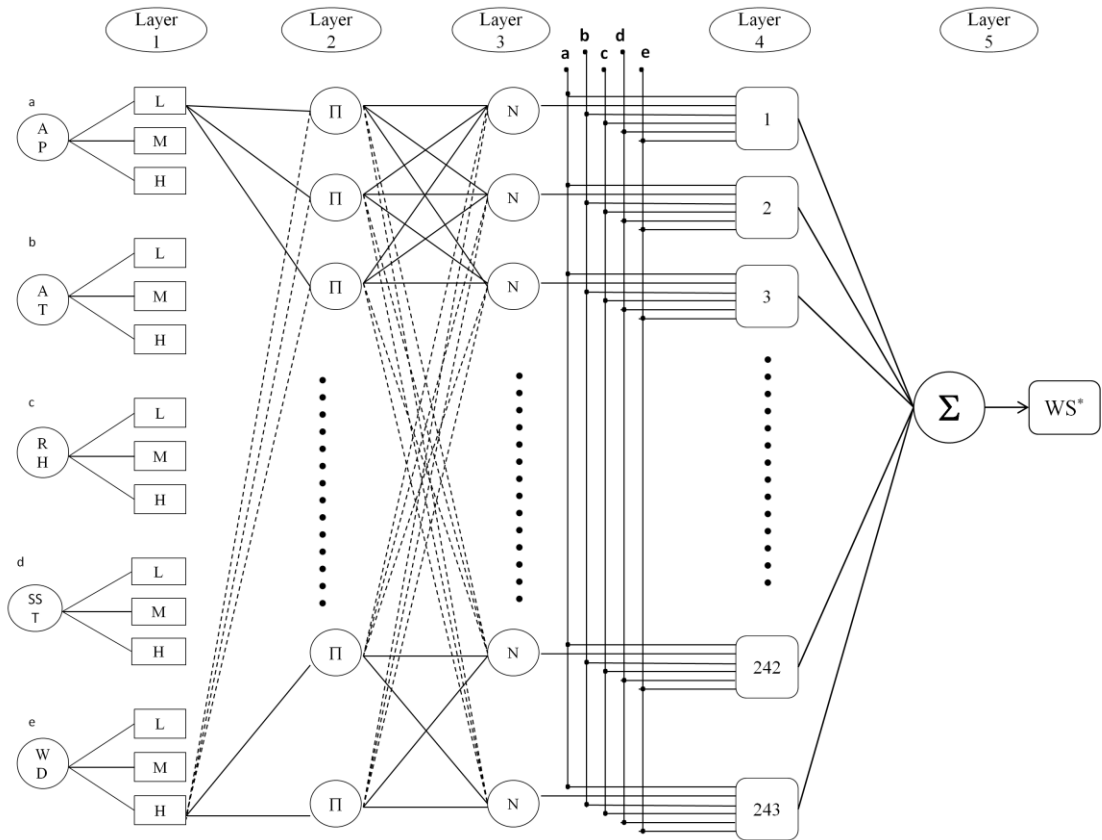


Fig. 2.4: Architecture of ANFIS for present study

In layer 1 the inputs are fuzzified, using the membership functions (MF): low (L), medium (M) and high (H) and Gaussian MF type. Layer 2 is where rules are formed, the number of rules depend on number of the MF's (m) and number of inputs (n) as -  $m^n$ . In the figure only a set of rules and connections are shown to provide a clear picture of the processes. Layer 3 is where the normalization of firing strengths occurs, which is calculated as the ratio of firing strength of a given rule to the sum of firing strength of all rules (Haque, et al. 2012). Defuzzification is carried out in layer 4, which receives inputs from each node from layer 3 and also is connected to all inputs. Layer 5 is the last step before the output is obtained, where in the summation of all the outputs of layer 4 is performed. Layer 5 gives the model output- wind speed ( $WS^*$ ), which can be estimated or forecasted wind speed with different lead times.

### 2.4.3. COMBINATION OF WAVELET TRANSFORM AND ANFIS (WT+ANFIS)

Wavelet transform is similar to Fourier transform as the signal is divided in to subclasses that help in smoothening of the input signal. The subclasses generated by the wavelet transform are called “wavelets”, which are scaled and shifted versions of the “mother wavelet” (Stecki and Altmann, 2000). Appropriate mother wavelet has to be selected which can follow or imitate the input signal (time series). Further, the decomposition of wavelets at different levels provides us with a signal whose mean is around zero. These synthesized signals are free of non-stationary property that is associated with the target signal, thus aiding for better analysis. The present study uses Debauchies (db) wavelet (mother wavelet) series from 1 to 10 on the observed wind speed time series data, nomenclature as db1 to db10. The decomposition levels are set to obtain the synthesized signal for both buoy locations. The sub classes are inputted to the ANFIS. The process of wavelet decomposition can be considered similar to a pre-processing of dataset in order to remove the noise in the dataset. Fig. 2.5 represents the architecture of one dimension (1D) wavelet transform process. The input signal is passed through high pass filter (HPF) and low pass filter (LPF). The noise or sharp trends in the signals are stored in the HPF as coefficients and the smoothened signal in LPF as approximations. On decomposition, the same procedure is repeated and the original signal can be obtained by adding the approximation at the level of decomposition and all the previous coefficients. Considering the input signal to be ‘s’, approximation to be ‘a’ and coefficients to be ‘d’, then after level 4 decomposition the signal will be synthesized as-  $a_4, d_1, d_2, d_3$  and  $d_4$ . The original signal can be obtained by simply adding all the coefficients and approximation as:  $s = a_4 + d_4 + d_3 + d_2 + d_1$ .

In the present study, the approximations generated after each level of decomposition were considered as subclasses and were used for forecasting wind speeds.

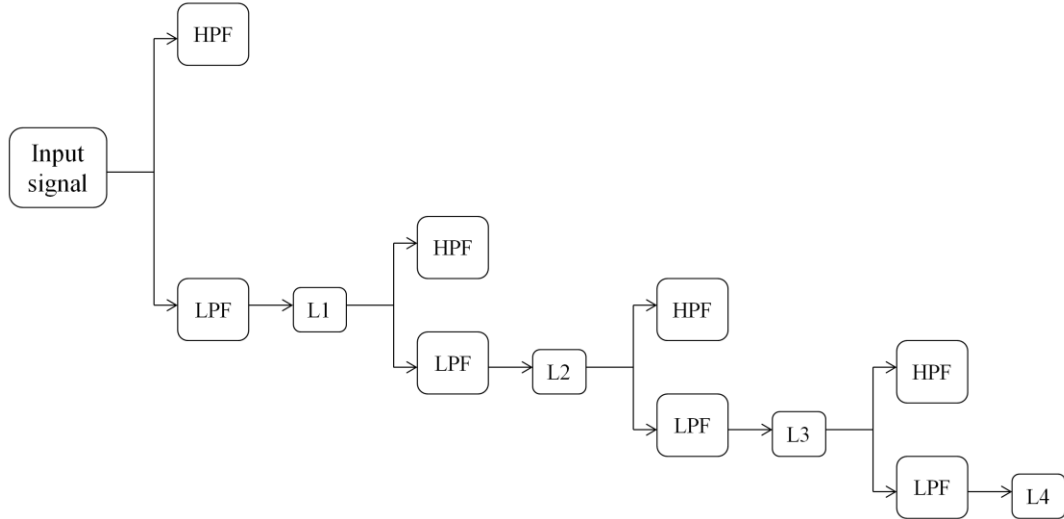


Fig. 2.5: Architecture of 1D wavelet transform

#### 2.4.4. POWER LAW METHOD

In the relationship between wind speeds and height of measurement,  $\alpha$  is the exponent, which is a function of atmospheric stability and underlying surface characteristics. The power law wind profile is accurate and useful in engineering applications. Range of values for  $\alpha$  for different terrain types are well established and are presented in table 2.2.

Power law can be expressed as:

$$\frac{U_1}{U_2} = \left( \frac{z_2}{z_1} \right)^\alpha \quad (2.2)$$

where,  $U_1$  is the wind speed at height  $z_1$ ,  $U_2$  is the wind speed at height  $z_2$ ,  $\alpha$  is the friction coefficient (exponent),  $z_1$  is the height at which wind speed data are available, and  $z_2$  is the height at which wind speed is to be determined.

Table 2.2: Friction Coefficient ( $\alpha$ ) of different terrain types (Patel, 2012)

Terrain type	Friction coefficient ( $\alpha$ )
Lake, ocean, and smooth, hard ground	0.10
Foot-high grass on level ground	0.15
Tall crops, hedges, and shrubs	0.20
Wooded country with many trees	0.25
Small town with some trees and shrubs	0.30
City area with tall buildings	0.40

#### 2.4.5. LOGARITHMIC (log) METHOD

Wind speed increases approximately logarithmically with height, the wind speed at the required height  $z$  is given as follows-

$$U_z = U_{\text{ref}} \left( \ln \frac{z}{z_o} / \ln \frac{z_{\text{ref}}}{z_o} \right) \quad (2.3)$$

where,  $U_z$  is the wind speed at height  $z$ ,  $U_{\text{ref}}$  is the wind speed at the known height,  $z_{\text{ref}}$  is the known height,  $z_o$  is the roughness length, and  $z$  is the height at which wind speed  $U_z$  is to be determined. The extrapolation height ( $z$ ) of 10 m, reference height ( $z_{\text{ref}}$ ) of 3 m, and the roughness length of about  $1.52 \times 10^{-4}$  m for open seas were adopted in the estimation of  $U_z$ .

The logarithmic approach does not consider the effect of changes in atmospheric stability, thus assuming a homogeneous atmosphere, which may lead to error (Singh, et al. 2013).

#### 2.4.6. LIU-KATSAROS-BUSINGER (LKB) METHOD

The assumption that the surface fluxes are uniform may not always hold true for the surface layer. Fluxes are affected by the atmospheric stability, the variation from a log-profile depends largely on atmospheric stability. Atmospheric stability refers to

the stratification of the air near the surface. A stable stratification will reduce mixing (and surface stress), and an unstable stratification will increase mixing. This in turn is influenced by other meteorological parameters, and thus a more general approach towards finding wind speed dependence on height is now given. This method is based on Monin–Obukhov similarity theory and is expressed as-

$$U_z = U_s + \frac{U_*}{\kappa} \left[ \left( \ln \frac{z}{z_o} - \psi \left( \frac{z}{L} \right) \right) \right] \quad (2.4)$$

where,  $U_z$  is the wind speed at height  $z$ ,  $z$  is the extrapolation height,  $U_s$  is the surface wind speed,  $\psi \left( \frac{z}{L} \right)$  is the atmospheric stability,  $U_*$  is the friction velocity ( $\text{m s}^{-1}$ ),  $\kappa$  is the von Kármán constant,  $z_o$  is the ocean roughness length, and  $L$  is Monin–Obukhov length. Under neutral atmospheric conditions, atmospheric stability is considered to be zero (i.e.  $\psi \left( \frac{z}{L} \right) = 0$ ). The following equation can be written:

$$U_z = U_s + \frac{U_*}{\kappa} \left[ \left( \ln \frac{z}{z_o} \right) \right] \quad (2.5)$$

$z_o$  is the ocean roughness length, calculated by the Charnock relationship:

$$z_o = z_{\text{ch}} \frac{U_*^2}{g} \quad (2.6)$$

where,  $z_{\text{ch}}$  is the Charnock constant and  $g$  is the acceleration due to gravity. In equation (2.5), the value adopted for extrapolation height ( $z$ ) is 10 m, von Kármán constant is 0.41, and with the magnitude of  $U_s$  being very small, this can be neglected. In equation (2.6), the value of the Charnock constant adopted is 0.0185.

#### 2.4.7. WIND POWER DENSITY (WPD)

WPD represents the quantity of energy present in the wind. WPD is calculated at hub height of turbine. WPD is expressed as shown in equation (2.7) (Pimenta, et al. 2008) and unit of WPD is  $\text{W m}^{-2}$ .

$$P = \frac{1}{2} \rho V^3 \quad (2.7)$$

where,  $\rho$  is the air density (constant,  $\rho = 1.225 \text{ kg m}^{-3}$ ).  $V$  = wind speed ( $\text{m s}^{-1}$ ) at 90 m (hub height).

Theoretical Power ( $P_t$ ) is obtained by multiplying WPD with known swept area ( $A$ ) and power coefficient ( $C_p$ ). It can be expressed as-  $P_t = (P \times A \times C_p)$

$P_t$  depends on turbine characteristics, whereas WPD is independent of turbine characteristics. Fig. 2.6 represents power curve for Siemens SWT 2.3 (blue), Vestas V90 (brown) and REpower 5 MW (black) and respective theoretical power ( $P_t$ ).  $C_p = 59.3\%$  is the Betz limit or maximum theoretical efficiency of a turbine rotor. All three turbines have hub height of 90 m (Staffell, 2012). The capacity of turbines considered for installation at site may depend on many economical factors, which should be explored by the institutionalized agencies.

#### 2.4.8. CAPACITANCE FACTOR (CF)

Capacitance Factor can be defined as an indicator of how much electricity a generator actually produces relative to the maximum that it could produce at continuous full power of operation during the same period. The calculation of CF in Sheridan, et al. (2012) was based on the averaged hourly wind speeds and corresponding hourly power values. Therefore this hourly power represented the kWh of energy produced during that hour. The equation to estimate CF is expressed as follows-

$$CF = \left( \frac{\text{Annual Energy Production (kWh / year)}}{\text{Rated Power (kW)} \times 8760 \text{ (h / year)}} \right) \quad (2.8)$$

The work in section (2.8) uses scatterometer data, which is assumed to represent averaged daily winds; a modified approach was adopted to calculate CF. The OSCAT data was averaged over a two-year period (2011 and 2012) for study area. The averaged wind speed data was then inputted in to ArcGIS 9.3 and Kriging spatial interpolation was performed. Then from the interpolated winds, an average value for the study area was calculated. From the power curve for REpower 5 MW,



corresponding to average wind speed output power is obtained. Further the CF can be estimated after modifying the equation (2.8) as follows-

$$CF = \left( \frac{\text{Annual Energy Production (kW)}}{\text{Rated Power (kW)}} \right) \quad (2.9)$$

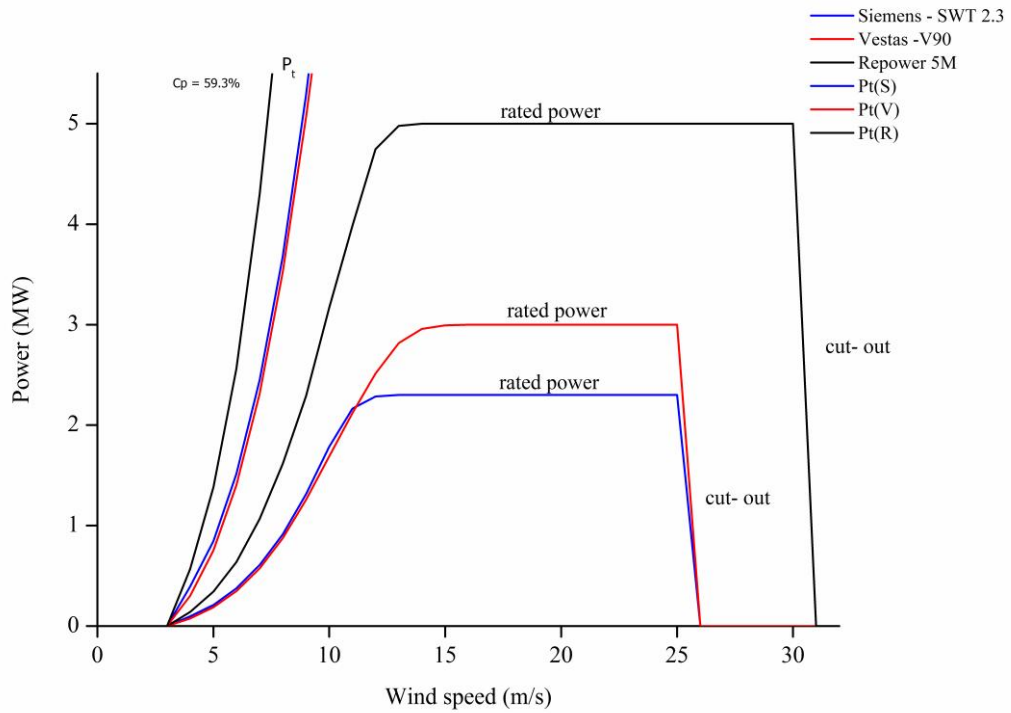


Fig. 2.6: Turbine power curves for Siemens- SWT 2.3 (blue), Vestas-V90 (brown), REpower 5M (black). Dotted lines represent max theoretical  $P_t$  (Betz limit,  $C_p = 59.3\%$ ) for three-turbine manufacturers

## 2.5. SHORT-TERM OFFSHORE WIND SPEED FORECASTING USING ANFIS AND RELATIVE HUMIDITY INFLUENCE ON THE ACCURACY OF ANFIS

Offshore winds are irregular and non-stationary in nature. To mimic the stochastic nature of winds, a hybrid technique- ANFIS was employed. The procedure so developed; to assess the capability of ANFIS to perform short-term forecasting of offshore wind speed can be seen in Fig. 2.7. The study area (Arabian Sea) belongs to tropical humid climate region; hence the investigation of influence of RH on ANFIS to estimate and forecast was considered to be of importance. To perform this exercise, two models (1 and 2) were developed with different input combinations and have been applied for both the buoys (AD07 and CB02). Gaussian input membership function (MF) type with three input MF's (small, medium and high) were employed for both the models.

	Input	Outputs		Inputs	Outputs
Model 1 (ANFIS)	AP, AT, RH, SST, WD	WS	Model 2 (ANFIS*)	AP, AT, SST, WD	WS

The scenario 1, was carried out to evaluate the accuracy of both the models to estimate the offshore wind speeds. The scenario 2 consists of conducting the same procedure, to obtain multi-step ahead forecasts. Model 1 (also represented as ANFIS) has 5 inputs and 1 output. The number of rules generated is ( $m^n = 3^5$ ) 243. Model 2 (also represented as ANFIS\*) has 4 inputs and 1 output type architecture with 81 number of fuzzy rules. Ratio of training to testing dataset considered was 80% to 20% for both the models. Root Mean Square Error (RMSE) and Mean Absolute Percentage Error (MAPE) are the indices considered to assess the performance of the models.

Scenario 1 helps to understand the capability of models to estimate the offshore wind speeds and to conduct a inter comparison between the model performance. Scenario 2 is aimed at obtaining wind speed forecasts at different ahead time steps by each models and compare the accuracy of the models with Persistence Method (PM).The output of the exercise was aimed at assessing the accuracy of estimates and forecasts of wind speeds by the models. Persistence method was considered as the benchmark method for comparing the forecast accuracy of the developed models.

The dataset was structured using the buoy observations from October 2012 to October 2013 at AD07 and at CB02, from January 2013 to January 2014. Fig. 2.8 represents the time series plot of wind speed data at both buoy locations. Red line in the figure represents the mean of the wind speed data. The variation in the wind speed observations at AD07 show almost uniform tendency during the post-monsoon season (October to January) and pre-monsoon season (February to May). With the onset of monsoon in the Arabian Sea, magnitude of wind speeds vary and high wind speeds can be observed in this season (June to September) and withdrawal of monsoon leads to reduction in the wind speed magnitude. Winds at AD07 ranges from 2.0 to 14.2 m s<sup>-1</sup>. At CB02, the prevailing winds were varying from 1.5 to 10.2 m s<sup>-1</sup>. There are large variations from mean, seen during the pre-monsoon season (February to May) with few spikes in measurements.

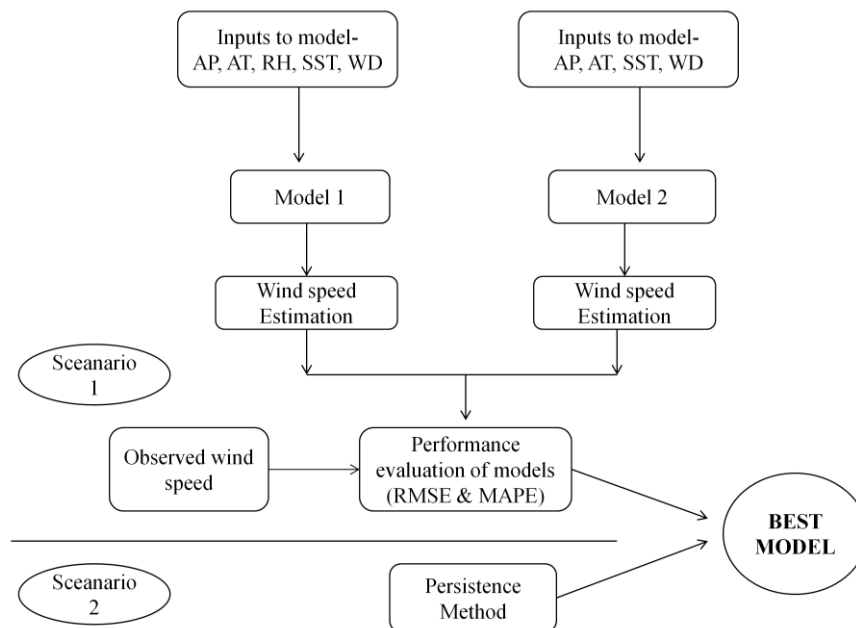


Fig. 2.7: Flowchart of scheme developed for short-term forecasting with multiple input combinations

During the monsoon season (June to September) winds are of high magnitude (mostly above mean observations) and with the withdrawal of monsoon, magnitude of wind speed reduces. For the post-monsoon season (October to January) it can be observed

that the wind speed is low ( $< 4 \text{ m s}^{-1}$ ). Statistics of the dataset have been tabulated as seen in Table 2.3. The magnitude of winds at CB02 was smaller than in AD07. The variation from mean in the case of AD07 is larger than CB02.

Table 2.3: Statistics of wind speed dataset at both buoys

Buoy	Minimum ( $\text{m s}^{-1}$ )	Maximum ( $\text{m s}^{-1}$ )	Mean ( $\text{m s}^{-1}$ )	Standard Deviation ( $\text{m s}^{-1}$ )
AD07	2	14.2	5.3	2.3
CB02	1.5	10.2	3.5	1.5

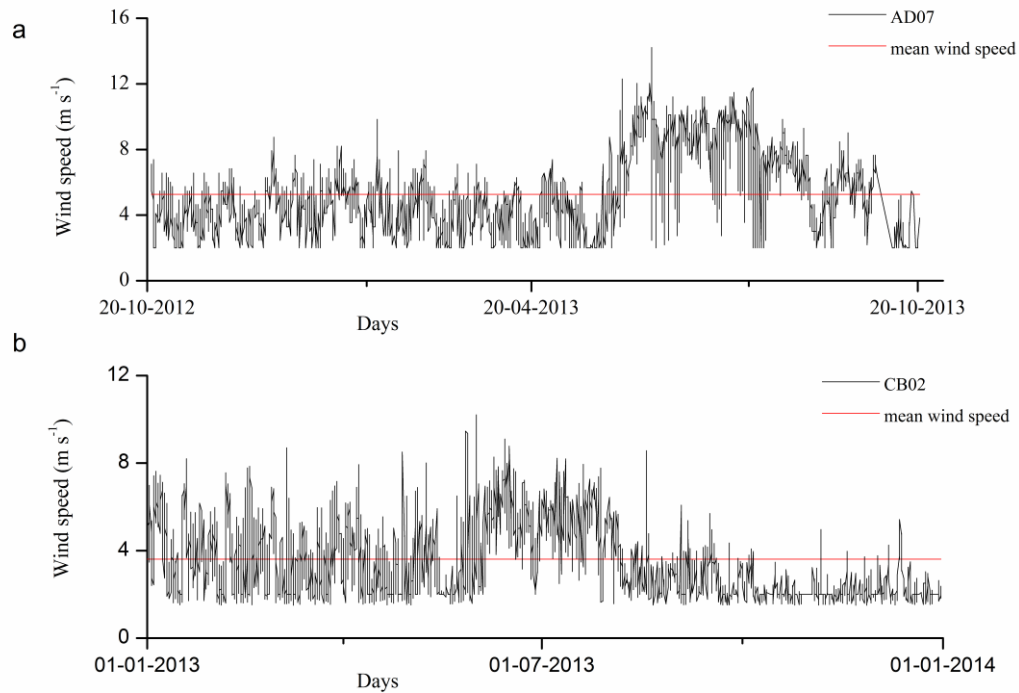


Fig. 2.8: Time series plot of observed wind speeds at a) AD07 and b) CB02

Therefore the performance evaluation of ANFIS was conducted in the present exercise and while there are other possible combinations of approaches that can be applied for short-term forecasting, there is a need to explore suitability of these methods. One such combination that was significant from literature was application of Wavelet transformation in combination with other techniques. Hence in following section, Wavelet-ANFIS combination is proposed for short-term wind speed forecasting.

## 2.6. SHORT-TERM OFFSHORE WIND SPEED FORECASTING BY ANFIS AND WT+ANFIS HYBRID TECHNIQUES

Hybrid techniques are combination of two or more approaches, which overcome the limitations of individual approaches. In case of offshore wind forecasting, there are limited literatures on the application of hybrid techniques for forecasting in short-term horizon. This section focuses on comparing two hybrid techniques that were developed using ANFIS and Wavelet transformations. Fig. 2.9 represents the development of step-wise procedure to achieve the best model suitable over different locations and forecasting horizons. Model 3 represents ANFIS method and Model 4 represents the Wavelet+ANFIS method.

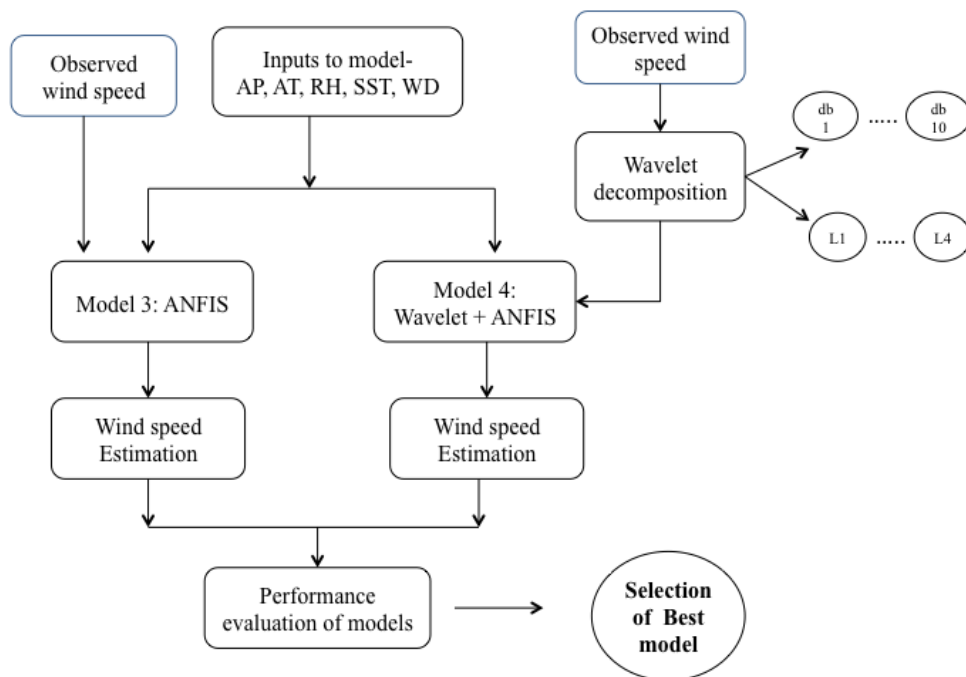


Fig. 2.9: Flowchart of scheme developed for short-term forecasting by hybrid techniques

The dataset was constructed using the observations at AD07 for duration of one year (from October 2012 to October 2013) and at CB02 from January 2013 to January 2014. The statistics of the dataset are presented in table 2.3. The dataset developed for the study in preceding section (2.5) for AD07 and CB02 was adopted in this section in

order to provide one-year data for performance comparison between the developed hybrid models. The time series plot (Fig. 2.8) and description of wind regime at the buoy locations remains unchanged as described in the section 2.6, since the dataset is the same.

In offshore region, the in situ data measurements by buoys are in range of 3-5 m, ship observations may range between 10-30 m, sensors mounted on offshore platforms (like oil rigs) and stand alone meteorological masts of designed height may be installed. Masts and ship data are expensive and hence are limited to specific area in accordance to funding agency. Buoy data are however provided at low or no cost to public. Also, before the installation of offshore wind turbines, measurements at hub heights are seldom conducted. It is conventional to use methods to extrapolate wind speeds from known height to required height. There are a number of approaches developed and tested on-shore (as it is easy to validate the method), in offshore scenario, these approaches are required to be tested and validated for their accuracy. Thence, the following section has been designed to evaluate the traditional methods that are widely adopted and accepted as highly accurate extrapolation methods for Arabian Sea. In addition, due to scarcity (both spatial and temporal) of offshore wind data, in the following section (2.7) accuracy assessment of satellite-based winds to represent actual winds over the region and its spatial distribution are analyzed and presented.

## **2.7. ESTIMATION OF ENW AND PERFORMANCE EVALUATION OF OCEANSAT-2 SCATTEROMETER WINDS**

The Equivalent Neutral Wind (ENW) speed may be defined as- “it is the mean wind speed that would be observed if there was neutral atmospheric stratification” (Geernaert and Katsaros, 1986). The height of 10 m above sea level is considered to be neutral layer height and wind speeds at this height are known as *neutral winds*. Wind speed increases considerably with height, particularly over rough terrain. For this reason, a standard height of 10 m above surface is specified for the exposure of wind instruments (Jarraud, 2008). Scatterometer based on principle of Bragg’s

scattering measures surface wind speed as a function of backscatter power, which depends on the intensity of surface roughness (waves). A geo-physical model function (GMF) is used to provide empirical relation between wind and backscatter (Hersbach, 2010). Therefore scatterometer do not respond directly to changes in the wind speed and hence are calibrated to ENW rather than actual wind speeds. The process of converting offshore winds from lower height to 10 m above sea level (ENW) can be much less complex than the converting ENW to actual winds. The flowchart presented in Fig. 2.10, represents the procedure developed for this section. Performance indices like- Root Mean Square Deviation (RMSD) and Mean Absolute Percentage Error (MAPE) are considered in the study. Generally, the observations at buoys are in range of 3-5 m above sea level. The moored buoys used in the study record observations at 3 m height.

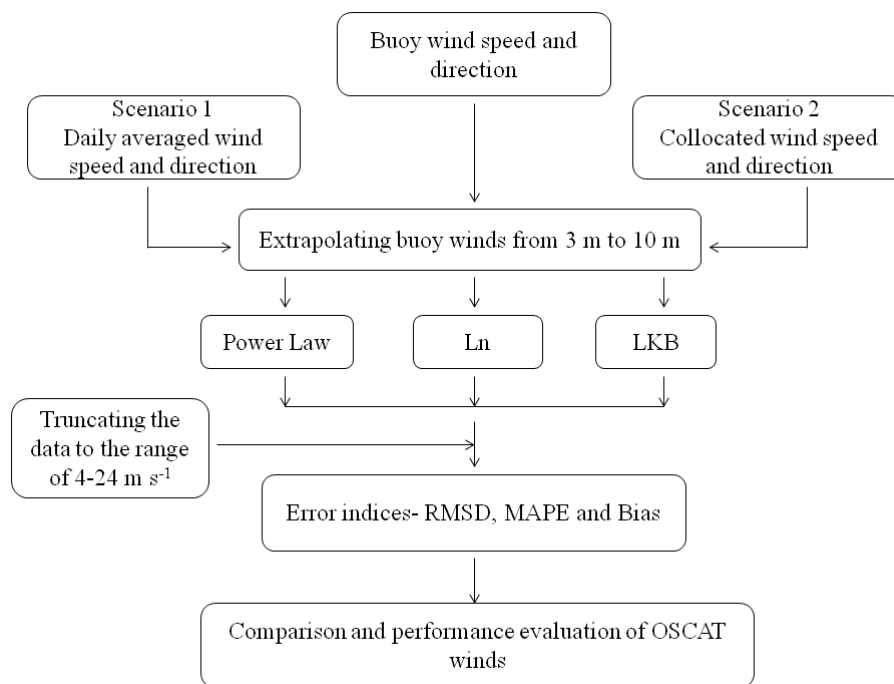


Fig. 2.10: Flowchart of scheme developed for estimation of ENW and comparison with OSCAT

The location details of buoys are- AD02 [15° N and 69° E] and CB02 [10° 15' 12" N and 72° 12' 36" E] can be seen in Fig. 2.11. In addition in the figure the bathymetric details of the study area has been plotted using the improvised version of ETOPOS data, made available by the National Institute of Oceanography (NIO), Goa. The

resolution of data is 5 arc minutes (Sindhu et al. 2007) and the depth of buoys AD02 and CB02 can be considered as around 4000 and 1000 m, respectively. The study uses wind observations during the monsoon season (June-September) of 2011 at buoys AD02 and CB02 and OSCAT wind data. The wind direction during this period is predominantly southwesterly (Rani and Gupta 2013). Fig. 2.12 shows the mean monthly average wind speed for the year 2011 recorded at buoys AD02 and CB02 at 3 m height. During the monsoon season, the variation in observed wind speed is found to be high, ranging from  $< 4$  to  $> 15 \text{ m s}^{-1}$ . From Fig. 2.12, it can be observed that the average wind speeds recorded during this period were no higher than  $9 \text{ m s}^{-1}$ . However, records exist showing wind speeds magnitude over  $12 \text{ m s}^{-1}$ . Thus, in order to consider the dynamic variability associated with offshore winds in the monsoon period, these four months were selected for this study.

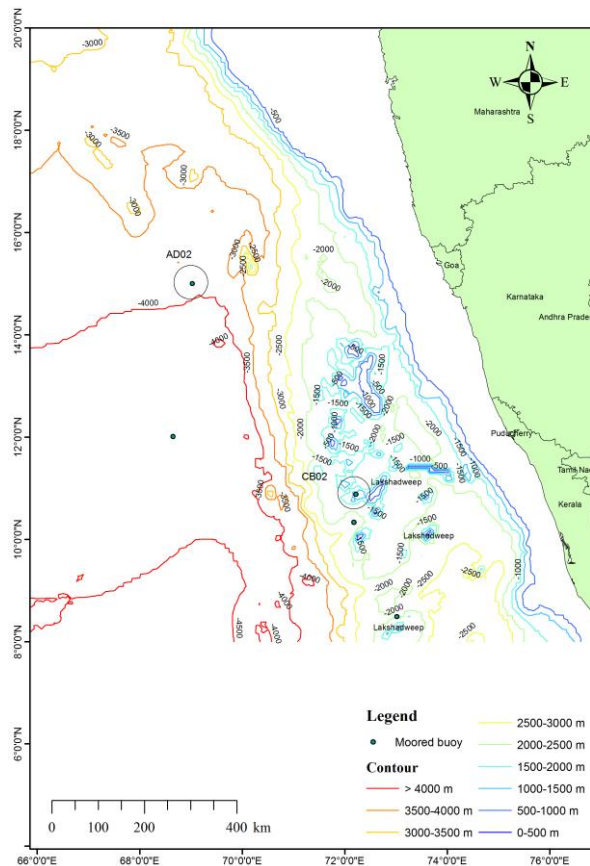


Fig. 2.11: Buoy location and bathymetry map of study area



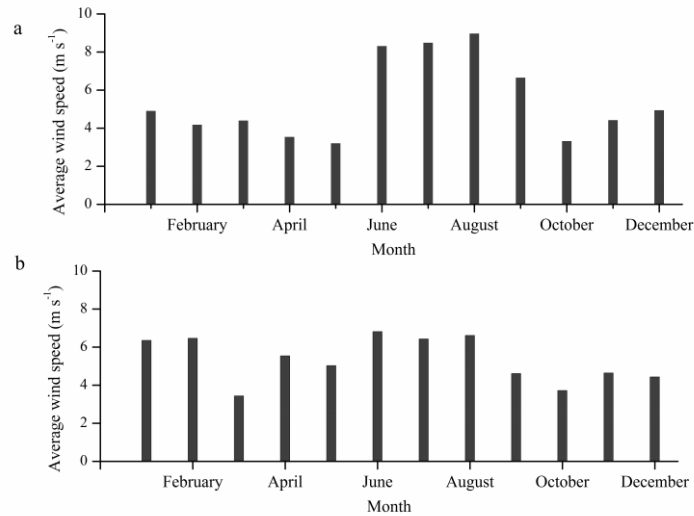


Fig. 2.12: Monthly mean wind speeds for 2011 at buoys (a) AD02 and (b) CB02

The aim of the exercise is to evaluate the best-suited method of extrapolation of buoy winds to ENW for the Arabian Sea. Then ENW and OSCAT winds (at 10 m) are compared. The comparison of these winds is a measure that can be used to evaluate the accuracy of Oceansat-2 scatterometer winds. For the comparison, the collocation of OSCAT and ENW was carried out using spatial window of  $0.5^\circ \times 0.5^\circ$  and temporal window as-

- Scenario 1: Daily averaged wind speeds; and
- Scenario 2:  $\pm 60$  min of buoy measurements and filtered data.

Scenario 1 was constructed based on the assumption that the scatterometer winds represent the average daily wind. The L2B data set consists of ascending and descending passes of OSCAT averaged to obtain daily observation of wind speeds during the study period. Through this assumption the study aims to determine whether OSCAT winds can represent averaged daily wind speed and reflect the diurnal behavior. The averaging of wind speed observation is carried out at the buoys to obtain daily buoy wind values. The kriging method of interpolation is employed where more than one collocated datum exists. Furthermore, the outcome from the Scenario 1 is aimed highlighting suitable method for ENW estimation.

Scenario 2 was adopted to validate OSCAT winds over the study area. This approach is generally adopted for comparison of OSCAT winds and accuracy determination with respect to in situ observations. The buoys selected are deployed at different

geographical locations in the Arabian Sea, which will help in understanding the pattern of spatial variation. The buoys are at some distance from coast, implying that the influence of landward wind on offshore winds can be ignored. Hence, the outcome from scenario 2 will be assessment of the quality of OSCAT winds for future assimilation into models for wind power estimation. Different approaches are available; in general, the adopted methods described provide accurate estimates of wind speeds. The advantage of selecting the monsoon period can also be demonstrated in comparison and performance assessment and, since wind speeds are generally over  $4 \text{ m s}^{-1}$ , an improvement is expected in this regard.

Consequently, in the section (2.7) the aim to establish satellite-based winds over region was conducted to address a major assumption in offshore wind resource assessment. The assumption, generally adopted due to unavailability of diverse offshore data is that, the buoy data are considered to be representative of wind regime over entire study area. This assumption may be justified due to the accuracy of buoy measurements and the temporal resolution required to frequency analysis of wind speeds and corresponding power density estimation. But the major limitation will be the difference in the spatial distribution of winds in the region, thus economics of conducting site based measurements for installation of turbines may turn expensive. The following section (2.8) was structured to address this very limitation of assuming constant wind regime over study area using satellite-based wind data. It aims at regional scale wind power assessment using satellite data and GIS based methodology to help decision makers in formulating stage wise development plans.

## **2.8. REGIONAL SCALE OFFSHORE WIND POWER RESOURCE ASSESSMENT USING OCEANSAT-2 SCATTEROMETER WINDS**

The work is aimed at evaluating the offshore wind power resource off the Karnataka coast. Karnataka state has 320 km long coastline available for energy development and in course of work assessment of potential has been carried out up to Exclusive Economic Zone (EEZ) of India as per draft policy guidelines (Govt. of India, 2013). Fig. 2.13 is a schematic representation of methodology adopted for the present work.

Offshore wind energy resource studies are generally carried out in accordance with turbine foundation technologies. The classification of foundation technologies has been tabulated, as seen in table 2.4. To the best of researcher’s knowledge there are no previous assessment studies or document available for Karnataka state’s offshore wind power potential, to present date.

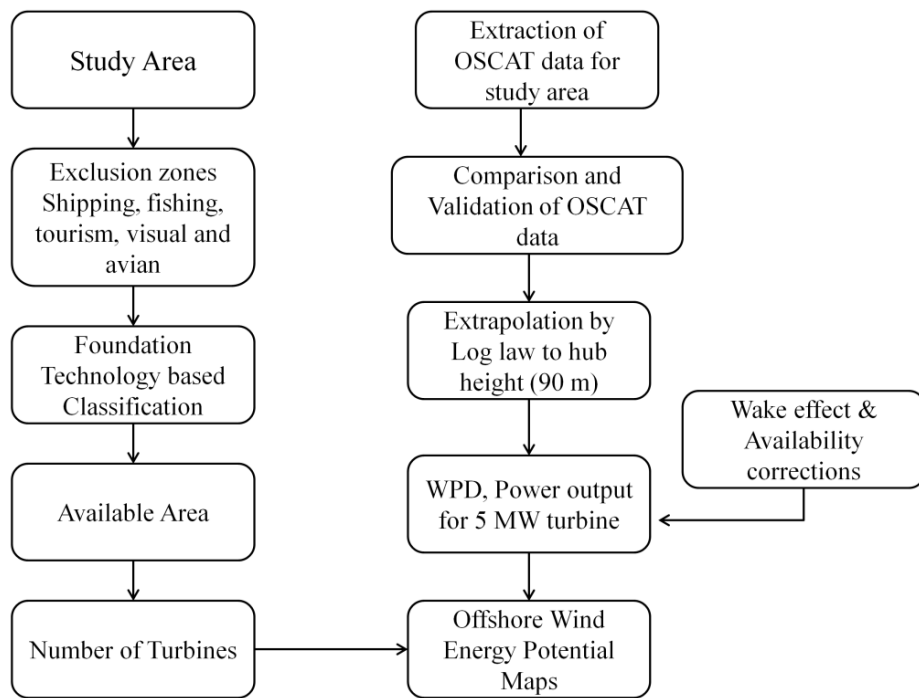


Fig. 2.13: Methodology modified after Sheridan, et al. (2012)

Table 2.4: Offshore wind turbine foundation technologies based on operational water depths

Foundation Technology	Depth range (m)
Monopile	0-35
Jacket	35-50
Advanced Jacket	50-100
Floating	100-1000

The classification of foundation types suitable for installing turbines, based on water depth range can be found in earlier works of Dhanju, et al. (2007); Pimenta, et al. (2008) and Sheridan, et al. (2012). Fig. 2.14 represents the bathymetric details of the

study area and the classification is based on the water depth intervals from table 2.4. The study area is extended up to EEZ (370 km from coastline), which in the map is represented by continuous black line. Monopile foundation has been most widely adopted type of foundation. Also monopile foundation can be less expensive than other foundation technologies. Lattice monopile (Jacket) foundation type can be adopted up to 50 m water depth as in the case of Beatrice Demonstrator Wind farm located in North Sea is at a depth of 45 m (Seidel, 2007). Beyond 50 m depth, advanced jacket type and floating structures can be adopted but may be expensive than other type of foundation. Fig. 2.2 shows the point of observations of IRAWS data during cruise in the study area. The IRAWS data and OSCAT data for duration of 2011 to 2013 in the Arabian Sea have been considered for the accuracy assessment of OSCAT data in this section. Earlier studies have accounted for the accuracy of scatterometer wind data by comparing it with in situ observations- buoys and ships, by Kent, et al. (1998); Satheesan, et al. (2007); Pimenta, et al. (2008); Singh, (2012); Rani and Gupta (2013); Kumar, et al. (2013), Peng, et al. (2013) and Doubrawa, et al. (2015). These works established the accuracy of scatterometer winds over global scale, however at regional scale, there are variations in geophysical parameters, attenuation of radiation by atmosphere (which is function of location and time of year). Therefore the assessment has to be carried out to ascertain that, the scatterometer winds at regional scale, represent the actual winds at site and the data can be incorporated for future analysis. It is a primary effort, to validate OSCAT data with IRAWS data in the Arabian Sea. The spatial and temporal windows considered for collocation are  $0.5^{\circ} \times 0.5^{\circ}$  and  $\pm 60$  min. It is believed that the choice of windows for validation is appropriate for the study, since with increase in the spatial window the variation in geophysical parameters may lead to incorrect comparisons. Thus, better assessment of accuracy of OSCAT data may be achieved. After the demarcation of study area, bathymetric classification of area based on the foundation technologies, it is vital to consider the exclusion areas, which may lead to conflict of interests with multiple sea users.

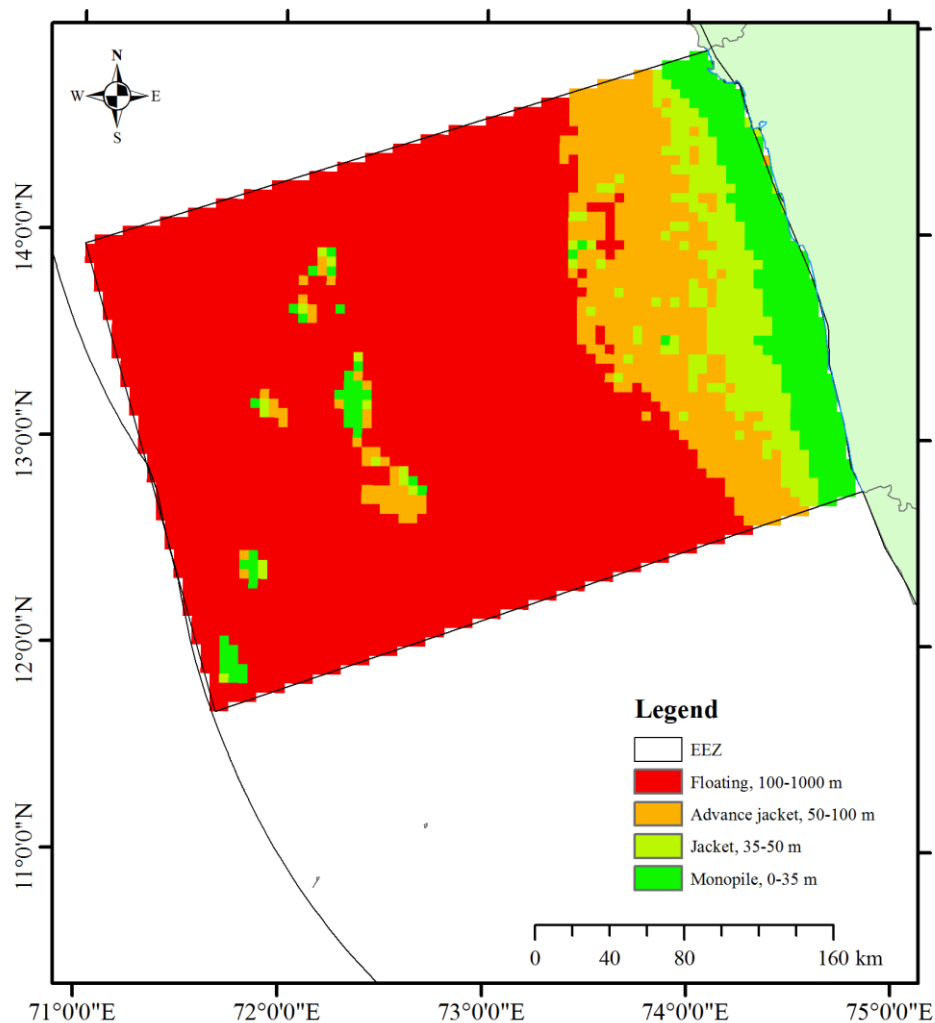


Fig. 2.14: Bathymetry of study area based on offshore foundation technologies

Significant activities that require demarcation, as exclusion zones are as follows-

*i. Potential Shipping Area*

In order to reduce the conflicts of area between turbine layout to be developed and the shipping traffic, the exclusion area should consider shipping lanes and area for operation of ships. Due to unavailability of accurate information regarding the commercial or tourist ship lanes, the exclusion zone considered in the study may be less precise. The Karnataka state has ports at Mangalore and Karwar. The New Mangalore Port (NMP) is a major port that handles various types of ship traffic ranging from commercial to tourist ships. The Karwar port is smaller than NMP and handles only specific types of cargo, majorly petroleum products. However the

exclusion zone has been set according to Survey of India (SOI) map representing information regarding Indian Railways and Sea Routes, the file is freely downloadable (<http://www.surveyofindia.gov.in/upload/downloads/Download-21.pdf>). Since the ship routes are generally planned considering- shortest distance between ports and minimum fuel consumption, the manoeuvring of ships from set routes are not advised. Hence larger exclusion area may be adopted, taking in to account future increase in ship traffic and operations.

*ii. Potential Fishing Zones (PFZ)*

The Ministry of Earth Sciences (MoES) initiated Marine Satellite Information Services (MARSIS) programme in June 1990. One of objective of MARSIS was to apply satellite data to harvest food from sea. INCOIS is involved in providing advisories to fisherman community on daily basis the details of fish landing centers, more details can be found in INCOIS web link: <http://www.incois.gov.in/MarineFisheries/PfzAdvisory>. The PFZ locations off the coast of Karnataka have been tabulated in table 2.5. The exclusion area should consider these locations and also consider the fishing boat cruises (which may not have fixed routes). Focus of exclusion zone must be towards reducing the impacts on fish habitats, mammals and proving to be minimum disturbance to eco-system that exists in sea.

*iii. Tourism Zones*

Beaches and islands attract local and tourists to shore. Tourism activities can provide source of livelihood for population located in coastal areas. The offshore wind energy development should consider the impact of turbines on beach recreational activities, marine ecosystems in shallow waters, sea vegetation etc. This requires a detailed study involving local community and wide range of people visiting beaches; such an analysis is out of scope of present work. However an assumption for exclusion has been made for the study.

*iv. Avian and Visual Zones*

Along with the tourism activities, exclusion zone for environment, bird population, and migratory birds should also be considered before and after construction. The aim should be towards reducing the interference and impact of offshore turbine on environment. The installed turbines should not reduce the aesthetics of beach, lower

familiar viewsapes and potentially reduce the number of people visiting the beach. As it could negatively impact on the tourism revenue. A detailed analysis will require large data and consultations with experts, which will lead towards proper offshore wind turbine planning (not scope of this study).

Since study focuses on energy potential estimation, an approximation of 10 km exclusion parallel to coastline was assumed for tourism, avian and visual exclusions. Future studies should focus on the details of each area's exclusion zones, in order to more accurately calculate amount of available area for development.

Table 2.5: Details of PFZ locations off-coast of Karnataka (source: INCOIS)

From the coast of	Direction	Bearing (°)	Distance (km) From-To	Depth (m) From-To	Latitude (D M S)	Longitude (D M S)
Gangoli	SW	266	175-180	1609-1614	13 32 35 N	73 1 25 E
Baindur	SW	262	154-159	1146-1151	13 40 28 N	73 11 52 E
Shirali	SW	262	136-141	699-704	13 51 57 N	73 15 4 E
Coondapoor (gangoli)	SW	265	186-191	1874-1879	13 27 49 N	72 56 23 E
Navunda	SW	264	165-170	1421-1426	13 35 22 N	73 6 11 E
Bhatkal	SW	261	140-145	977-982	13 45 39 N	73 14 6 E





## CHAPTER 3

### RESULTS AND DISCUSSION

#### 3.0 GENERAL

The work comprises of four subdivision that have been designed to explore the capability of the hybrid techniques, to address the need for efficient offshore wind speed forecasting tool, to study the influence of a selected parameter on the developed model's performance, to upscale the study of offshore winds on an spatial domain and to overcome the limitation of scarcity of data for regional scale analysis. Furthermore, works carried out to explore an efficient method for extrapolating the offshore wind speeds and validate satellite winds using in situ data from different sources. The validated satellite data is then employed for regional scale wind power resource assessment in nexus with GIS methodology. The results indicate that, the methodology can be applicable to other offshore regions as well. The deliverables of study hence are presented in four sections as follows.

#### 3.1 SHORT-TERM OFFSHORE WIND SPEED FORECASTING USING ANFIS AND RELATIVE HUMIDITY INFLUENCE ON THE ACCURACY OF ANFIS

##### 3.1.1 Scenario 1: Evaluate the accuracy of models to estimate the offshore wind speeds

The atmospheric parameters recorded at a buoy (AP, AT, RH, SST, WD and WS) are all interdependent factors, which are responsible for generation and movement of winds. Using these parameters as inputs to the ANFIS, effort was made to assess the capability of the models to estimate offshore wind speeds. Since, the Arabian Sea belongs to tropical humid climate zone, it was considered important to investigate the behavior of ANFIS model without RH as an input to the system. Thus, two different models (1 and 2) were developed for the purpose. The performance indices used are RMSE and MAPE for the models and results are presented the in table 3.1. From the table, it can be observed that the RMSE of training dataset at AD07 was found to be around  $0.9 \text{ m s}^{-1}$  and  $1.1 \text{ m s}^{-1}$  for model 1 and 2 respectively. However, for the testing

dataset the RMSE was found to be around  $1.0 \text{ m s}^{-1}$  and  $1.4 \text{ m s}^{-1}$  for model 1 and 2 respectively. The MAPE at AD07, for the training dataset was found to be around 16% and 20% for model 1 and 2 respectively. Similarly, for the testing dataset, MAPE was observed to be around 22% and 28% for model 1 and 2 respectively.

In case of CB02, RMSE of the training dataset for model 1 and 2 was found to be around  $0.9 \text{ m s}^{-1}$  and  $1.1 \text{ m s}^{-1}$  respectively. Correspondingly, for testing dataset the RMSE was found to be around  $1.1 \text{ m s}^{-1}$  and  $1.6 \text{ m s}^{-1}$  for model 1 and 2 respectively. The MAPE for training dataset was observed to be about 23% and 27% for model 1 and 2 respectively. MAPE of model 1 and 2 for testing dataset was observed to be about 26% and 35% respectively. Similarity in the performance of model 1 and 2 can be observed from the training datasets at both the buoys. However, from the testing dataset it can be noticed that the RMSE and MAPE of model 1 are lower than the model 2. It reveals that the model 1 performed better than model 2 and estimated wind speeds were close to observed wind speeds. Thus, substantial influence of RH can be seen on the ANFIS technique at both the buoys. Fig. 3.1 represents the scatter plot of estimated wind speeds for model 1, to examine the over and under-estimation of observed wind speeds. The density of data points at CB02 was high than AD07, which can be noticed from the scatter plot, since the observations were hourly averaged at CB02 compared to three hourly averaged at AD07.

Table 3.1: Error analysis of model 1 and 2 estimated wind speeds at AD07 and CB02

Buoy	RMSE ( $\text{m s}^{-1}$ )			
	Model 1 (ANFIS)		Model 2 (ANFIS*)	
	Training	Testing	Training	Testing
AD07	0.92	1.03	1.17	1.40
CB02	0.96	1.10	1.18	1.58
	MAPE (%)			
	Training	Testing	Training	Testing
	AD07	16.24	22.40	20.92
CB02	23.22	26.18	26.90	35.14

From model 1 estimates, it was found that at AD07, the scatter is uniformly distributed around the  $45^\circ$  line. Minor over-estimation can be seen when prevailing

winds were up to  $5 \text{ m s}^{-1}$  and minor under-estimation was observed when magnitude of winds were greater than  $10 \text{ m s}^{-1}$ . At CB02, the scatter distribution differs in comparison to AD07, initially over-estimation is seen when the observed winds were up to  $5 \text{ m s}^{-1}$ . Further, the model 1 shows slight under-estimation for wind speeds  $> 6 \text{ m s}^{-1}$ , however the distribution was found to around  $45^\circ$  line.

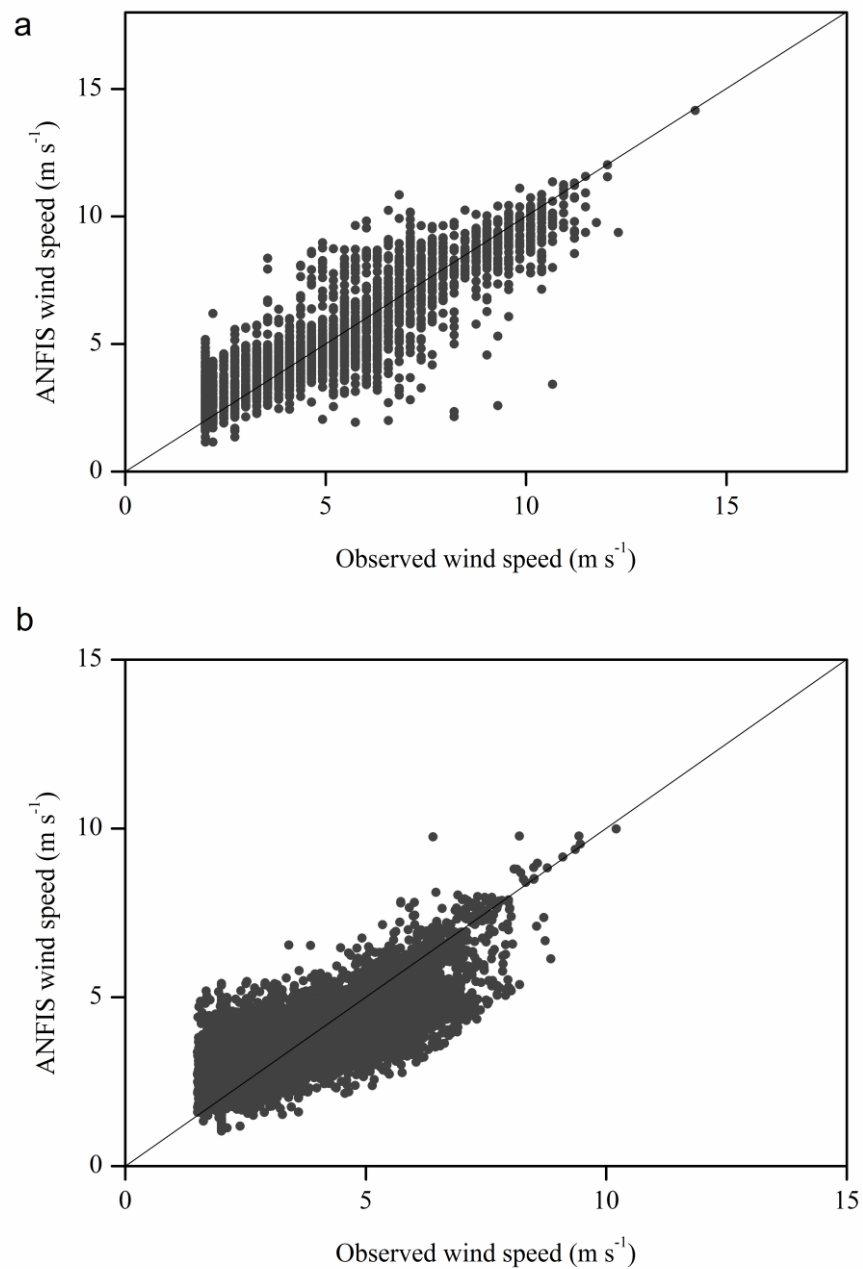


Fig. 3.1: Observed versus model 1 estimated wind speed at a) AD07 and b) CB02

Also, for model 2 the estimated versus observed wind speeds was plotted and can be seen in Fig. 3.2. The scatter plot demonstrates the trend in the estimated wind speeds, showing clear over-estimation of observed wind speeds.

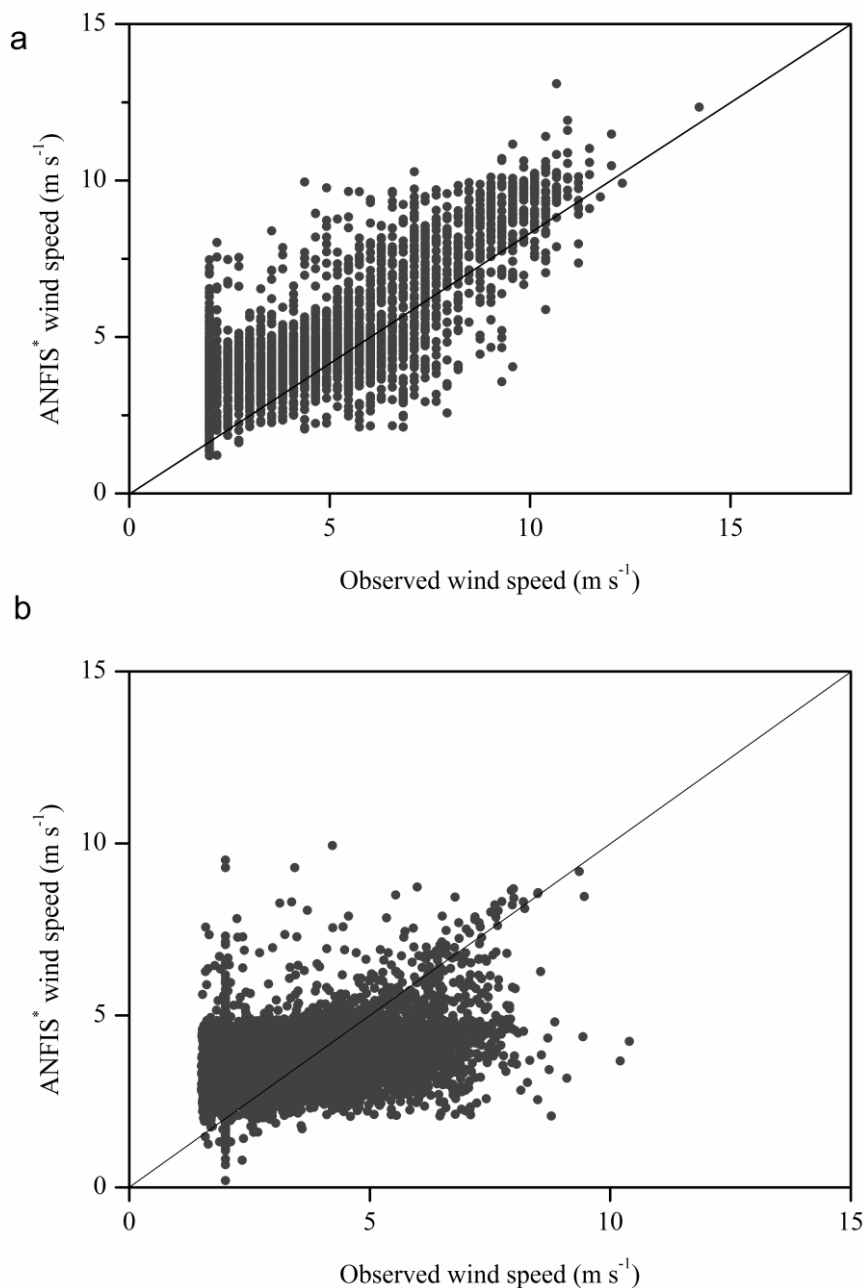


Fig. 3.2: Observed versus model 2 estimated wind speed at a) AD07 and b) CB02

At both the buoys, winds were over-estimated when observed wind speeds were in the range of 0-5 m s<sup>-1</sup>. Further, at AD07 when the wind speeds > 10 m s<sup>-1</sup> there occurs a clear case of over-estimation trend. However, when the prevailing winds were in the

range of 5-10 m s<sup>-1</sup> the points are uniformly scattered around 45° line. This may be the cause of lower RMSE at AD07 when compared to model performance at CB02.

In the case of CB02, with prevailing wind speeds > 5 m s<sup>-1</sup> the model clearly shows under-estimation of observed winds and thus the overall error was high. In addition from Fig. 2.8 it can be observed that, the observed wind speeds at CB02 are varying in between 2 and 10 m s<sup>-1</sup> with majority of testing dataset concentrated around 2 to 4 m s<sup>-1</sup>. Also, the occurrence of winds > 3.5 m s<sup>-1</sup> are also limited in number therefore making the testing dataset approximately stationary in nature, which may be affecting the performance of ANFIS and leading to lower accurate estimates. Overall, it can be considered that model 1 estimated wind speeds were better than model 2. Also, the influence of RH on short-term forecasting using ANFIS technique needs to be investigated.

### 3.1.2 Scenario 2: Wind Speed forecasting at different ahead time steps and comparison with Persistence Method (PM).

The developed models were applied to obtain forecasts of different time steps at AD07 and CB02. The RMSE and MAPE have been presented in Tables 3.2 and 3.3. In the earlier section (3.1.1), it was demonstrated that the RH could influence ANFIS model accuracy to estimate the wind speeds. Further in this section, the RH influence on short-term wind speed forecasts obtained using model 1 and 2 has been investigated. The aim of carrying out this exercise was to consider the probable event of non-availability of RH measurements at a site. In such cases, if ANFIS was to be applied to obtain wind speed forecasts, then the quantity of error in the forecasts needs to be assessed. In the present section only two buoys (locations) are considered, as the atmospheric parameters are function of geographic locations, generalization of the effect can be difficult. In addition, the performance of methods applied to obtain forecasts may be site specific in nature. Thus, the study demonstrates the performance of ANFIS model at two sites with and without RH observations. PM method was considered as the benchmark method to assess the accuracy of wind speed forecasts obtained from model 1 and 2.

In case of AD07 the data are three hourly averaged therefore, (t+1) represents 3<sup>rd</sup> hour forecast, (t+2) represents 6<sup>th</sup> hour and (t+3) represents the 9<sup>th</sup> hour forecasts. From Table 3.2 it can be seen that, the RMSE and MAPE of model 1 are lower than other two models. The RMSE of model 1 for training dataset for the three time steps were found to be around 1.1, 1.3 and 1.4 m s<sup>-1</sup> respectively. The RMSE of model 2 for training dataset was found to be about 1.3, 1.5 and 1.55 m s<sup>-1</sup> for the three time steps respectively. For the testing dataset the model 1 RMSE was found to be around 1.3, 1.5 and 1.6 m s<sup>-1</sup> for the three time steps respectively. In the case of model 2 it was found that RMSE was around 1.9 m s<sup>-1</sup> for first two time steps and around 2.1 m s<sup>-1</sup> for third time step. The training of model 1 was observed to better than model 2 and model 1 forecasts were better than model 2.

Consequently, the MAPE of model 1 for training dataset was found to be around 19%, 23% and 28% for the three time steps respectively. For testing dataset, it was seen that the MAPE was about 24%, 27% and 28% for the three time steps respectively. However, the MAPE of model 2 for training dataset was found to be around 23%, 32% and 33% for the three time steps respectively. For testing dataset, it was seen that MAPE for the three time steps was about 32%, 37% and 38% respectively. On comparison, it reveals that model 1 performs better than model 2.

PM is considered as benchmark method, to assess the forecast accuracies of model 1 and 2. From the table it can be observed that RMSE of model 1 for training and testing datasets was small than that of PM. Similarly, in case of MAPE for training and testing dataset it was found that PM is better than model 1 for the first time step, but error for consecutive time steps is higher than model 1.

In addition for all time steps, PM was found to be better than model 2. Also, it can be noticed that as the lead-time increases the performance of model 1 was found to be better than PM. Therefore, from the performance indices it can be inferred that the model 1 outperforms PM and model 2 at AD07.

Table 3.2: RMSE and MAPE of PM, model 1 and 2 for multiple forecast at AD07

Forecast time step	Training RMSE ( $\text{m s}^{-1}$ )			Testing RMSE ( $\text{m s}^{-1}$ )		
	PM	Model 1	Model 2	PM	Model 1	Model 2
t+1	1.16	1.09	1.27	1.28	1.30	1.92
t+2	1.47	1.28	1.51	1.63	1.47	1.93
t+3	1.65	1.43	1.55	1.81	1.59	2.12
	Training MAPE (%)			Testing MAPE (%)		
t+1	17.88	19.31	23.20	18.50	24.58	32.28
t+2	24.36	22.87	31.95	26.16	26.95	36.88
t+3	28.43	27.95	33.05	30.52	28.08	38.22

At CB02 the data are hourly averaged, hence (t+1) represents 1<sup>st</sup> hour forecast, (t+2) and (t+3) represent 2<sup>nd</sup> hour and 3<sup>rd</sup> hour forecasts respectively. PM method provides the most accurate forecasts when the lead-time step is hourly, which is clearly seen in Table 3.3. The RMSE of model 1 for training dataset was found to be around 1.1, 1.27 and 1.3  $\text{m s}^{-1}$  respectively for the three time steps. For testing dataset, RMSE was found to be about 1.3, 1.4 and 1.6  $\text{m s}^{-1}$  respectively for the three time steps. On the other hand, RMSE of model 2 for training dataset was found to be around 1.2, 1.3 and 1.4  $\text{m s}^{-1}$  respectively for the three time steps. Similarly for testing dataset, the RMSE was found to be around 1.5, 1.6 and 1.7  $\text{m s}^{-1}$  for the three time steps respectively. Thus, the forecasts of model 1 were found to be better than model 2, as the RMSE of later was closer to PM's. The MAPE values of model 1 for training dataset were found to be varying from 27% to 34% and for testing dataset were found to vary from 38% to 48% for the three time steps. The model 2 MAPE values were found to be varying from 30% to 36% for the training dataset and for testing dataset it was found to be varying from 43% to 50% for the three time steps. Thus, model 1 was found to perform better than model 2 but considerably lower in comparison to the PM.

Further, from Fig. 2.8 it can be noticed that the wind speeds in the testing dataset of CB02 were around 2  $\text{m s}^{-1}$  with no much variation seen in the magnitude of the observed winds. MAPE depends on the statistics of the dataset, the performance of ANFIS depends on the number of rules, fuzzy subsets formed based on the inputs. All the above may have been responsible for the low performance of models. Also, it

should be considered that the (t+1) forecasts were used as inputs for (t+2) and (t+2) as input for (t+3), thus the error in the forecasts obtained in the first time step are carried forward to other time steps.

Table 3.3: RMSE and MAPE of PM, model 1 and 2 for multiple forecast at CB02

Forecast time step	Training RMSE (m s <sup>-1</sup> )			Testing RMSE (m s <sup>-1</sup> )		
	PM	Model 1	Model 2	PM	Model 1	Model 2
t+1	0.81	1.13	1.25	0.93	1.26	1.53
t+2	1.03	1.27	1.31	1.05	1.44	1.65
t+3	1.10	1.31	1.37	1.07	1.62	1.72
	Training MAPE (%)			Testing MAPE (%)		
t+1	15.67	26.98	30.16	18.13	38.16	43.54
t+2	20.48	32.21	32.30	20.84	42.29	46.59
t+3	23.94	34.47	36.07	21.51	47.99	50.05

Overall, by performance indices at both buoys it can be inferred that the model 1 demonstrated the capability to perform better than other two models for obtaining multi-time step wind speed forecasts at two sites. Further, to assess the quantity of error in the model 2 with respect to model 1, equation 3.1 was formulated. The RMSE of model 1 and 2 was used in equation 3.1. The % error in wind speed forecasts due to absence of RH observations as input, was calculated as –

$$\%error = \frac{ANFIS^* - ANFIS}{ANFIS} \times 100 \quad (3.1)$$

The %error for each time step at both the buoys has been presented in table 3.4. At AD07, the % error is seen varying from 47% to 32% for testing dataset and at CB02 the %error was found to vary from 24% to 13% for testing dataset. This also quantifies that the error in forecasts from previous time step are carried forward to next time step, thus a decreasing trend in the error can be observed.



Table 3.4: Percentage error in model 2 forecasted wind speed at both the buoy locations

Station Time step	Percentage error			
	AD07		CB02	
	Training	Testing	Training	Testing
t+1	16.51	47.70	10.61	21.42
t+2	17.96	31.30	3.14	14.58
t+3	8.39	33.33	4.58	6.17

If an average of the %error were considered then, approximately 37% higher RMSE would be computed in obtaining wind speed forecasts using ANFIS technique (when RH measurements are not available) at AD07 for forecasts up to three time steps. Similarly at CB02 approximately 14% higher RMSE of the wind speed forecasts would be occurring if ANFIS technique were employed without RH observations as input, to obtain forecasts up to three time steps. Therefore, by adopting the correction to RMSE, the model 2 forecasts could be adjusted to achieve higher accuracy. In addition, it is important to acknowledge that ANFIS can be employed at sites without RH or limited RH observations.

## 3.2 SHORT-TERM FORECASTING BY ANFIS AND WAVELET-ANFIS HYBRID TECHNIQUES

### 3.2.1 Adaptive Neuro-Fuzzy Inference System (ANFIS)

To understand the modeling capacity of ANFIS, initial assessment was carried out where in the raw inputs (AP, AT, RH, SST and WD) from the observations were inputted in to the model with wind speeds (WS) as target output. The model was built using Gaussian Membership Function (Gauss) type and 3 (low, medium and high) number of membership functions for input and linear membership function type for the output. Table 3.5 presents the performance of ANFIS model to estimate wind speeds at both the buoys. The RMSE for training and testing dataset at AD07 was found to be around 0.9 and 1.1 m s<sup>-1</sup> respectively. At CB02, the RMSE was found to be around 1 m s<sup>-1</sup> for training and testing dataset. Therefore, the error between ANFIS

estimated and observed wind speeds were found to small. On other hand, the MAPE at AD07 was found to be about 16% and 24% for training and testing dataset respectively. In case of training and testing dataset at CB02, MAPE was found to be about 23% and 30% respectively. From the results, similarity in the performance of ANFIS to estimate offshore wind speeds can be noticed for both buoy locations.

Table 3.5: Performance indices of ANFIS model estimates at both the buoys

Buoy	RMSE ( $\text{m s}^{-1}$ )		MAPE (%)	
	Training	Testing	Training	Testing
AD07	0.92	1.16	16.22	23.84
CB07	0.97	1.01	23.22	29.83

Fig. 3.3 represents the scatter plot of estimated wind speeds versus observed wind speeds at AD07 and CB02. From the figure, it can be observed that for AD07 there exists clear distinction in distribution of points. It can be observed that for low wind speeds ( $2\text{-}4 \text{ m s}^{-1}$ ), the points are distributed above the  $45^\circ$  line indicating overestimation by the model. For medium wind speeds ( $4\text{-}7 \text{ m s}^{-1}$ ), almost uniform distribution around  $45^\circ$  line can be seen and for high winds ( $> 7 \text{ m s}^{-1}$ ), the distribution of winds was found to be around and beneath the  $45^\circ$  line. The model estimates for medium and high wind speeds were found to be relatively accurate.

At CB02, the bulk of the data were concentrated in the low wind speeds ( $2\text{-}4 \text{ m s}^{-1}$ ). In this region, the distribution of points in the scatter plot was observed to be above  $45^\circ$  line indicating overestimation of wind speeds. In the medium wind speeds ( $4\text{-}7 \text{ m s}^{-1}$ ), the points show uniform distribution around  $45^\circ$  line, while very few points below the line. For high wind speeds ( $> 7 \text{ m s}^{-1}$ ), which were small in number, the distribution is almost along  $45^\circ$  line. Therefore, the model estimates were found to be precise in the medium and high wind speed range. The performance of the ANFIS at AD07 and CB02 was found to be similar.

Overall, the ANFIS model with Gaussian MF type can be considered to be capable of estimating the observed wind speeds at different locations with higher accuracy. In table 3.6 and 3.7, results of ANFIS model performance for forecasting at buoy AD07 and CB02 respectively are presented.

Table 3.6: Performance of ANFIS, forecast up to 3 time steps at buoy AD07

Forecast time step	Training		Testing	
	RMSE (m s <sup>-1</sup> )	MAPE (%)	RMSE (m s <sup>-1</sup> )	MAPE (%)
t+1	1.09	19.31	1.30	24.58
t+2	1.28	22.87	1.47	26.95
t+3	1.43	27.95	1.59	28.08

In the short-term forecast horizon, forecasting of offshore wind speed up to three time steps was considered for both the buoy locations. For AD07, Table 3.6 records the performance of ANFIS forecasted wind speed up to three lead-time steps. Since the wind speeds at AD07 are averaged over three hours the (t+1) time step represents the 3<sup>rd</sup> hour forecast, (t+2) represents 6<sup>th</sup> hour forecast and (t+3) represents the 9<sup>th</sup> hour forecast. The RMSE of forecasted wind speeds was found to range from 1.30 to 1.59 m s<sup>-1</sup> and MAPE ranges from 23% to 28% for the testing dataset. The low error in forecasted wind speeds demonstrates the ability of ANFIS to model offshore wind speeds with greater accuracy. However, it can also be noted that the model accuracy reduces with increase in the lead-time.

Table 3.7: Performance of ANFIS, forecast up to 3 time steps at buoy CB02

Forecast time step	Training		Testing	
	RMSE (m s <sup>-1</sup> )	MAPE (%)	RMSE (m s <sup>-1</sup> )	MAPE (%)
t+1	1.13	26.98	1.26	38.16
t+2	1.27	32.47	1.44	42.29
t+3	1.31	34.21	1.72	47.99

In the case of CB02, the time steps differ as the wind speeds recorded are hourly averaged and the time steps, (t+1) represents 1<sup>st</sup> hour forecast, (t+2) represents 2<sup>nd</sup> hour forecast and (t+3) represents 3<sup>rd</sup> hour forecast.

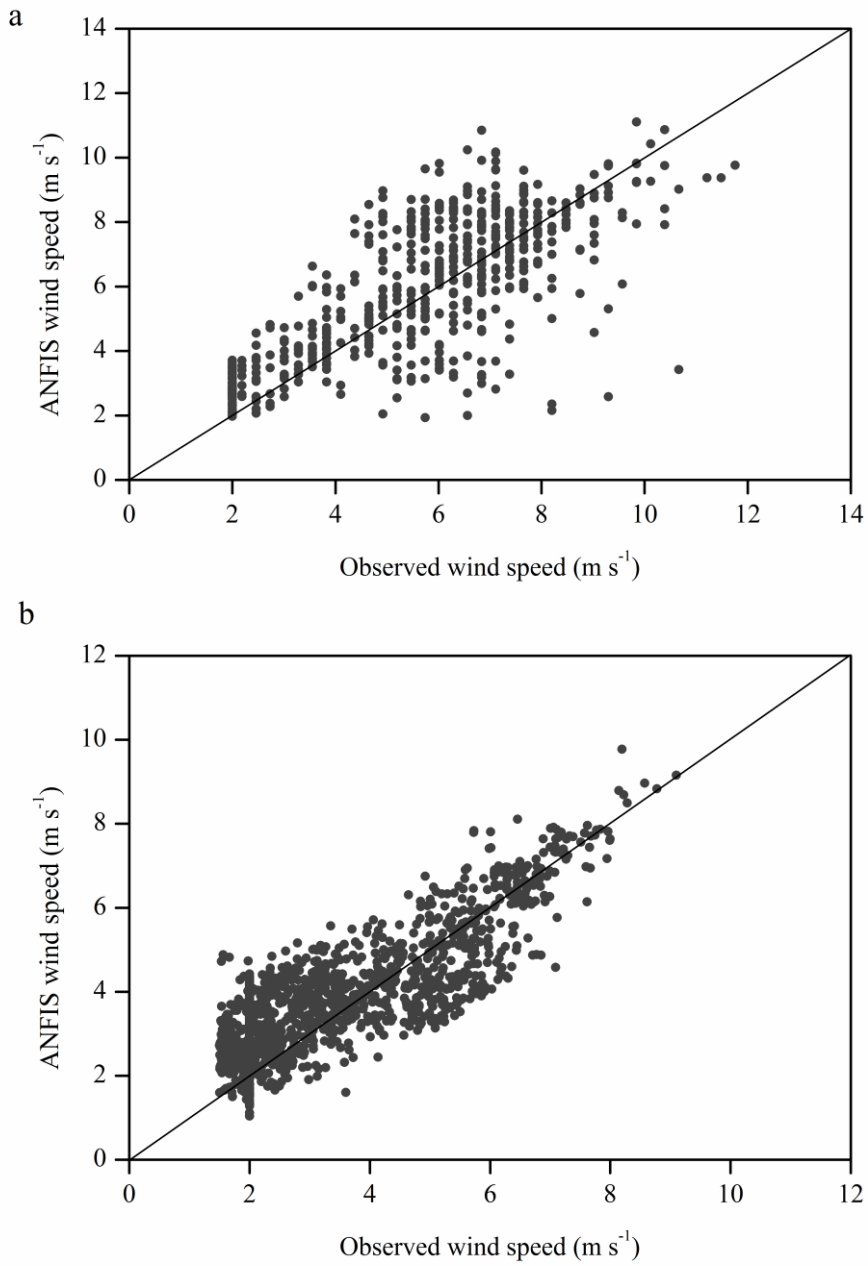


Fig. 3.3: Scatter plot of observed and ANFIS wind speeds at buoy a) AD07 and b) CB02

From Table 3.7, the RMSE for the testing dataset ranges from 1.26 to 1.72 m s<sup>-1</sup> and MAPE was found to vary from 38% to 48% for the time steps. The probable cause for high MAPE value could be the statistical characteristics of the dataset. The performance of ANFIS depends on the number of rules, fuzzy subsets formed based on the inputs. During training, almost all possible cases of observed wind speeds were covered and the hence model performed better. However in the testing dataset, as seen in Fig. 2.8 (time series plot for CB02), the magnitude of winds were low (around 2 m s<sup>-1</sup>). There was no much variation in the wind speeds noticed; consequently it may be affecting the performance of ANFIS. There may be a case of over-training of model too, which requires further investigation.

Fig. 3.4 is a plot of observed and ANFIS forecasted wind speeds at both the buoys. For AD07, when the wind speeds are low (around 2 m s<sup>-1</sup>), error between the forecasted and observed wind speeds was observed to be more, for all three time steps. With the change in the magnitude of wind speeds, the trend followed by observed and forecasted wind speeds was observed to be similar. The 1<sup>st</sup> time step forecast (t+1: red line) was the most accurate among the forecasted wind speeds when compared to the observed wind speeds. The (t+1) forecasted wind speeds were then used as input for the 2<sup>nd</sup> time step (t+2: blue line) forecasts and similarly (t+2) was used as input for 3<sup>rd</sup> time step (t+3: pink line) forecasts, the error gets carried on with the increase in lead-time. Therefore, the accuracy of wind speed forecasts reduced with increase in the lead-time. Overall, it can be inferred that the performance of ANFIS was found to be satisfactory.

In the case of CB02, the observed and forecasted wind speeds were found to be dissimilar. The disparity between observed and forecasted wind speeds can be seen initially. Since the observed wind speed at the CB02 were around 2 m s<sup>-1</sup> (as seen in Fig. 2.8) with insignificant changes in the magnitude, ANFIS overestimated wind speeds for all the lead-time steps. With the increase in time (on *x*-axis), a change in wind speeds was effectively captured. ANFIS is capable of handling vagueness but during the training of the model, it may be unlikely that such low wind speeds were available in the dataset.

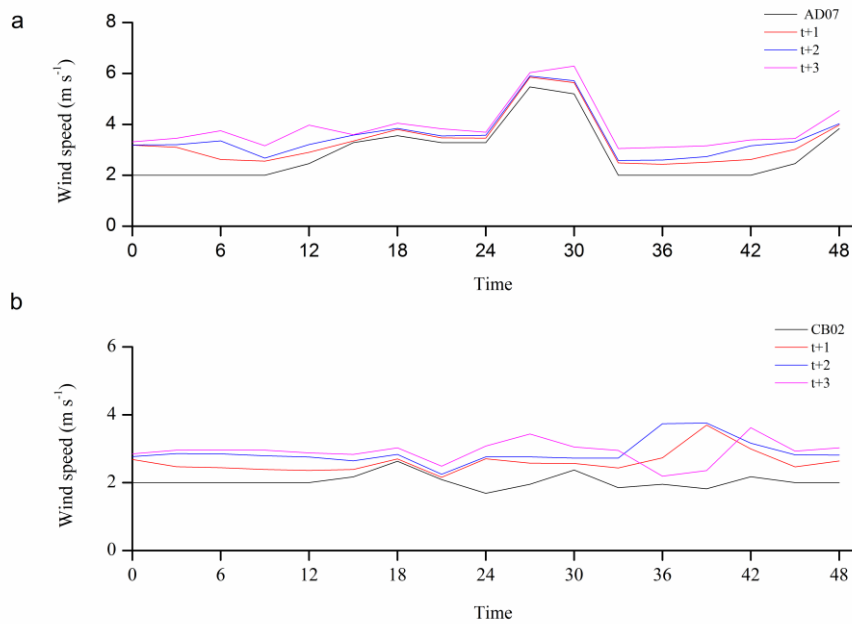


Fig. 3.4: Observed versus ANFIS forecasted wind speeds at buoy a) AD07 and b) CB02

So the ANFIS, with the formulated rules and fuzzy sets was found to be generally overestimating low wind speeds in testing dataset. This could have been the cause for high error in ANFIS forecasted wind speeds. For sites with low wind speed conditions and with little variations, ANFIS performance may increase subject to more number of fuzzy subsets with small domain and more rules. On the basis of RMSE ( $< 2 \text{ m s}^{-1}$ ) for both the buoy locations, we observe that the ANFIS method performance were similar and possess the ability to be appropriate tool for short-term forecasts.

### 3.2.2 Combination of Wavelet transform and ANFIS (WT+ANFIS)

In this section, the focus was on evaluating the performance of ANFIS and WT+ANFIS method, as to which method can be (more) suitable tool for short-term offshore wind forecasting. Wavelet transformation is similar to a pre-processing tool that provides smooth synthesized signals after decomposition of original signal. The synthesized wind speeds were then inputted to the ANFIS and the steps illustrated in the methodology flowchart were carried out. All subclasses that were obtained after wavelet decomposition have been used in the study. The proposed hybrid method

(WT+ANFIS) was used to forecast offshore wind speeds at both the buoy locations (AD07 and CB02).

Debauchies wavelets from 1 to 10 were considered to obtain a most suited mother wavelet that could represent the input signal (observed wind speed), decomposition level 1 (constant) was considered. The synthesized signals were compared to the input signal, at both the buoys. From the analysis, it was found that for AD07 wavelet *db8* was closest to the original signal with coefficient of correlation (R) of 0.97. In case of CB02, *db7* wavelet was the closest to the original signal and the R was found to be 0.98. Further, using Gaussian membership function in the ANFIS model the offshore winds were estimated. At both the buoys, the decomposition level 3 (L3) produced the best results, which are presented in bold font in Table 3.8. The RMSE for training and testing dataset at both the buoys were found to be around  $1 \text{ m s}^{-1}$ .

Table 3.8: Performance indices for WT+ANFIS model estimates at both the buoys

Buoy	Training RMSE ( $\text{m s}^{-1}$ )				Testing RMSE ( $\text{m s}^{-1}$ )			
	L1	L2	L3	L4	L1	L2	L3	L4
AD07	0.94	1.00	<b>0.99</b>	1.02	1.27	1.59	<b>1.17</b>	1.09
CB07	0.98	1.05	<b>0.94</b>	0.98	1.04	1.08	<b>1.05</b>	1.04
	Training MAPE (%)				Testing MAPE (%)			
AD07	16.58	17.89	<b>16.23</b>	17.20	19.90	24.60	<b>18.75</b>	18.95
CB07	24.52	26.56	<b>23.98</b>	24.67	29.1	29.51	<b>26.48</b>	32.01

The MAPE for training and testing dataset at AD07 was found to be around 16% and 19% respectively. At CB02, the MAPE was found to be about 24% and 26% for training and testing dataset. Therefore, new approach is better than ANFIS for estimating offshore winds at both the buoys. Table 3.9 and 3.10 shows the performance of the hybrid method applied for the same lead-time steps as in section 3.2.1, for both the buoys respectively. The RMSE of developed model with L3 (bold font in table 3.9) for training dataset at AD07 varied from 1 to  $1.36 \text{ m s}^{-1}$  for time steps (t+1) to (t+3). The RMSE for testing dataset for time steps (t+1) to (t+3) was found to range from  $1.50$  to  $1.72 \text{ m s}^{-1}$ .

Table 3.9: Performance of WT+ANFIS for forecast up to 3 time steps at buoy AD07

Forecast time step	Decomposition Levels							
	Training RMSE (m s <sup>-1</sup> )				Testing RMSE (m s <sup>-1</sup> )			
	L1	L2	<b>L3</b>	L4	L1	L2	<b>L3</b>	L4
t+1	1.19	1.19	<b>1.07</b>	1.11	1.64	1.70	<b>1.50</b>	1.70
t+2	1.26	1.24	<b>1.18</b>	1.19	1.84	1.73	<b>1.62</b>	1.82
t+3	1.41	1.28	<b>1.36</b>	1.24	1.91	1.80	<b>1.74</b>	1.87
	TRAINING MAPE (%)				TESTING MAPE (%)			
t+1	22.40	22.70	<b>19.46</b>	20.65	25.87	27.21	<b>24.73</b>	26.60
t+2	22.99	23.02	<b>21.72</b>	22.23	28.00	28.42	<b>27.22</b>	27.99
t+3	28.10	23.72	<b>27.06</b>	23.13	31.48	28.79	<b>30.00</b>	32.56

Similarly, the MAPE for training dataset ranged from 19% to 27% and for testing dataset it was found to varying from 25% to 30% for time steps (t+1) to (t+3).

Consequently at CB02, the RMSE of training dataset (from table 3.10) for time steps (t+1) to (t+3) varied from 1.1 to 1.28 m s<sup>-1</sup> and for testing dataset it was found to vary from 1.20 to 1.37 m s<sup>-1</sup> for (t+1) to (t+3) time steps. The variation in MAPE for training dataset was found to be around 27% to 29% and for testing dataset it was ranged from 31% to 37%.

When compared to the ANFIS, WT+ANFIS produced more accurate results (based on RMSE) at CB02. At AD07, it was observed that there was insignificant improvement. In the case of AD07, it was observed that the MAPE was in the range of 25% to 30% (for testing dataset) similar to results in previous section (3.2.1). However, at CB02 the MAPE was found to be high (30% to 37%) for the testing dataset in comparison to the ANFIS performance in the previous section (3.2.1).

Fig. 3.5 shows the plot of observed and WT+ANFIS forecasted wind speeds. From the figure it can be noticed that for AD07, the 1<sup>st</sup> hour forecasted wind speed (t+1: red line) are more accurate when compared to 2<sup>nd</sup> (t+2: blue line) and 3<sup>rd</sup> (t+3: pink line) hour forecasted wind speeds.



Table 3.10: Performance of WT+ANFIS, forecast up to 3 time steps at buoy CB02

Forecast time step	Training RMSE ( $\text{m s}^{-1}$ )				Testing RMSE ( $\text{m s}^{-1}$ )			
	Decomposition Levels							
	L1	L2	<b>L3</b>	L4	L1	L2	<b>L3</b>	L4
t+1	1.10	1.13	<b>1.13</b>	1.14	1.05	1.19	<b>1.20</b>	1.33
t+2	1.21	1.26	<b>1.21</b>	1.30	1.42	1.29	<b>1.29</b>	1.42
t+3	1.27	1.32	<b>1.28</b>	1.32	1.69	1.55	<b>1.37</b>	1.67
	Training MAPE (%)				Testing MAPE (%)			
t+1	27.36	27.48	<b>27.19</b>	27.87	31.11	34.56	<b>30.91</b>	39.56
t+2	28.93	28.83	<b>28.17</b>	33.64	36.68	36.78	<b>33.71</b>	41.08
t+3	30.78	34.54	<b>28.59</b>	35.18	38.46	42.04	<b>36.84</b>	44.05

Similarly in the case of CB02, the accuracy reduces with increase in the lead-time, (t+1) being most accurate than the other two lead-time steps. It can also be noted that the model performance is affected by the magnitude of observed wind speeds. As in the case of AD07, large error between observed and forecasted wind speeds exist when the observed wind speeds were low (around  $2 \text{ m s}^{-1}$ ) and the wind speeds become stationary. The stationary wind speeds may be limiting the wavelet performance, which can be noticed in the initial time period ( $x$ -axis) and at towards the end. This error from (t+1) time step was carried forward to the future time steps. For the CB02, the scenario was different as the observed wind speeds were low (around  $2 \text{ m s}^{-1}$ ) but continuously varying. The synthesized signal closely followed the observed wind speeds, which reveals higher forecast accuracy. The WT+ANFIS hybrid model showed significant improvement in performance over ANFIS method.

In order to understand the probable cause for high MAPE in the methods for offshore wind speed forecasts, the observed wind speeds were classified in to two classes. The classification was based on the consideration that in the wind energy industry, generally wind speeds above  $4 \text{ m s}^{-1}$  are of interest. Therefore, the observed wind speeds were classified as -

- class (i) : High winds, where observed wind speed were greater ( $>$ ) than  $7 \text{ m s}^{-1}$  and
- class (ii) : Medium winds, wherein the observed wind speeds were between  $4\text{-}7 \text{ m s}^{-1}$

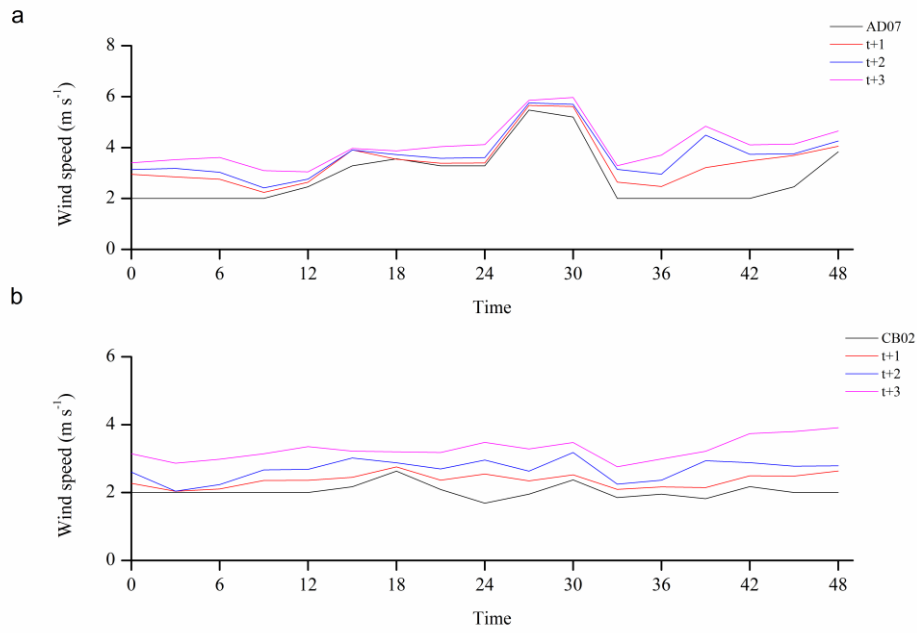


Fig. 3.5: Observed versus WT+ANFIS forecasted wind speeds at buoy a) AD07 and b) CB02

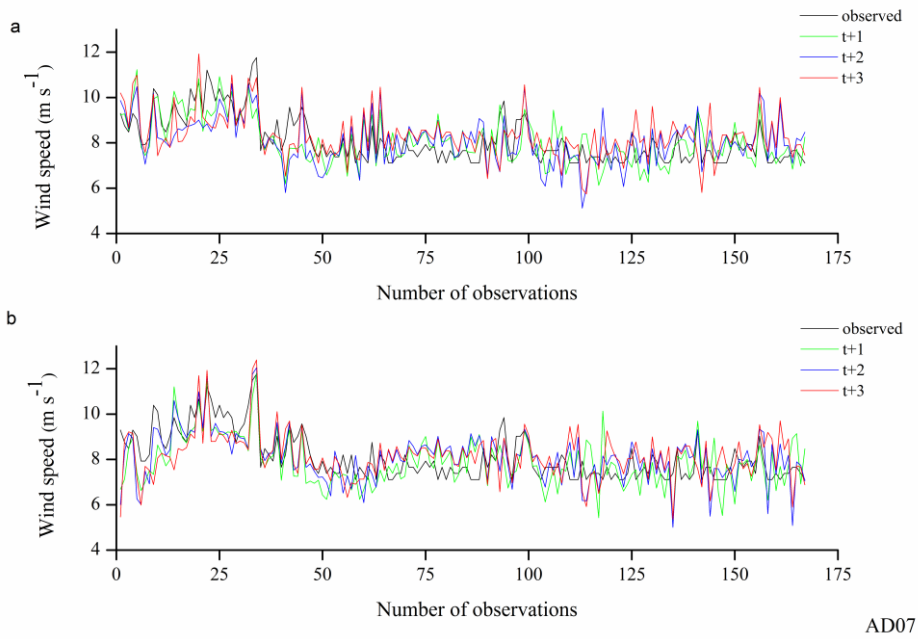


Fig. 3.6: Comparison of observed and forecasted wind speeds a) ANFIS and b) WT+ANFIS at AD07, observed wind speed  $> 7 \text{ m s}^{-1}$

Fig. 3.6 represents the plot of class (i): high winds and corresponding forecasted wind speeds a) ANFIS and b) WT+ANFIS at AD07. The number of events in this class was around 170 in the testing dataset. From the figure, it can be noticed that the WT+ANFIS is able to model high wind speeds more accurately than ANFIS. In case of (t+3) time step forecasted wind speeds, the performance was found to be unsatisfactory for both the methods and (t+1) forecasted wind speeds were closest to the observed wind speeds in both methods.

The plot of class (ii): medium winds versus a) ANFIS and b) WT+ANFIS at AD07 are seen in Fig. 3.7. The number of events in this class was around 250 in the testing dataset. The difference between the numbers of events in the class (i) and (ii) is comparatively small, thus the dataset has relatively even mix of high and medium winds. The forecasted wind speeds by ANFIS and WT+ANFIS follow approximately similar trend. The (t+1) forecasted wind speeds were the closest to the observed wind speeds, however when compared between the two methods, WT+ANFIS outperforms ANFIS method. The (t+2) and (t+3) forecasted wind speeds are over estimated in case of ANFIS than WT+ANFIS, for the same time steps. Thus, the results points towards the capacity of ANFIS to forecast wind speed limited up to 3 hour lead-time and WT+ANFIS method may be applicable up to 6 hour lead-time forecast of offshore wind speeds.

At CB02, the plot of class (i): high winds versus ANFIS and WT+ANFIS forecasted wind speeds could be seen in Fig. 3.8. From the testing dataset the number of events was found to be around 45°. The WT+ANFIS forecasted wind speeds show good agreement with the observed wind speeds when compared to ANFIS forecasted wind speeds. In the case of ANFIS forecasted wind speeds, the (t+1) time step forecasted wind speeds were found to be following trend similar to the observed wind speeds. From the other two time steps, forecasted wind speeds show sharp changes in the trend and are less accurate when compared to observed wind speeds.

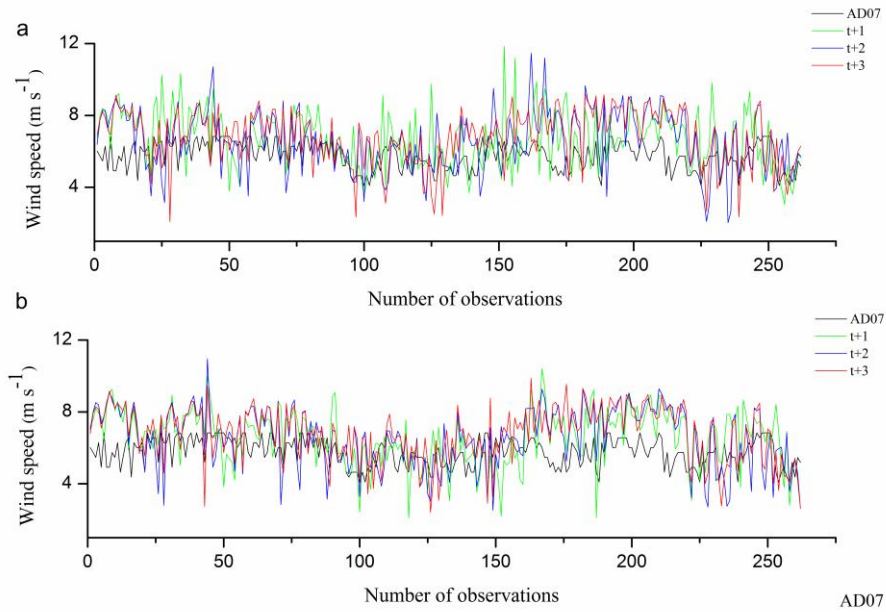


Fig. 3.7: Comparison of observed and forecasted wind speeds a) ANFIS and b) WT+ANFIS at AD07, observed wind speed between 4-7 m s<sup>-1</sup>

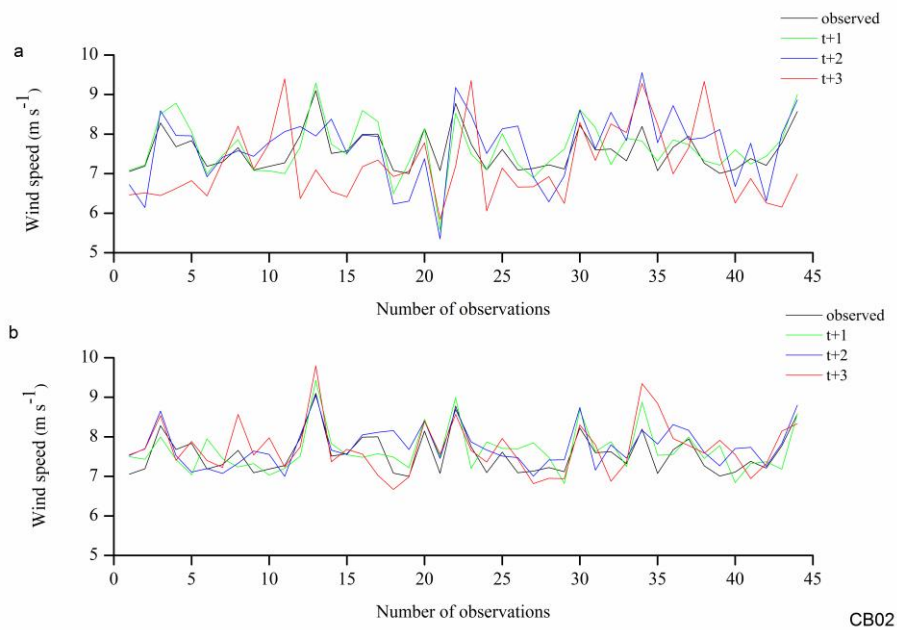


Fig. 3.8: Comparison of observed and forecasted wind speeds a) ANFIS and b) WT+ANFIS at CB02, observed wind speed > 7 m s<sup>-1</sup>

While the WT+ANFIS forecasted handle the variations in the observed wind speeds well, (t+3) forecasted wind speeds had large error. The accuracy of models reduces with increase in lead-time as found in the earlier analysis.

Fig. 3.9 represents the plot of comparison between class (ii): medium observed and forecasted wind speeds by a) ANFIS and b) WT+ANFIS methods. The number of events was found to be around 400 from testing dataset at CB02. This high number of events represents that winds at CB02 showed sharp changes in trend. This may have been a reason for high MAPE value in case of ANFIS forecasted wind speeds when compared to WT+ANFIS forecasted wind speeds. The wavelet decomposition produces subclass that helps in reducing the sharp trends (coefficients) and produce smoother wind speed. When these subclasses (approximations) were used with ANFIS, it was effective in modeling observed wind speeds and may be responsible for better modeling of medium winds.

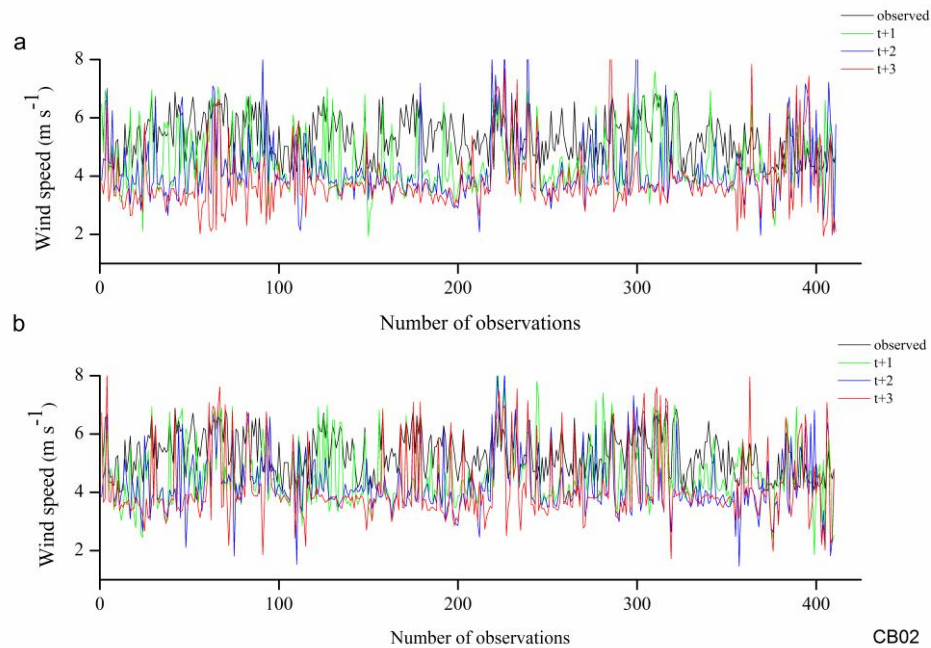


Fig. 3.9: Comparison of observed and forecasted wind speeds a) ANFIS and b) WT+ANFIS at CB02, observed wind speed between 4-7 m s<sup>-1</sup>

### 3.2.3 Comparison of ANFIS, WT+ANFIS with PM

Persistence Method (PM), benchmark method for short-term forecasts and used as reference to assess the performance of the hybrid methods. The results have been tabulated in table 3.11 for AD07 and CB02. Both the methods- ANFIS and WT+ANFIS were well trained and the same can be noticed, as the RMSE for training dataset was less than  $1.5 \text{ m s}^{-1}$ . The PM forecast at AD07 for (t+2) and (t+3) time steps were found to be less accurate. The wind speed forecasts from testing dataset at AD07 highlights the performance of ANFIS, as it produces more accurate forecasts than the other two methods. It can be inferred that at AD07 buoy location, ANFIS slightly performs better than WT+ANFIS model. In the case of CB02, the PM performs well for both training and testing dataset. PM produces most accurate forecasts in hourly forecast intervals and performed well up to three-hour lead-time at the CB02 buoy location. Furthermore the WT+ANFIS method for both training and testing dataset outperforms ANFIS for all forecast time steps. It is important to emphasize that the difference between PM and WT+ANFIS is comparatively small.

Table 3.11: Comparison of PM, ANFIS and WT+ANFIS forecasts at both buoys

Forecast time step	AD07					
	Training RMSE ( $\text{m s}^{-1}$ )			Testing RMSE ( $\text{m s}^{-1}$ )		
	PM	ANFIS	WT+ANFIS	PM	ANFIS	WT+ANFIS
t+1	1.16	1.09	1.07	1.28	1.30	1.50
t+2	1.47	1.28	1.18	1.63	1.47	1.62
t+3	1.65	1.43	1.36	1.81	1.59	1.74
Forecast time step	CB02					
	PM	ANFIS	WT+ANFIS	PM	ANFIS	WT+ANFIS
	t+1	0.81	1.13	1.13	0.93	1.21
t+2	1.03	1.27	1.21	1.05	1.44	1.29
t+3	1.16	1.31	1.28	1.07	1.72	1.37

When both the buoy sites are considered, WT+ANFIS method was found to produce steady, accurate forecasts and consistent in performance. This ascertains the ability of the hybrid method to handle different wind scenarios and multiple lead-times for offshore wind speed forecasting.

### 3.3 ESTIMATION OF ENW AND PERFORMANCE EVALUATION OF OCEANSAT-2 SCATTEROMETER WINDS

#### 3.3.1 Equivalent Neutral Winds (ENW) estimation

Wind speeds observations are averaged over 3-hourly at buoy AD02 and hourly at CB02. As the data recording interval is different for the two buoys and OSCAT data are available twice per day, daily averaging of wind speed was performed. The daily averaged data are further utilized in the scenario 1 analysis. Wind speed is a function of height and generally increases logarithmically with height. Therefore, the log method was considered as base method to compare the other two methods (Singh, et al. 2011). Table 3.12 provides the correlation coefficient of power law and LKB method with log method. From the table, it can be observed that root mean square deviation (RMSD) of power law estimates with respect to log method was found to be 0.2 and 0.9  $\text{m s}^{-1}$  at AD02 and CB02 respectively. However, the RMSD of LKB estimates with respect to log method were low ( $<0.5 \text{ m s}^{-1}$ ) for both the buoys. It was found that the LKB and power law method estimates were in good agreement with the logarithmic wind profile.

Table 3.12: RMSD and Correlation between methods

Buoy	Correlation (R)		RMSD ( $\text{m s}^{-1}$ )	
	Power Law-Log	LKB-Log	Power Law-Log	LKB-Log
AD02	1	0.99	0.20	0.35
CB02	0.9	0.99	0.96	0.40

Fig. 3.10 displays the time series plot of observed wind speeds at 3 m and ENW. From the graph, it can be seen that the power law method overestimated wind speed at the CB02 buoy. It is established that the friction coefficient (exponent factor),  $\alpha = 0.11$  is a good approximation for the sea surface (Hsu et al. 1994), and the same was adopted for buoy AD02. Nevertheless, there is an overlap between the CB02 buoy location and satellite pass, and thus from collocation and time of overlap, the exponent factor was determined as  $\alpha = 0.2$  using equation (2.2), and the same was adopted for buoy CB02. This  $\alpha$  value may be the reason for overestimation of CB02 and mean absolute error was found to be  $0.8 \text{ m s}^{-1}$  (if  $\alpha = 0.11$  was used). While the

estimation of wind speed is higher, this was used in the study to represent the in situ wind profile.

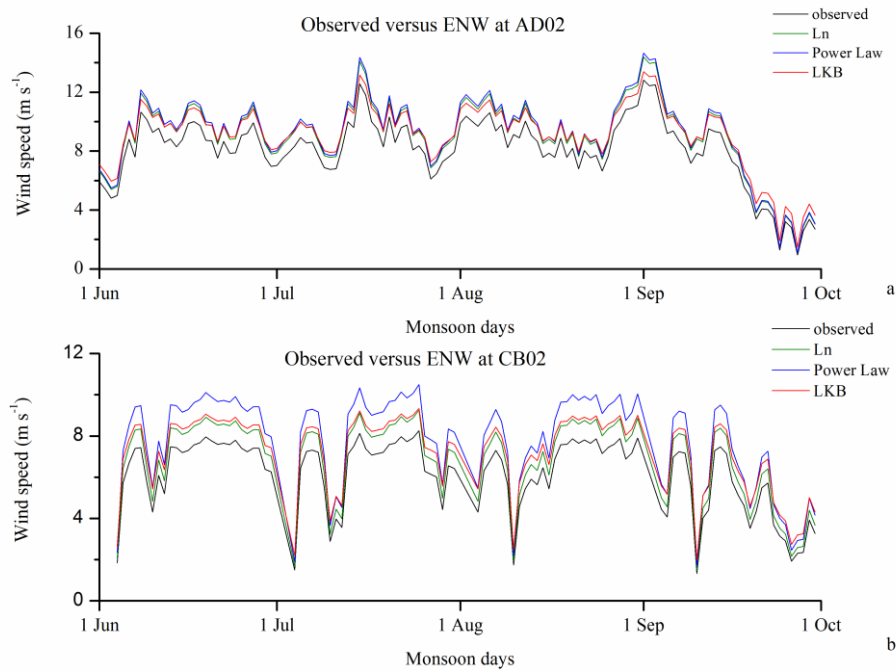


Fig. 3.10: Comparison of observed and ENW winds at buoy (a) AD02 and (b) CB02

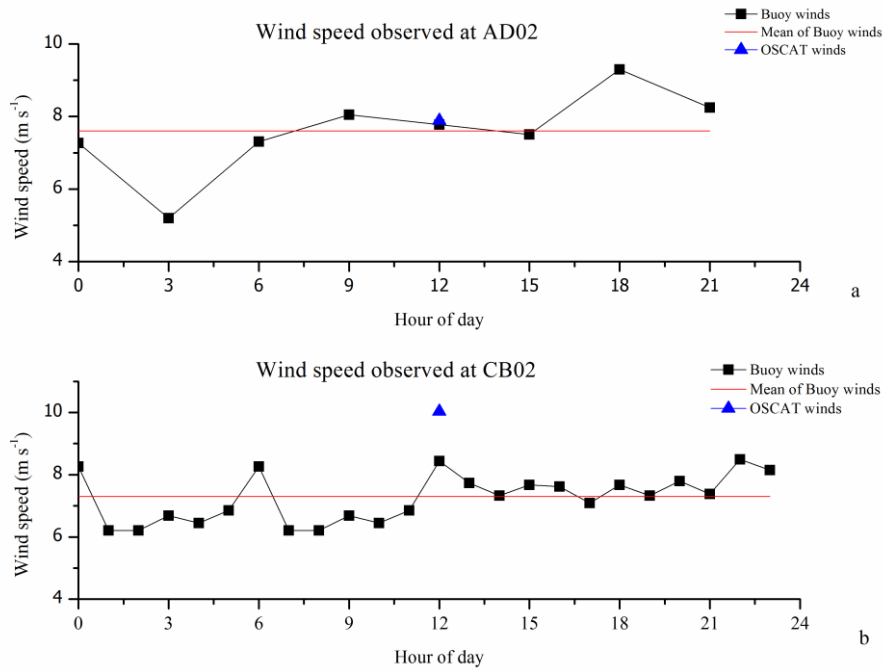


Fig. 3.11: Daily wind speed profile, buoy winds at (a) AD02 and (b) CB02 versus time of the day, and OSCAT wind (local time)



### 3.3.1.1 Scenario 1: Daily averaged buoy winds compared to OSCAT winds

Fig. 3.11 shows the daily wind speed profile at the buoy locations, with the mean of buoy observations denoted by the red line and OSCAT data on a particular day during the monsoon period. The figure highlights the relation of OSCAT data to the average of buoy observations. The ascending and descending passes of Oceansat-2 satellite over the Indian Ocean are approximately 18.00 and 06.00 hours UTC (+5:30 hours local time), while over the study area these are approximately 00.00 and 12.00 hours (local time), respectively. At AD02, the observed winds (at 3 m) were low in the morning and increased through the day. Winds changed continuously throughout the day and maximum speed was observed around 18.00 hours local time.

At CB02, the wind speeds (at 3 m) show a gradual trend of increasing and decreasing throughout the day with the maximum wind speed observed around 06.00 hours local time. The average of wind data throughout the day was considered and conversion was performed for comparison to the satellite data. Table 3.13 summarizes the comparative statistics between OSCAT-measured winds and the power law, log, and LKB methods.

Table 3.13: Correlation, RMSD and MAPE for different methods with OSCAT winds (scenario 1)

Buoy versus OSCAT (daily averaged)			
Methods	Buoy: AD02		
	Correlation (R)	RMSD (m s <sup>-1</sup> )	MAPE (%)
Power Law	0.78	1.53	10.76
Log method	0.78	1.55	11.10
LKB method	<b>0.78</b>	<b>1.46</b>	<b>10.80</b>
Methods	Buoy: CB02		
	Correlation (R)	RMSD (m s <sup>-1</sup> )	MAPE (%)
Power Law	0.18	2.69	26.71
Log method	0.32	2.38	29.20
LKB method	<b>0.32</b>	<b>2.26</b>	<b>19.58</b>

The log and power law estimates were equivalent to each other. Correlation was found to be 0.78 for all the methods at AD02. The RMSD for power law method was found to be around  $1.53 \text{ m s}^{-1}$ , for LKB method it was observed to be around  $1.46 \text{ m s}^{-1}$  and for log method it was around  $1.55 \text{ m s}^{-1}$ . Similarly, the MAPE was found to be about 10.8%, 11.1% and 10.8% for power law, log and LKB methods respectively. On comparing the methods, the maximum error was observed to be in the case of log method and the in LKB method was small indicating that the LKB estimated winds were closest to the OSCAT winds.

At CB02, the correlation was observed to be small as it was 0.18 for power law and 0.32 for log and LKB methods. The RMSD was found to be around  $2.69 \text{ m s}^{-1}$ ,  $2.38 \text{ m s}^{-1}$  and  $2.26 \text{ m s}^{-1}$  for power law, log and LKB methods respectively. Consequently, the MAPE was found to be around 26.7%, 29.2% and 19.6% for power law, log and LKB methods respectively. The RMSD was found to be high in the case of power law estimated winds whereas, the MAPE was found to be high for log method.

All the three methods were found to be almost similar with the LKB method slightly edged over others considering the error R, RMSD and MAPE. These poor results can be attributed to the lower wind speeds observed at CB02; furthermore, the daily averaged values may have lowered the magnitude of winds considered for comparison. The LKB wind speed estimates were found to be the closest to OSCAT winds, with the lowest error indices. However, the aim of the exercise was to determine the best method for estimating ENW, and the LKB method yielded the best results. At a height of 10 m above sea level, atmospheric stratification is considered to be neutral. In the logarithmic and power law methods, the assumption is that the wind speeds at 10 m are free from the influence of atmospheric parameters. Conventionally, these methods have been employed with corrections and are known to yield acceptable results. The neutral condition reduces the atmospheric stability function in the LKB equation to zero. The LKB method, by incorporating roughness length ( $z_o$ ) and friction velocity ( $u_*$ ) in the estimation of wind speeds, provides a more realistic wind estimates than estimates obtained from log and power law methods.

On the basis of scenario 1, the LKB method performed better; hence, it has been adopted for scenario 2. The optimal performance can be linked to the mechanism of

wind speed and direction observations observed from the scatterometer and LKB methods. Scatterometer data are based on backscattering, and backscattering power is a function of surface roughness, which in turn is highly correlated to near-surface wind speeds and direction. Thus, ENW from the LKB method and OSCAT wind comparison seems to be more appropriate than comparison of OSCAT and ENW estimated by the other two methods.

### 3.3.2 Scenario 2: $\pm 60$ minutes of buoy measurements and filtered data

This data set is constructed based on scatterometer wind cells within  $0.5^\circ$  of buoy location and a temporal window of  $\pm 60$  min. Scatterometer is designed to measure wind speeds in the range of 4 to  $24 \text{ m s}^{-1}$ , so truncation of data was performed on neutral winds estimated by the LKB method. Table 3.14 presents the results for comparison between OSCAT and LKB ENW wind speeds. It can be observed that the number of collocated points at both the buoys is almost similar. In case of AD02, the RMSD for wind speed and direction was found to be around  $2.2 \text{ m s}^{-1}$  and around  $22^\circ$  respectively. There was small bias observed in the wind speed of the magnitude  $0.23 \text{ m s}^{-1}$  and in case of wind direction the bias was found to be  $0.14^\circ$ . At CB02, the RMSD was found to be around  $2.4 \text{ m s}^{-1}$  slightly higher than at AD02. The RMSD for wind direction was found to be around  $22.4^\circ$  similar to AD02. The bias in wind speed at CB02 was  $0.11 \text{ m s}^{-1}$  similar to the bias seen at AD02. Bias in wind direction was observed to be  $0.18^\circ$  at CB02. A small positive bias was observed for wind speed and wind direction for both buoys.

The bias seen can be attributed to under- or over-estimation of winds by the scatterometer in the event of low and high winds, respectively. The RMSD of AD02 observed to be lower than for CB02. A good agreement between AD02 and OSCAT winds can be observed. This may be due to the dataset characteristics: as at CB02 the data recording interval is hourly, the preceding and succeeding winds are considered while averaging and comparing to OSCAT winds. In the case of AD02, the data are recorded at 3 h intervals, with no averaging of winds, and thus the effect of preceding and subsequent winds is not considered. In addition, other mechanisms may be involved, such as waves, air-sea interactions, and humidity flux variation (Bourassa, et al. 1999; Barthelmie, et al. 2010) that can influence the wind regime. This

phenomenon needs to be investigated and quantified, but is beyond the scope of the present work.

Table 3.14: RMSD and Bias for OSCAT winds against buoy winds (scenario 2)

Buoy versus OSCAT					
Buoy	No. of collocated points	RMSD		Bias	
		Wind speed ( $\text{m s}^{-1}$ )	Wind direction ( $^{\circ}$ )	Wind speed ( $\text{m s}^{-1}$ )	Wind direction ( $^{\circ}$ )
AD02	120	2.2	22.35	0.23	0.14
CB02	110	2.4	22.40	0.11	0.18

The scatter plots for OSCAT and buoy winds are shown in Fig. 3.12. In the case of OSCAT winds versus AD02 winds, there is considerable dispersion from the  $45^{\circ}$  line for low buoy winds, and better agreement can be observed for winds in the range  $5\text{--}8 \text{ m s}^{-1}$ . OSCAT winds show good agreement with AD02 winds in the range  $7\text{--}12 \text{ m s}^{-1}$ . At CB02, from the scatter plot it can be seen that points are distributed around the  $45^{\circ}$  line. For wind speeds up to  $5 \text{ m s}^{-1}$ , it can be seen that the points are distributed above the  $45^{\circ}$  line clearly representing over-estimation of wind speeds. For wind speeds in the range of  $5\text{--}10 \text{ m s}^{-1}$ , the uniform distribution can be seen around the  $45^{\circ}$  line with few outliers (y-axis). Since, there were hardly wind speeds  $> 10 \text{ m s}^{-1}$  observed at CB02, it was difficult to understand the trend. In general, the winds measured at CB02 were found to be lower in magnitude than those at AD02. At AD02, the winds are generally high and uniform in nature and are concentrated within the range  $7\text{--}12 \text{ m s}^{-1}$ . At AD02, the wind observations are 3-hourly averaged and some outliers ( $>12 \text{ m s}^{-1}$ ) can be seen on the graph (y-axis), which may be attributed to spikes in measurement.

Also, there may be the influence of rain on scatterometer data, which causes overestimation and lower agreement (Stiles and Yueh 2002; Kumar et al. 2013). However, this effect is limited to fewer data since the RMSD is less ( $2.2 \text{ m s}^{-1}$ ). The scatter plot of wind direction measurements is shown in Fig. 3.13. There is symmetry between OSCAT and buoy recordings. The bias was found to be small and RMSD was observed to be approximately  $22^{\circ}$ . Considering the southwest monsoon season of

June–September 2011, the OSCAT wind direction measurements are in accordance with the buoys, and within the mission limit of around 20°.

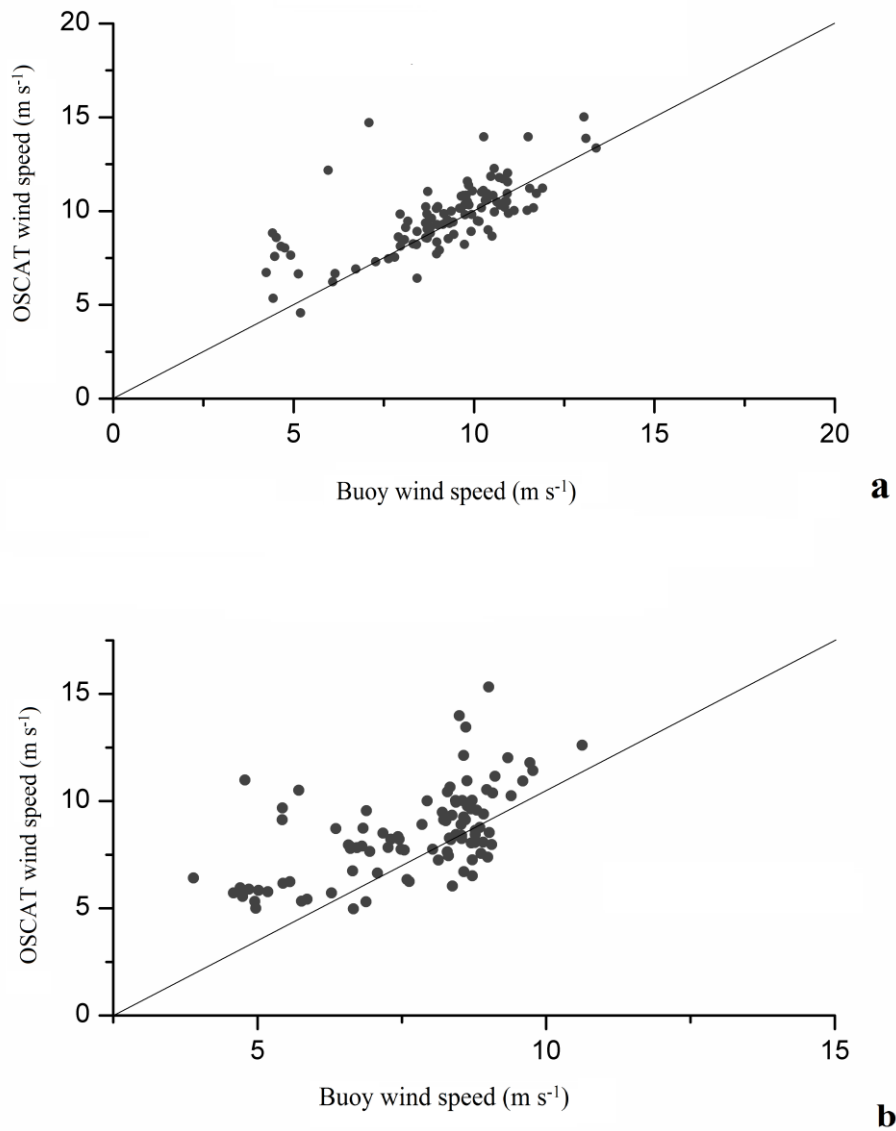


Fig. 3.12: Scatter plot of buoy (a) AD02 (b) CB02 against OSCAT wind speeds

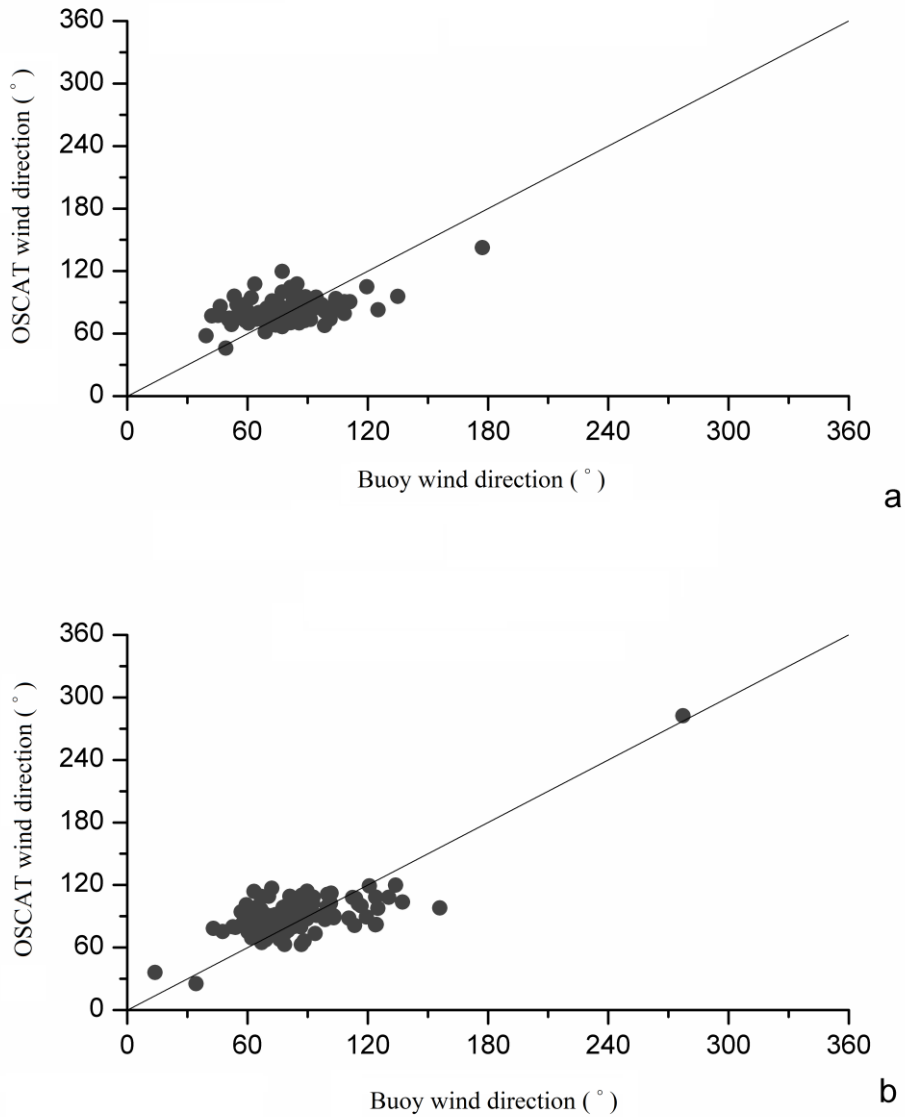


Fig. 3.13: Scatter plot of buoy (a) AD02 (b) CB02 against OSCAT wind direction

The scatter plot of residual wind speeds,  $dW$  (OSCAT–buoy ENW) and residual wind direction,  $dD$  (OSAT–buoy) against observed buoy wind speed (3 m) is shown in Fig. 3.14 and 3.15. These figures also show the dependence of residual wind speed and direction over wind speeds measured at the buoys. The residual wind speeds in the case of AD02 are uniformly scattered: for low wind speeds ( $<4 \text{ m s}^{-1}$ ), high residual winds are observed and the maximum difference is around  $5 \text{ m s}^{-1}$  winds; for wind speeds in the range  $5\text{--}12 \text{ m s}^{-1}$ , the magnitude of residual winds is less. High winds

(>12 m s<sup>-1</sup>) are limited in occurrence and the scatterometer may underestimate wind speeds >15 m s<sup>-1</sup> (Kumar et al. 2013).

In the case of CB02, the concentration of winds is in the range 5 to 10 m s<sup>-1</sup> and the residual wind magnitude is low within the range. For low speeds (<4 m s<sup>-1</sup>), as expected the scatterometer overestimated and hence higher residual values and maximum difference were observed in this range. No high winds (>12 m s<sup>-1</sup>) were observed at CB02. Thus, a positive dW implies the scatterometer overestimation while a negative dW suggests under estimation. Symmetry in wind direction data was observed between OSCAT and the buoys. Uniform scattering and bias can be observed along the wind axis, as seen in Fig. 3.15. From the analysis, it will be noted that the mission requirements of OSCAT (i.e. RMSD of less than around 2 m s<sup>-1</sup> for wind speed and less than around 20° for wind direction) are satisfied, and hence the wind vectors retrieved from OSCAT over the Arabian Sea are accurate enough to be used for further studies.

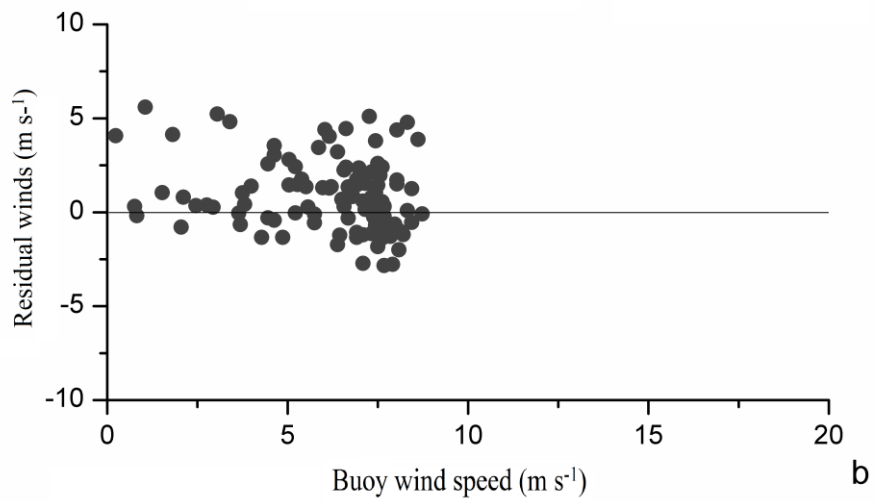
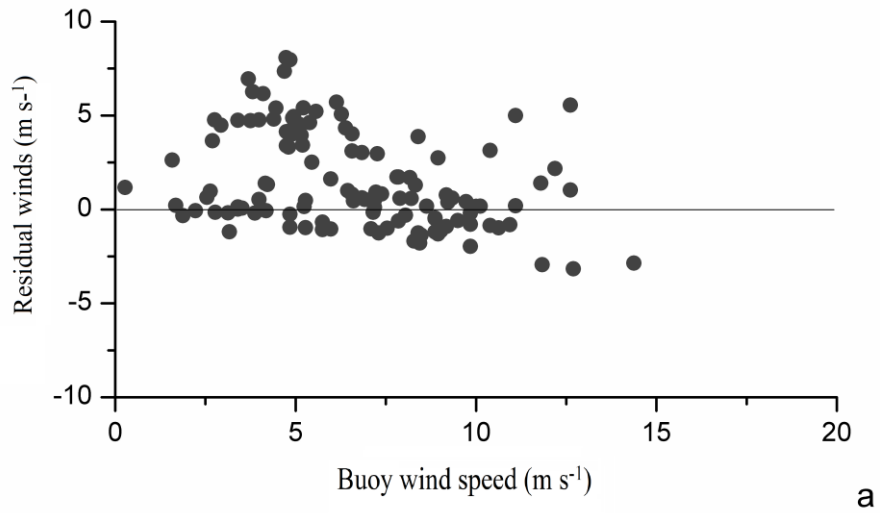


Fig. 3.14: Scatter plot of residual versus buoy (a) AD02 and (b) CB02 wind speeds



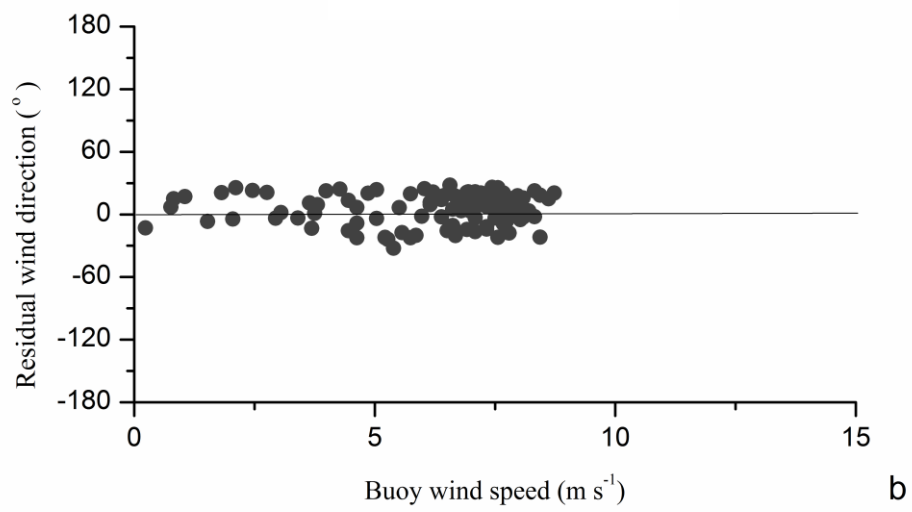
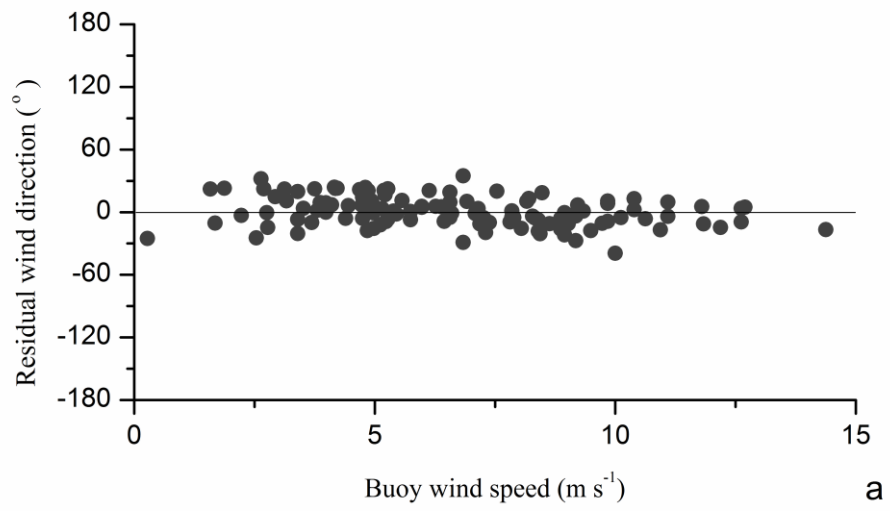


Fig. 3.15: Scatter plot of residual versus buoy (a) AD02 and (b) CB02 wind direction

### 3.3.3 Wind maps

Spatial wind speed maps are developed in the ArcGIS environment for the monsoon months (June–September) of 2011. Generally, the Kriging method of interpolation is applied to obtain spatial interpolation (Johnston, et al. 2001; Childs, 2004). The Kriging method assumes that the distance between points reflects a spatial correlation that can be used to explain variation in the surface (Luo, et al. 2008; Sliz-Szkliniarz and Vogt 2011). Ordinary Kriging with a semivariogram (spherical model) is used for calculating estimates of the surface at the grid points. The raster maps so generated have wind speeds ranging from 6 to 13 m s<sup>-1</sup>. The red color scheme in the legend indicates the zone of maximum wind speed and green indicates that of lower wind speed, as shown in figures 3.16 to 3.19. The arrows in the images represent monthly averaged OSCAT data. The orientation of arrows represents the wind direction, and their length indicates wind intensity.

The development of wind maps can be helpful in understanding the distribution of wind, variation in space, and in identifying pockets of high wind. This can be a preliminary step towards the identification of sites of importance for energy harnessing. Once a site is identified, the instruments required for high-precision (in both time and space) in situ data acquisition can be installed, thus providing an economically viable solution for the micrositing process. The interpolated wind speeds in the month of June were in the range of 8 to 12 m s<sup>-1</sup>, for July the wind speeds varied from 7 to 12 m s<sup>-1</sup>, in the August month the wind speed were observed to be in the range of 6 to 10 m s<sup>-1</sup> and in September month the wind speeds were found to vary from 6 to 8 m s<sup>-1</sup>. From the maps it can be observed that, as the monsoon progresses from June to September, there is an increase in area of wind speed in the range of 6 to 9 m s<sup>-1</sup>. Spatially high winds prevail off the coast and nearby to the coasts of Maharashtra, Goa, and Karnataka states, India.

The monthly winds at buoy location AD02 are higher than at buoy CB02, as noted from Table 3.15. Thus, by point location data the inference may be drawn that there is a decrease in wind speed from deep ocean to shallower ocean depths. On the other hand, it can be observed from the maps that nearer to the coast, there is an increase in wind speed and concentration of winds in the range 6 to 10 m s<sup>-1</sup>.

Table 3.15: Monsoon period maximum and minimum OSCAT and buoy wind speeds

Month of 2011	AD02		CB02	
	Max ( $\text{m s}^{-1}$ )	Min ( $\text{m s}^{-1}$ )	Max ( $\text{m s}^{-1}$ )	Min ( $\text{m s}^{-1}$ )
June	13.3	1.8	9.30	1.1
July	15.3	2.8	12.48	2.0
August	14.4	3.2	12.42	2.8
September	14.8	2.4	10.31	1.4

Therefore, the inference based on the buoy data that there will be a continuously decreasing trend in winds towards the coast was contradicted by OSCAT data. OSCAT data may lead to the inference that wind speeds increase with the monsoon and decrease subsequently.

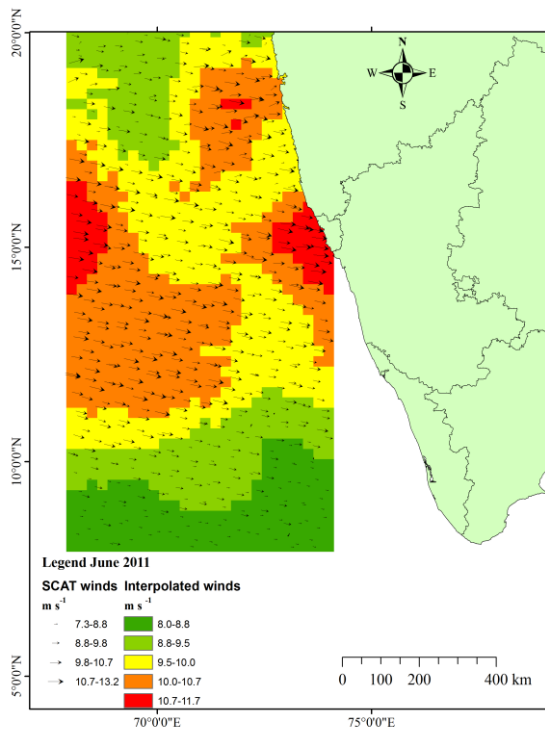


Fig. 3.16: Spatial wind map at 10 m for June 2011

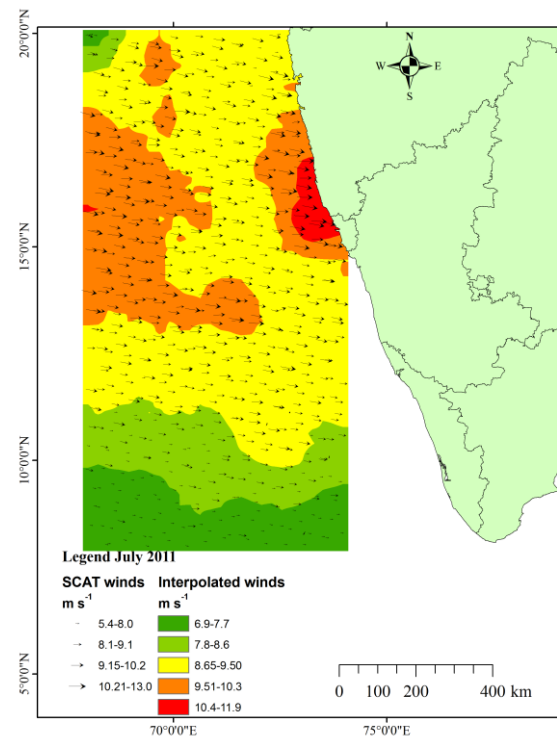


Fig. 3.17: Spatial wind map at 10 m for July 2011

The concentration of high wind speeds is maximal near the coast. This effect may be due to the complex phenomenon existing in the offshore environment involving the interaction of land and sea breezes which is beyond the scope of this work. Thus, greater focus for power calculations should be on the areas of high-intensity winds.

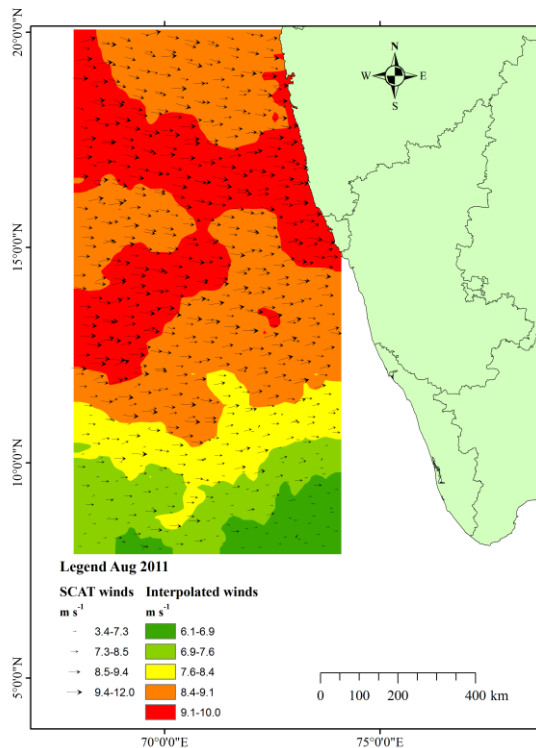


Fig. 3.18: Spatial wind map at 10 m for August 2011

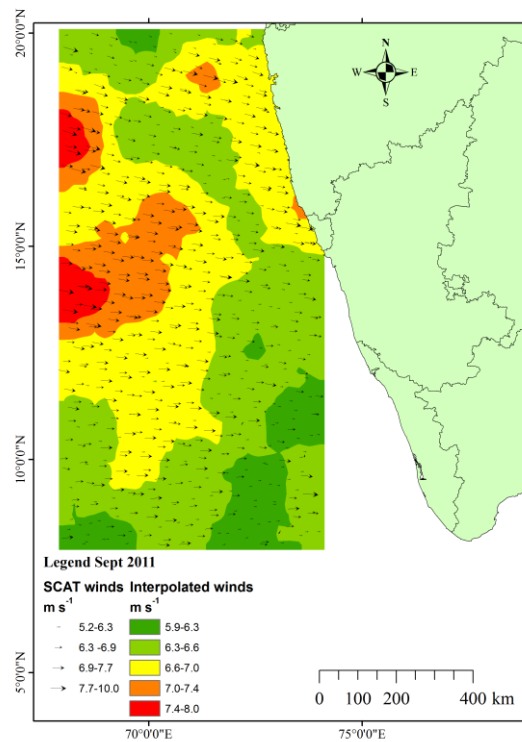


Fig. 3.19: Spatial wind map at 10 m for September 2011

Wind speeds at hub height of 90 m or higher are required to be evaluated and the correspondingly wind power generation by turbine need to be assessed. From the maps, the areas colored yellow–orange and red represent strong winds throughout the monsoon season, and thus indicating that the turbines in this region would be operational for most of the season. At higher altitudes, the wind speed will be even greater, requiring consideration at the design stage of the issues of wind turbine safety and efficiency. Detailed in situ measurement at different heights is required for a period of 1–2 years to validate the predicted wind speeds and wind power.

### **3.4 REGIONAL SCALE OFFSHORE WIND POWER RESOURCE ASSESSMENT USING OCEANSAT-2 SCATTEROMETER WINDS**

#### **3.4.1 OSCAT data comparison with IRAWs ship data**

Collocation between OSCAT and IRAWs data was carried out based on spatial window of  $0.5^\circ$  and temporal window of  $\pm 60$  min. The OSCAT data from both swath retrievals (ascending and descending) are used for the accuracy assessment. The IRAWs data at 10 m above sea level was estimated by using logarithmic method. OSCAT is known to perform best in wind speed range of 4 to  $24 \text{ m s}^{-1}$  so the IRAWs data was truncated to the same range and filtered data (62 number of observations) was used. Kriging interpolation technique was applied to OSCAT data to obtain wind speeds at collocated points. Fig. 3.20a shows the plot of OSCAT versus IRAWs wind speeds at 10 m height above sea level. From the plot, it can be observed that there is good correlation between two data sets for winds in range of  $5$  to  $10 \text{ m s}^{-1}$ . From the analysis, it was found that  $\text{RMSE} = 1.9 \text{ m s}^{-1}$  and (correlation coefficient)  $R = 0.6$ .

Further, similar approach was adopted to assess the directional accuracy. Fig. 3.20b represents the plot of OSCAT wind direction versus IRAWs wind direction observations. From the plot, it can be observed that there is good agreement between the direction measurements,  $R = 0.6$  and the RMSE was around  $20^\circ$ . However, better correlation can be achieved with increase in temporal resolution and with more number of observation vessels in the Arabian Sea. The advantage of considering IRAWs ship observations over buoy observations is that the observation points are spatially well distributed in study area and thus contribute to improved accuracy assessment of OSCAT data. Mission limits for the Oceansat-2 scatterometer data are  $\pm 2 \text{ m s}^{-1}$  for wind speed and  $\pm 20^\circ$  for wind direction. Thus, it can be inferred that the scatterometer data is accurate and within mission limits for the study area. The validated OSCAT data can be further incorporated in assessment of wind speed and wind power at hub heights.

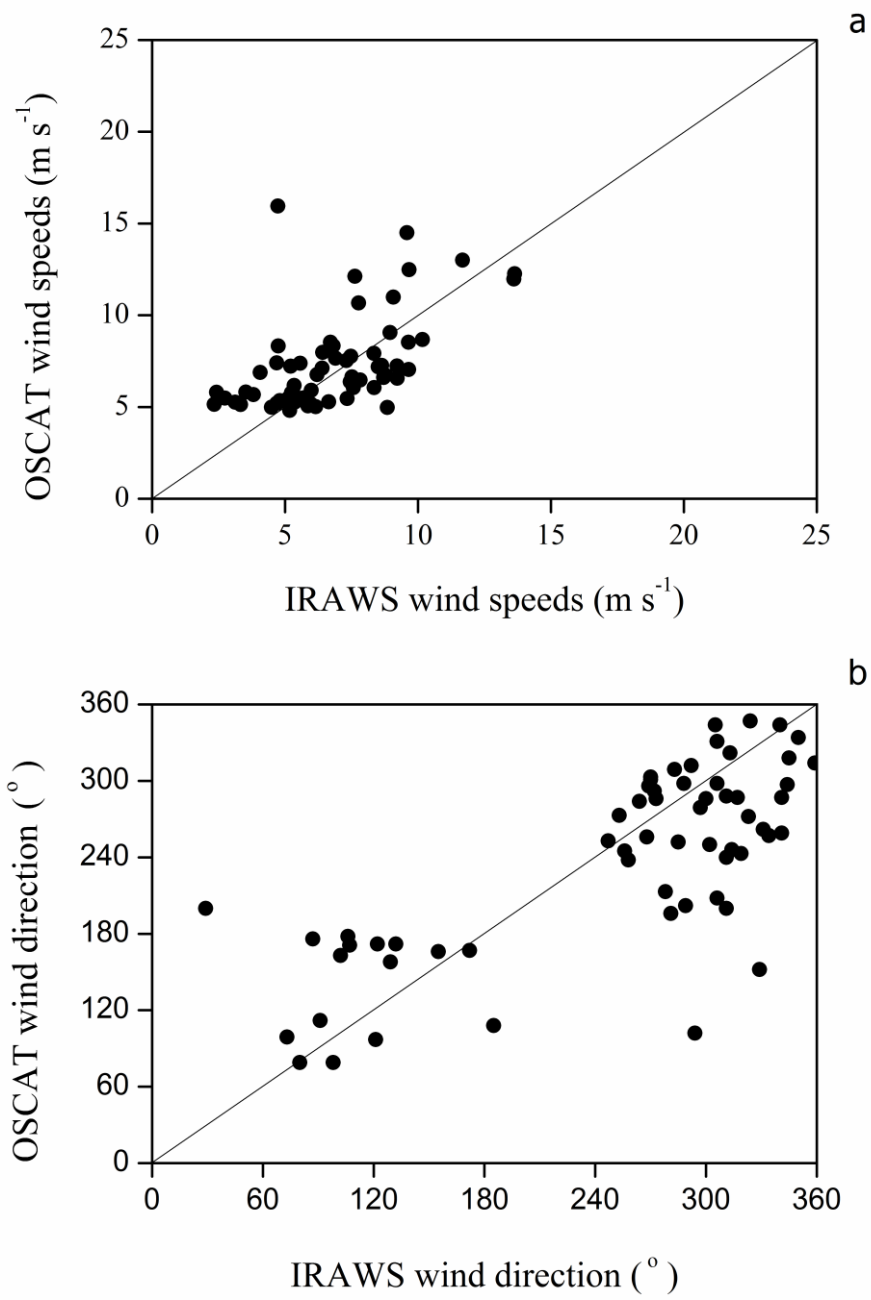


Fig. 3.20: Comparison of OSCAT and IRAWS (a) wind speeds and (b) wind directions

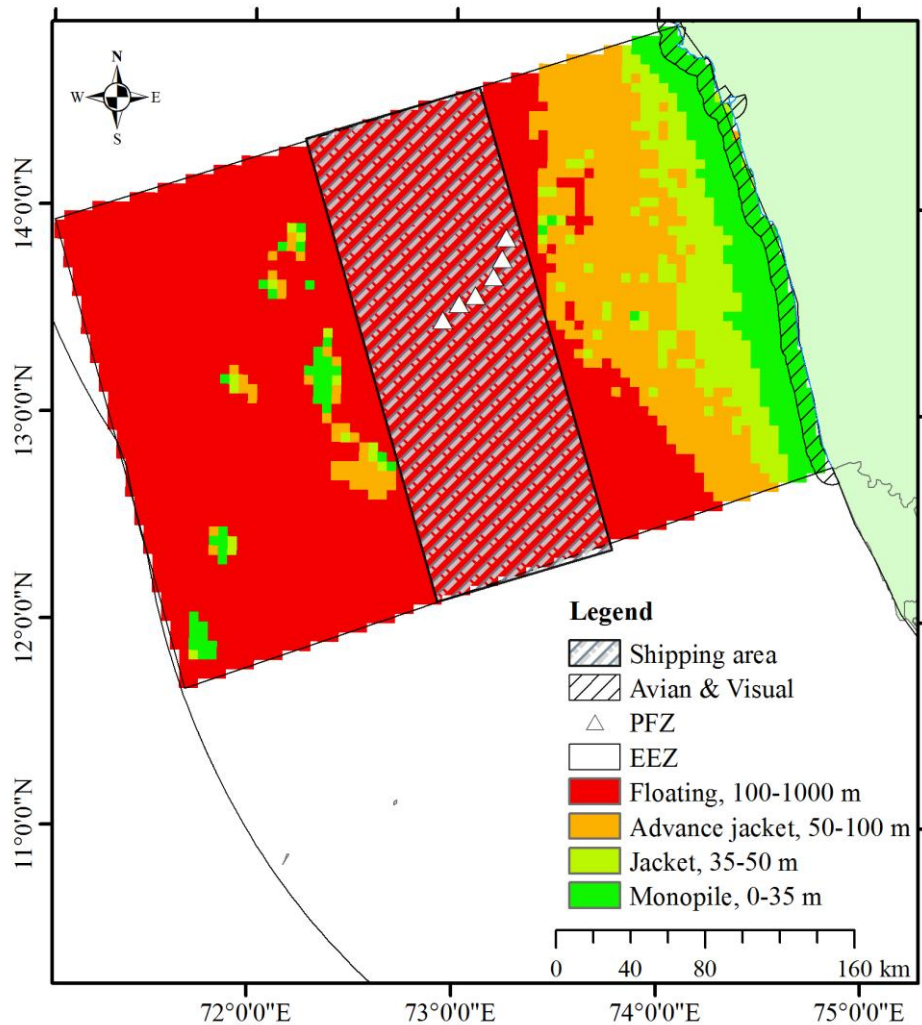


Fig. 3.21: Exclusion zones and shipping exclusion area for study area

### 3.4.2 Mapping Available Area

The exclusion zones help in reducing the conflicts with different types of sea users. Exclusion zones play vital role in wind power potential assessment studies as they directly influence the wind farm development. The exclusion zone of 10 km parallel to coastline has been considered for Tourism, Beach recreational activities, Avian and Visual zones. Fig. 3.21 represents the exclusion zones considered in the study. The 10 km limit in the map is labeled, as Avian and Visual, would be sufficient for the above exclusions. In Karnataka, the beach tourism may not extend beyond 10 km and is restricted to very few locations. The visibility over waters beyond 10 km can be considered as low, thus the viewshed may be less affected. However, the aesthetics

and impact on local residents and livelihood may require a social survey, which can be conducted in future.

Further, major exclusion should be considered for fishing activity and ship traffic. These are among the two major activities in the Arabian Sea. In Fig. 3.21, the PFZ locations as per INCOIS advisory are represented as triangular points. The shipping zone is marked by rectangular shaded area. Since the exclusion zone is in deep waters, the impact on wind energy development may be less as foundation technology for offshore turbines at deeper water depths is still in prototype stage and major studies are focused offshore wind farm development up to 100 m water depth.

### 3.4.3 Calculating Capacity Factor (CF) for turbine

The wind speeds averaged over two years (2011 and 2012) were obtained and this averaged wind speed data was then plotted over study area. By Kriging interpolation, smooth spatial distribution of winds over study area was obtained. The magnitude of interpolated winds in the study area was in range of 5.5 to 10 m s<sup>-1</sup>. Thus the average value of 7.8 m s<sup>-1</sup> was adopted and by equation (2.9) the CF was estimated. The CF (for REpower 5 MW turbine) was estimated to be 0.32. However, losses like wake effect and turbine availability have to be considered while calculating the generation capacity. Accounting these effects (assuming 10% wake effect and 90% availability) (Sheridan, et al. 2012) the adjusted CF was found to be 0.27. Thus the CF (=0.27) value was used in power generation capacity calculation.

### 3.4.4 Mapping Wind Potential

Monthly averaged OSCAT winds over the study area were computed. Histograms of the winds obtained were computed in bins of 1 m s<sup>-1</sup>. Fig. 3.22 presents the histograms for two years (2011 and 2012). From the figure, it can be noticed that winds during the year 2012 were stronger than in year 2011. During the year 2011, the concentration of OSCAT winds in 0-5 m s<sup>-1</sup> range was high, whereas for the year 2012, prevailing winds were in the range of 5-10 m s<sup>-1</sup>. The wind speeds between 7 and 11 m s<sup>-1</sup> are generally seen during the southwest monsoon period (June to September) (Tyagi and Pai, 2012; Pai and Bhan, 2013). During year 2011, the delayed



monsoon and early withdrawal in comparison to the monsoon period during year 2012, may be one of the reasons for smaller number of high winds ( $> 6 \text{ m s}^{-1}$ ) in 2011. For remaining part of the year, the winds are generally in the range of 5 to  $10 \text{ m s}^{-1}$  at 10 m, which may be considered as favorable wind speed range for operation and development of offshore wind farm.

The OSCAT winds at 10 m represented in Fig. 3.23a, are averaged winds over two years (2011 and 2012) for the study area. These winds were then used to develop the spatially interpolated map using kriging technique in ArcGIS 9.3. The interpolated wind speeds range from  $4.9$  to  $9.4 \text{ m s}^{-1}$  and relative color scheme from yellow to red can be seen in the figure. Correspondingly, the contour lines on the map represent the particular wind speed magnitude in the area. It can be observed that high magnitude winds are available near to coast and in deeper waters. Average wind speeds of magnitude approximately  $7 \text{ m s}^{-1}$  are distributed at central region of the study area. Log method is then applied on the 10 m OSCAT winds to extrapolate wind speeds up to turbine hub height of 90 m. The extrapolated winds are then spatially interpolated using Kriging technique in ArcGIS 9.3. The Kriging technique assumes that the distance between points reflects a spatial correlation that can be used to explain variation in the surface (Gadad and Deka, 2015).

In the study, Kriging with a semivariogram (spherical model) was used for calculating estimates of the surface at the grid points, hence the smoothed raster map (Fig. 3.23 a and b) was obtained. The contours overlaid on the interpolated map specifies wind speed magnitudes in the region. Spatial distribution of 90 m interpolated winds can be seen in Fig. 3.23b. The OSCAT winds at 90 m vary from  $5.9$  to  $11.3 \text{ m s}^{-1}$ . The high winds,  $>10 \text{ m s}^{-1}$  are concentrated in deeper water depths. Average winds (about  $6-9 \text{ m s}^{-1}$ ) can be seen around the coast, lower winds ( $< 6 \text{ m s}^{-1}$ ) are concentrated in southern region of study area. Focus on wind farm development should be considered in area of average winds ( $6-9 \text{ m s}^{-1}$ ) and nearer to the coast.

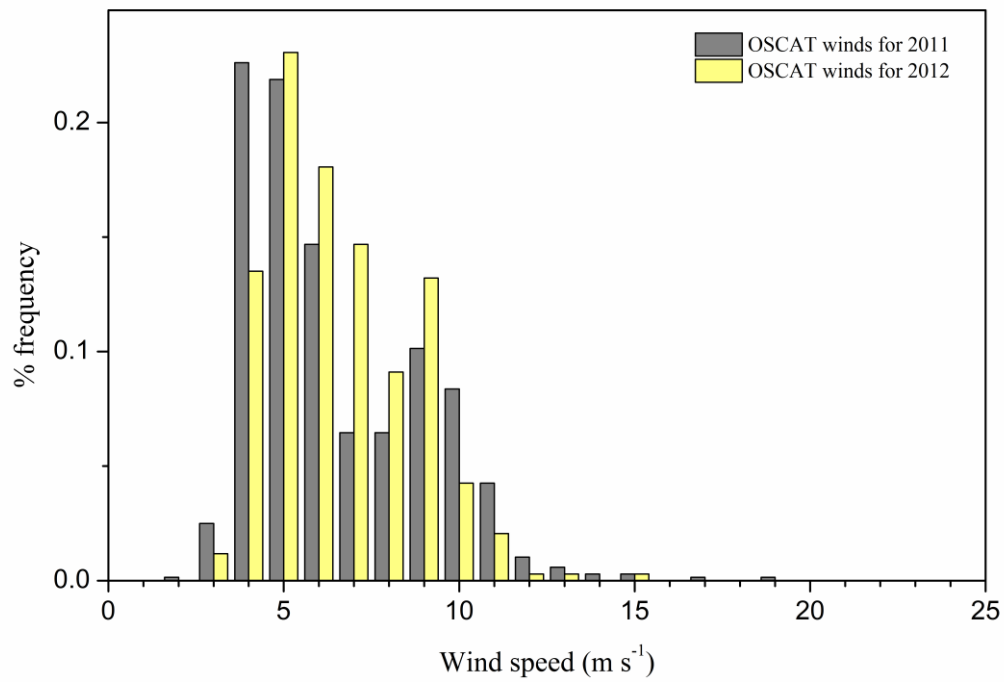


Fig. 3.22: Histograms of monthly averaged OSCAT winds for the study area

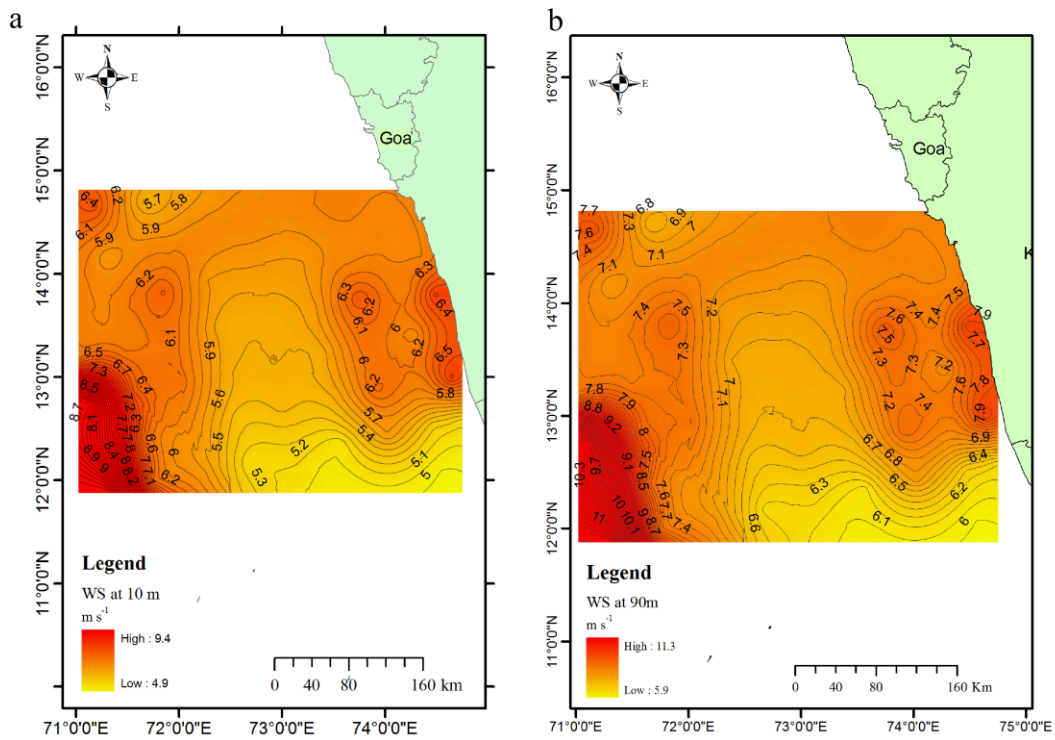


Fig. 3.23: OSCAT Winds at (a) 10 m and (b) 90 m over the study area

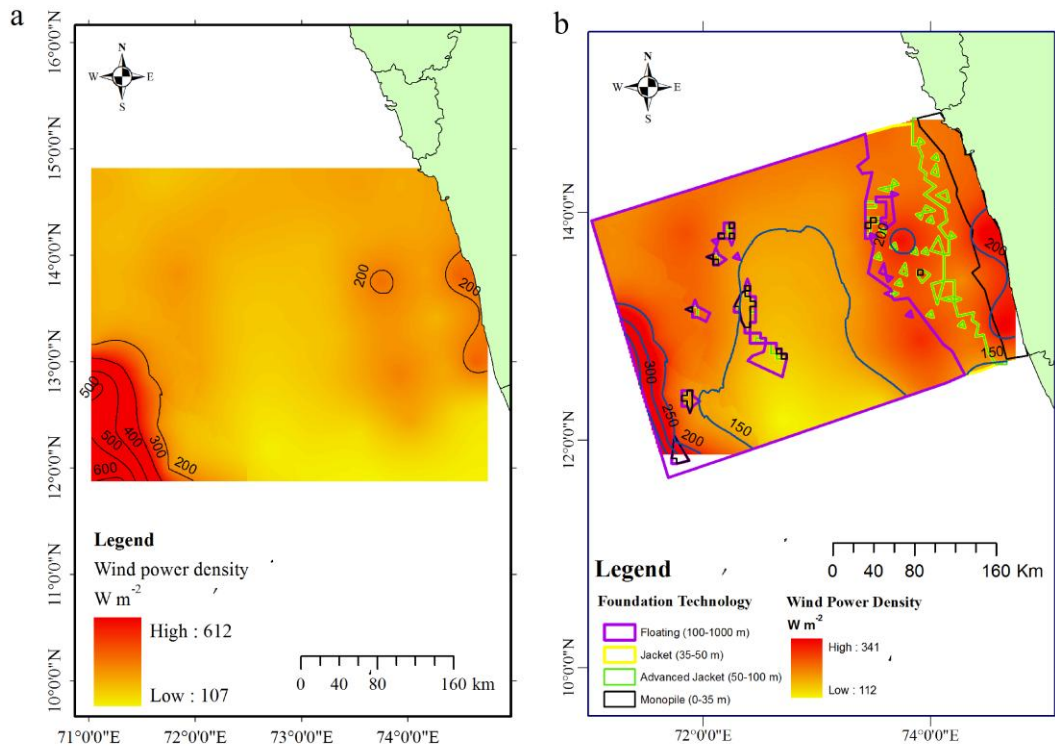


Fig. 3.24: (a) WPD at 90 m over the study area. (b) Classification of WPD (at 10m) based on foundation technology depths

Wind Power Density (WPD) has been approximately calculated based on the 90 m OSCAT wind data using equation (2.7). Then the WPD was spatially interpolated over the study area as seen in Fig. 3.24a. The power density ranges between 107 and 612  $W m^{-2}$ . The high power density (around 612  $W m^{-2}$ ) can be observed in lower left region of the study area and low power density (around 107  $W m^{-2}$ ) can be seen in lower right region of the figure. Contour lines are plotted representing the magnitude of WPD along the lines in the area. From Fig. 3.24a, it can be observed that major portion of study area has uniform variation in WPD distribution.

National Renewable Energy Laboratory (NREL), USA provides with the classification of WPD (NREL class) at 10 m and 50 m over land surface. The major factors influencing the wind power class are -

- a) the abundance and quality of wind data,
- b) the complexity of the terrain, and
- c) the geographical variability of the resource.

Based on the classification, NREL suggests that, wind power class 2 and above are favorable for installation of wind turbines. The classification of WPD has been presented in table 3.16

Table 3.16: Classes of wind power density at 10 m and 50 m (source: [http://www.nrel.gov/gis/wind\\_detail.html](http://www.nrel.gov/gis/wind_detail.html))

Wind Power Class	10 m		50 m (extrapolated using (1/7) <sup>th</sup> power law)	
	Wind Power Density (W m <sup>-2</sup> )	Wind Speed (m s <sup>-1</sup> )	Wind Power Density (W m <sup>-2</sup> )	Wind Speed (m s <sup>-1</sup> )
	0	0	0	0
1	100	4.4	200	5.6
2	150	5.1	300	6.4
3	200	5.6	400	7.0
4	250	6.0	500	7.5
5	300	6.4	600	8.0
6	400	7.0	800	8.8
7	1000	9.4	2000	11.9

Over the ocean surface the terrain complexity is almost non-existent, the offshore winds are abundant, satellite data provides for almost total global coverage and good quality data. Thus, in order to quantize the energy present in offshore winds, WPD over the study area using OSCAT data (at 10 m) was coarsely estimated and interpolated using Kriging technique, which was further classified according to water depth classes mentioned in table 2.4. The classified WPD map as seen in Fig. 3.24b, was developed considering Fig. 2.14 as reference. The polygons in the map represent the boundary for each water depth class. From the figure, WPD is seen varying from 112 to 341 W m<sup>-2</sup>. The contours plotted (blue lines) on the map represents the magnitude of WPD along the line. Considering the recommendations from NREL class, it is assumed that a threshold WPD of 200 W m<sup>-2</sup> (as minimum) is prerequisite for setting up of offshore wind turbines. Thus in the study area, regions with WPD ≥ 200 W m<sup>-2</sup> can be considered as potential areas for offshore wind farm development.

These areas fall under monopile foundation (0-35 m) and floating foundation (100-1000 m) type. More research is needed to explore the monopile foundation depth class in detail, as it is technologically well-established and closer to coast. It is also necessary to assess the power production potential over entire study area for different foundation technologies for future developments.

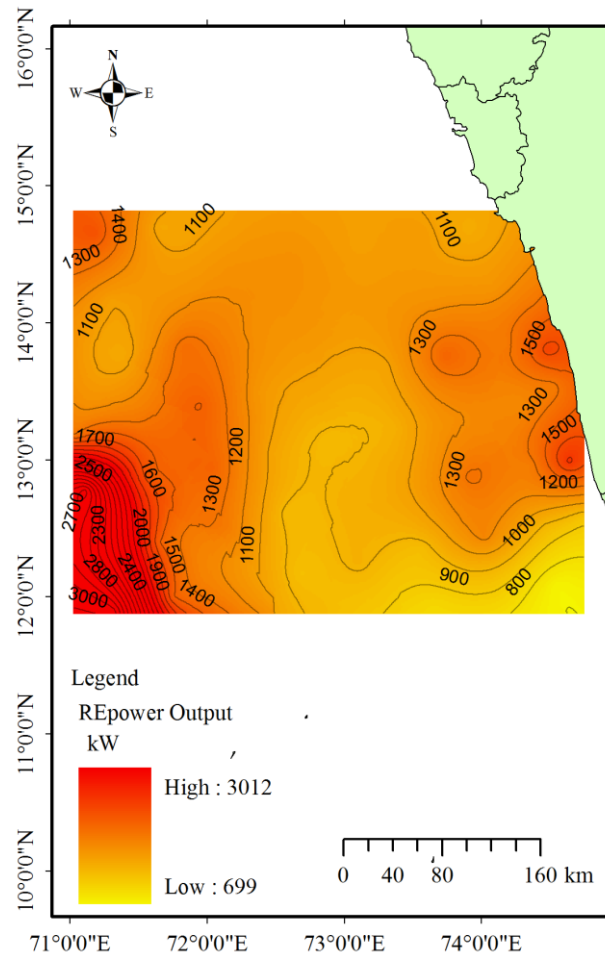


Fig. 3.25: Wind power output based on REpower 5 MW turbine

The power production and the spatial distribution of wind power over study area is represented in Fig. 3.25. The contour lines indicate the average power that can be produced when REpower 5 MW turbine is placed along a particular contour in area. The average output varies from 699 to 3012 kW. Since the focus is up to 100 m water depth, the potential areas for wind turbine can be from 13N to 14N latitude and around 74E longitude. The WPD classification (Fig. 3.24b) also implied that this region exhibits high wind potential. Further the average output in the target area is between 1300 and 1500 kW. The selected area is nearer to the coast and a control

centre is located near Padubidri town, bearing coordinates 13.08N 74.8E. Therefore the transmission, refinement and energy storage processes may be cost-effective for developing wind farm in the area. The map shows large potential (max up to 3000 kW) in deep water depths. In future, this area may be accessed and harnessing energy may be economical.

The next step to be outlined after the estimation of resources, would be placing of wind turbines in the most efficient way to optimize the energy production and reduce losses. This process requires knowledge of wind direction and variation occurring with respect to seasons. The wind direction data from OSCAT over study area was averaged season wise for two years (2011 and 2012). The OSCAT wind direction data was divided in to  $10^\circ$  intervals and 36 bins were obtained. The data was segregated in to three seasons as (a) Pre-Monsoon season (February to May), (b) Monsoon season (June to September) and (c) Post-Monsoon season (October to January). The seasonal rose plots of OSCAT winds are shown in Fig. 3.26. The color scheme represents the magnitude of wind speeds. Winds are strong during monsoon period ( $4$  to  $16 \text{ m s}^{-1}$ ) and are eastwards, almost perpendicular in direction to the Karnataka coast. Post-monsoon season winds are majorly towards south, with  $4$ - $8 \text{ m s}^{-1}$  winds prevailing. In pre-monsoon season winds are towards eastwards and in mostly in range of  $4$  to  $12 \text{ m s}^{-1}$ . Wind speeds prevailing above  $6 \text{ m s}^{-1}$  and consistent wind direction, will help to infer that turbine will be working for most part of seasons and aid in layout design.

For optimized power production turbines may be positioned in rows, 5 times rotor diameters apart crosswind and 10 times rotor diameters apart downward wind (Sheridan, et al. 2012). The array spacing for REpower 5 MW can be calculated by-

$$\text{Array Spacing} = (\text{rotor diameter})^2 \times \text{DSF} \times \text{CSF} \quad (3.2)$$

Downward Spacing Factor (DSF) = 10 times rotor diameter.

Crosswind Spacing Factor (CSF) = 5 times rotor diameter.

The equation (3.2) yields value of  $0.794 \text{ km}^2$ . Based on this spacing, the number of turbine units in estimated for each water depth class in the study area. Table 3.17 records the water depth classification and corresponding number of turbines in each class, nameplate generation capacity and average output (obtained by multiplying nameplate capacity and CF). The CF (= 0.27) used for calculation of average output

includes wake effect losses and turbine availability. The output represents average annual power production capacity.

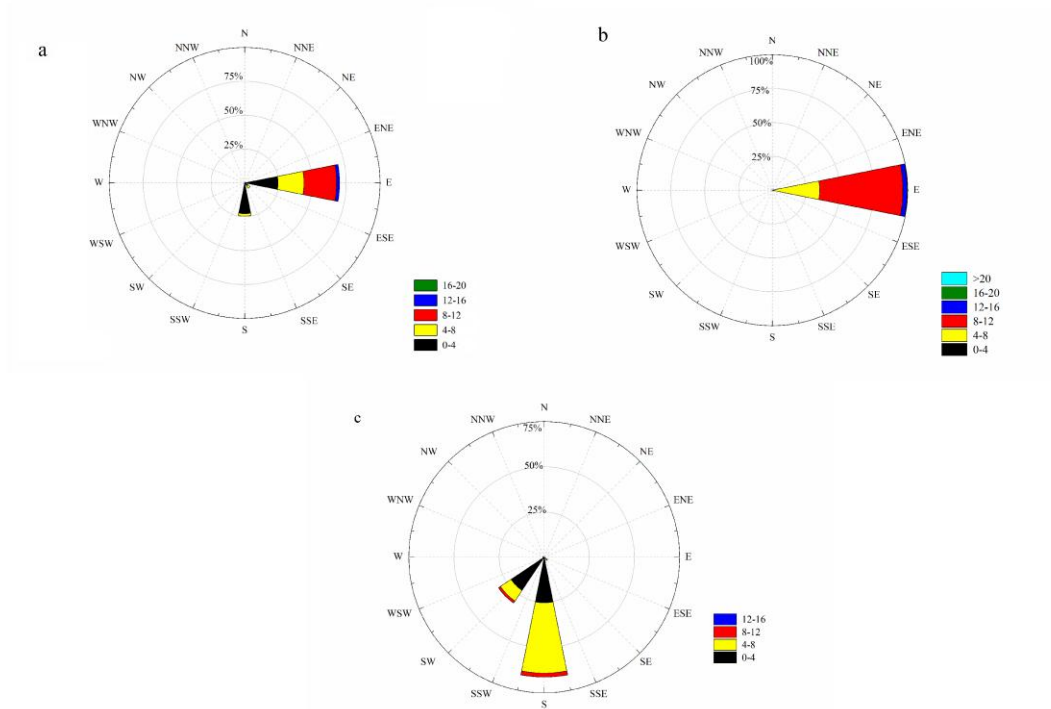


Fig. 3.26: Seasonal rose plots of OSCAT wind direction: (a) Pre-monsoon (b) Monsoon (c) Post-monsoon

The average output is expressed in terms of kW or MW in the present work, however the units generally used in power industry are expressed in terms of kWh or MWh per year. In order to get the output in kWh or MWh per year, the average output can be multiplied by 8760 hours per year.

The energy deficit for FY 2011-12 was 777 kW as per CII Karnataka-2012 report and the anticipated power deficit data for FY 2014-15, is 1142 kW as per Load Generation Balance Report (LGBR- 2014) by CEA, India. Considering the power generation capacity of 9.09 GW in the Monopile foundation class, if 10% of the estimated potential is developed as phase-I development, then the %power supply that offshore wind power can meet the current and anticipated power deficit have been tabulated in Table 3.17.

Table 3.17: Depth wise available area, power potential and annual output

Water depth (m)	Available Area (km <sup>2</sup> )	No. of Turbine Units	Generation capacity (MW)	Average Output (MW)	Annual Energy Deficit	Proposing 10% of potential (MW)	% Wind power supply for deficit
0 – 35	5156	6494	32469	9091.18	777 MW	909.11	116.9
35 – 50	6641	8364	41820	11709.57	(for FY 2011- 12)	1170.95	150.5
50 – 100	13435	16921	84603	23688.92	source: CII	2368.89	304.7
100 – 1000	66742	84058	420290	117681.11	Karnataka, 2012	11768.11	1514.5
0 – 35	5156	6494	32469	9091.18	1142 MW	909.11	79.6
35 – 50	6641	8364	41820	11709.57	(for FY 2014- 15)	1170.95	102.5
50 – 100	13435	16921	84603	23688.92	source: CEA,	2368.89	207.3
100 – 1000	66742	84058	420290	117681.11	2014	11768.11	1030.5

Considering the massive potential in 0-35 m water depth, turbines in Monopile foundation class can be instrumental in initiating the development of offshore wind farms in the state. Thus in Table 3.17, it is suggested to the state that by developing 10% of the estimated potential, 116% of energy deficit in FY 2011-12 and up to 79% of the energy deficit for FY14-15 can be met by 5 MW turbines in Monopile foundation class. The purchase of electricity and dependency on other short-term sources can be reduced, consecutively reducing the expenditures. The potential available can be further developed to meet the future requirements and also by selling the surplus electricity to grid, the state would be able to generate revenue.

As presented in Table 3.18, the estimate of overall potential for the area of 91974 km<sup>2</sup> was approximately 162 GW considering that the wind farm development was extended up to EEZ zone, without subtracting area for any of the exclusion zones. However, after exclusions, the net available area for development was 66690 km<sup>2</sup>, the power generation potential was estimated to be 117 GW, which is an enormous energy resource.



Table 3.18: Wind Power potential for Karnataka coast before and after subtracting shipping conflict areas

	Available Area (km <sup>2</sup> )	No. of Turbine Units	Generation capacity (MW)	Average Output (MW)
Before excluding shipping zone	91974	115836	579181	162170.78
Excluding shipping conflict area	66690	83992	419962	117589.42

It is suggested that, further research and studies can be focused in Monopile (0-35 m) foundation region, since it may be more economically viable than other type of foundations. Therefore the deliverables with practical implementation from the study will be- (a) better accuracy assessment of OSCAT winds using IRAWS ship based observations and assessing wind resource at regional scale. (b) GIS based methodology for understanding of spatial distribution of wind resource over study area that could be adopted for other offshore regions. (c) Setting a threshold limit of power density and identifying feasible potential zone for development of offshore wind farm. (d) OSCAT data based estimation of power generation capacity and optimal layout for the entire study area. Collaborating (c) and (d) identifying and recommending a possible region that can be developed. (e) Issue related to conflicts and exclusion zones required to minimize impact on operational exploitation of marine renewable energy (MRE). For the future scope of WRA study, it is suggested that meteorological masts can be established to obtain high frequency wind speed measurement at different heights, integrating multi-platform observations can lead to improved accuracy of WRA (Doubrawa, et al. 2015). Also, due to turbine availability losses and quality of wind speed measurement, there can be uncertainty in the estimation of the annual energy production (Jung, et al. 2013), which should be considered in future. Based on Fig. 3.25, the locations near to coast approximately around 13N and 14N latitudes have demonstrated a potential of 1300-1500 kW. More studies and in situ data are required to be carried out in this direction and wind farm development can be focused in this area.



## **CHAPTER 4**

### **CONCLUSION**

#### **4.0. GENERAL**

The study focused on evaluating the applicability of hybrid techniques for offshore wind speed estimation and obtaining short-term forecasts using buoy observations in the Arabian Sea. In addition, an investigation of influence of one atmospheric parameter such as Relative Humidity over the developed models was conducted. Then, the accuracy assessment of Oceansat-2 satellite, scatterometer (OSCAT) winds over the Arabian Sea using in situ buoy data was performed. The process required estimation of ENW (winds at 10 m above sea level) and consequently a best-suited method for obtaining ENW was established for the Arabian Sea. Scatterometer winds validated using in situ data from real-time ship based observations (IRAWS), were then incorporated in to satellite-based regional scale, offshore wind power resource assessment for the Karnataka state, India.

The key conclusions framed after results and discussions have been presented section wise, with brief summary for convenience. Also, limitations of the study and future scope of further studies are enumerated.

#### **4.1. SHORT-TERM OFFSHORE WIND SPEED FORECASTING USING ANFIS AND RELATIVE HUMIDITY INFLUENCE ON THE ACCURACY OF ANFIS**

The present study focuses on developing model using hybrid technique, to estimate and to obtain short-term wind speed forecasts in the Arabian Sea, which belongs to tropical humid climate zone. In addition, the objective of the work was to evaluate the performance of the developed model, with RH observations as input to the system, to estimate and forecast offshore wind speeds. Two buoys AD07 and CB02 were chosen for the study and multiple scenarios were developed to achieve the objectives of work. Persistence Method was considered to be the benchmark method to assess the accuracy of wind speed forecasts obtained from model 1 and 2.

1. From the scenario 1, it was found that the model 1 outperformed model 2 at both the buoy locations. There was a noticeable influence of RH observations over the ANFIS model performance, since the RMSE of model 2 was higher than model 1.
2. Further in scenario 2, wind speed forecasting with multiple time-steps was carried out. At AD07, it was found on comparing the RMSE and MAPE that the model 1 performed better than other two models. At CB02, the interval of data being hourly, it was observed that model 1 forecasts were closer to PM and the RMSE was lower than that of model 2. MAPE was high at CB02 wind speed forecasts with model 1 varying from 38% to 48% and 43% to 50% for model 2. The reason for low performance of ANFIS at CB02 may be associated with the statistics of wind speeds in the testing dataset and the fuzzy rules and subsets that are generated based on the inputs.
3. Further, the %error in RMSE between model 2 and 1 was computed and an averaged %error was suggested. The RMSE computed at AD07 would be approximately 37% higher and RMSE at CB02 would be approximately 14% higher when RH measurements are not available as input to the model to obtain wind speed forecasts up to three time steps.

#### *Salient Conclusions*

- a) The accuracy of wind speed forecasts of ANFIS model was found to be higher when RH measurements are available to the model.
- b) Statistics of the input datasets were found to influence the performance of the models.

## 4.2. SHORT-TERM FORECASTING BY ANFIS AND WAVELET-ANFIS HYBRID TECHNIQUES

In the present study two buoys (AD07 and CB02) were selected and the dataset from previous section was adopted. The selected buoy have different location and have different time interval of recording offshore wind speeds. Thus the methods considered for forecasting were subjected to multiple scenarios. Focus was on hybrid methods like ANFIS and combination of wavelet transform and ANFIS (WT+ANFIS) methods. Persistence method (PM) was considered as the benchmark method to assess the accuracy of forecasts obtained by the hybrid methods.

1. The modeling capability of ANFIS was studied with Gaussian MF type and three-membership function (low, medium, high). The RMSE for both buoy locations (training and testing) dataset was found to be less than  $1 \text{ m s}^{-1}$ . MAPE was found to be around 24% for AD07 and around 30% for CB02. The scatter plot indicated that the points are well distributed along  $45^\circ$  line. Then ANFIS was employed for wind speed forecasting with three lead-time steps. The RMSE of wind speed forecasts for testing dataset at AD07 was found to vary from  $1.3$  to  $1.59 \text{ m s}^{-1}$  for (t+1) to (t+3) time steps. At CB02, the RMSE was found to vary from  $1.26$  to  $1.72 \text{ m s}^{-1}$  for (t+1) to (t+3) time steps for the testing dataset.
2. The WT+ANFIS model, wavelet *db8* for AD07 and wavelet *db7* for CB02 were found to be the closet to the observed wind speed and correlation coefficient (R) was found to 0.98 and 0.97 respectively. The maximum decomposition level was calculated to be 4. L3 decomposition produced more accurate forecasts than the other decomposition levels. The forecasts obtained at AD07, for testing dataset showed RMSE varying from  $1.5$  to  $1.74 \text{ m s}^{-1}$  for (t+1) to (t+3) time steps. At CB02, the RMSE was found to vary from  $1.20$  to  $1.37 \text{ m s}^{-1}$  for (t+1) to (t+3) time steps.
3. On applying the WT+ANFIS method, it was found that the MAPE for testing dataset at AD07 was 24.73 to 30% for (t+1) to (t+3) time steps. In case of CB02 the MAPE was found to be 30.91 to 36.84% for (t+1) to (t+3) time

steps. Thus, the WT+ANFIS model performance was found to be better than the ANFIS alone, considering results at both the buoys.

4. The division of winds in to subclasses pointed towards the mix of winds in the testing dataset and the probable cause of low performance of the models. In the case of AD07, there was relatively even mix of high and medium winds and both the performance of the models was observed to be similar. Whereas in CB02, it was observed that there was an unequal mix of high and medium winds, with repeated spikes and sharp changes in the wind trend. This trend was better captured by WT+ANFIS than the ANFIS alone. Thus from the study for both the scenarios, it was found that the WT+ANFIS method produced forecasts with better accuracy than ANFIS.

#### *Salient Conclusions*

- a) ANFIS and Wavelet+ANFIS model were used for forecasting wind speeds up to three time steps at both the buoys. It was found that Wavelet+ANFIS model's performance was better.
- b) Investigation of wind speed characteristics on the model performance provided the role of wavelet in enhancing forecast accuracy.

#### **4.3. ESTIMATION OF ENW AND PERFORMANCE EVALUATION OF OCEANSAT-2 SCATTEROMETER WINDS**

OSCAT surface winds over the Arabian Sea were analyzed and compared against moored buoys (AD02 and CB02) for the monsoon period (June–September) of 2011. Collocation of OSCAT data with respect to buoy data was conducted, adopting a spatial and temporal window of within  $0.5^\circ$  and  $\pm 60$  min. The monsoon months generally see high winds and hence were selected with the aim of attaining a better comparison between scatterometer and buoy data. The comparison of satellite winds and buoys winds at 10 m required the conversion of in situ buoy measurements from 3 to 10 m above sea level. The present study offers a new approach in identifying and locating offshore areas with potentially high wind speeds.

1. The study compared three different methods for estimation of neutral winds – power law, logarithmic, and LKB. Neutral winds estimated by the LKB method were the closest to OSCAT winds, and thus a suitable method for estimation of ENW was established in the Arabian Sea.
2. The RMSD for wind speed and direction was found to be less than  $2.5 \text{ m s}^{-1}$  and around  $20^\circ$ , values within the OSCAT mission objectives. However, there exists a small bias in the OSCAT data. Consistency of OSCAT winds with in situ wind measurements was observed.
3. Further, wind maps were developed and spatial interpolation by the kriging. The smoothed raster maps demonstrated the distribution of wind speed, and assisted in identifying the zones of consistently high winds. Region around the coasts of Maharashtra, Goa and Karnataka states of India, show promising result.

##### *Salient Conclusions*

- a) LKB extrapolation method was determined to be suitable method to be adopted in the Arabian Sea.
- b) Using buoy data for monsoon month the accuracy of scatterometer winds was established. Wind atlases provided insight to the available offshore wind potential along the west coast of India

#### **4.4. REGIONAL SCALE OFFSHORE WIND POWER RESOURCE ASSESSMENT USING OCEANSAT-2 SCATTEROMETER WINDS**

The present study focuses on assessing and highlighting the offshore wind potential available for Karnataka state, located on west coast of India. The study is unique, as it is perhaps the first attempt to map the offshore wind energy potential, using satellite data and GIS based methodology for the state extended up to EEZ. The study also uses IRAWs data to validate the OSCAT data, which has not been attempted before. The merits of IRAWs data over other sources of in situ observations have been emphasized, which makes it a better validation data set. To assess the accuracy of OSCAT data in the study area, the collocated data between OSCAT and IRAWs data was obtained by adopting spatial resolution of  $0.5^\circ$  and temporal resolution of  $\pm 60$  min.

1. The RMSE for wind speed and wind direction was found to be  $1.9 \text{ m s}^{-1}$  and around  $20^\circ$  respectively. A good correlation of 0.6 for both wind speed and wind direction data was observed between OSCAT and IRAWs. RMSE of OSCAT data was observed to be within the mission limits ( $\pm 2 \text{ m s}^{-1}$  and  $\pm 20^\circ$ ). Thus the OSCAT data was found to be accurate and representative of real wind speeds in the study area.
2. The OSCAT wind data was extrapolated to 90 m height by logarithmic method, wind power density (WPD) was estimated and actual power from turbine that can be generated was carried out. WPD using OSCAT winds at 10 m was classified based on the available foundation technology for the study area. Threshold limit of  $200 \text{ W m}^{-2}$  was set for developing offshore wind that lead to identification of viable potential zone (between 13N and 14N latitudes), which was nearer to coast and in monopile foundation class.
3. The study used REpower 5 MW offshore turbine to estimate the actual power generation capacity. Optimal wind farm layout was considered and the number of turbines in each foundation type was estimated. Further, the foundation class wise generation capacity was estimated and tabulated. The total available area (up to EEZ) that can be considered for offshore wind energy development was estimated to be  $91,974 \text{ km}^2$ . After subtracting the exclusion zones and



conflict areas from the total area, the net area was estimated to be 66,690 km<sup>2</sup>. The average annual output power including and excluding conflict areas were found to be approximately 162,171 MW and 117,589 MW respectively.

4. In the Monopile (0-35 m) foundation type, the area of 5,156 km<sup>2</sup> and potential of 9,091 MW was estimated. Considering the energy deficit faced by the Karnataka state during FY 2011-12 of 777 MW, it is proposed as phase-I development that if, 10% of the estimated offshore wind potential in the Monopile foundation class can be developed then 116% of energy deficit can be met. Further the anticipated energy deficit for the state is 1142 MW for the FY 2014-15, the turbines in Monopile foundation class are capable of meeting the deficit up to 79%.

#### **4.5. LIMITATIONS OF THE STUDY**

- The selection of moored buoys for the analysis presented in the sections was subjected to availability of continuous time series observations.
- Limited IRAWS dataset was available only for duration 2011-2013 and for limited number of vessels, which restricted validation accuracy of the OSCAT wind data.
- Accuracy of wind power potential assessment is limited by the assumptions of exclusion zone and lack of in situ data at hub heights.

#### **4.6. SCOPE FOR FUTURE WORK**

- The hybrid model's performance at different buoy locations and larger dataset may be explored. Further, investigations on the influence of atmospheric parameters, for short-term forecast needs to be carried out.
- Retrieval of met-ocean parameters like- Air Temperature, Sea Surface Temperature, Relative Humidity and Wind Speed from space borne data and their interaction over the study area needs to be investigated.
- Extrapolation of offshore winds using LKB method to higher heights (hub height) and validation against in situ measurements may be carried out, which will help to establish the method as standard approach for extrapolation in the Arabian Sea.
- For higher accuracy in WRA studies it can be suggested that integration of multi-platform observations (like- buoys, masts, various satellite data products) would provide high quality dataset.



## REFERENCES

---

- Ali, M. M., Bhat, G. S., Long, D. G., Bharadwaj, S., and Bourassa, M. A. 2013. "Estimating wind stress at the Ocean surface from scatterometer observations." *Geoscience and Remote Sensing Letters, IEEE*, 10(5), 1129-1132.
- Allen, R. G., Pereira, L. S., Raes, D., and Smith, M. (1998). Chapter 3. Meteorological Data. Crop evapotranspiration-Guidelines for computing crop water requirements-FAO Irrigation and drainage paper 56. FAO, Rome, 300(9), D05109.
- Bagiorgas, H. S., Mihalakakou, G., Rehman, S., and Al-Hadhrami, L. M. (2012). "Offshore wind speed and wind power characteristics for ten locations in Aegean and Ionian Seas." *Journal of Earth System Science*, 121(4), 975-987.
- Bailey, B. H., McDonald, S. L., Bernadett, D. W., Markus, M. J., and Elsholz, K. V. (1997). "Wind resource assessment handbook." Albany-New York: AWS Scientific Inc.
- Barthelmie, R. J., and Pryor, S. C. (2003). "Can satellite sampling of offshore wind speeds realistically represent wind speed distributions?." *Journal of Applied Meteorology*, 42(1), 83-94.
- Barthelmie, R. J., Sempreviva, A. M., and Pryor, S. (2010). "The influence of humidity fluxes on offshore wind speed profiles." In *Annales Geophysicae*, 28(5), 1043-1052.
- Bentamy, A., Queffeuilou, P., Quilfen, Y., & Katsaros, K. (1994). "Intercomparisons of wind speed measurements derived from ERS-1 scatterometer and altimeter and SSM/I over the tropical Atlantic Ocean." In *OCEANS'94, September. 'Oceans Engineering for Today's Technology and Tomorrow's Preservation Proceedings 1*, 1-81. IEEE Brest. IEEE.
- Brower, M., and Bernadett, D. W. (2012). "Wind resource assessment: a practical guide to developing a wind project." John Wiley & Sons.
- Cadenas, E., Jaramillo, O. A., & Rivera, W. (2010). "Analysis and forecasting of wind velocity in chetumal, quintana roo, using the single exponential smoothing method." *Renewable Energy*, 35(5), 925-930.

- Cao, Q., Ewing, B. T., and Thompson, M. A. (2012). "Forecasting wind speed with recurrent neural networks." *European Journal of Operational Research*, 221(1), 148-154.
- Carvalho, D., Rocha, A., Gómez-Gesteira, M., & Santos, C. S. (2014). "Offshore wind energy resource simulation forced by different reanalyses: comparison with observed data in the Iberian Peninsula." *Applied Energy*, 134, 57-64.
- Carvalho, D., Rocha, A., Gómez-Gesteira, M., & Santos, C. S. (2014a). "WRF wind simulation and wind energy production estimates forced by different reanalyses: Comparison with observed data for Portugal." *Applied Energy*, 117, 116-126.
- Castellanos, F., and James, N. (2009). "Average hourly wind speed forecasting with ANFIS." In *11th Americas conference on Wind Engineering, June-2009*, 26-29.
- Census. 2011. ([http://www.censusindia.gov.in/2011census/PCA/PCA\\_Highlights/pca\\_highlights\\_file/India/Chapter-1.pdf](http://www.censusindia.gov.in/2011census/PCA/PCA_Highlights/pca_highlights_file/India/Chapter-1.pdf))
- CGMS. 2014. "Status of the wind scatterometer constellation." Presented to CGMS-42 Working Group III session, agenda item 2.2, URL: [http://www.eumetsat.int/website/wcm/idc/idcplg?IdcService=GET\\_FILE&RevisionSelectionMethod=LatestReleased&Rendition=Primary&dDocName=CWPT\\_1152](http://www.eumetsat.int/website/wcm/idc/idcplg?IdcService=GET_FILE&RevisionSelectionMethod=LatestReleased&Rendition=Primary&dDocName=CWPT_1152))
- Chang, R., Zhu, R., Badger, M., Hasager, C. B., Xing, X., & Jiang, Y. (2015). "Offshore wind resources assessment from multiple satellite data and WRF modeling over South China Sea." *Remote Sensing*, 7(1), 467-487.
- Chang, R., Zhu, R., Badger, M., Hasager, C. B., Zhou, R., Ye, D., & Zhang, X. (2014). "Applicability of Synthetic Aperture Radar wind retrievals on offshore wind resources assessment in Hangzhou Bay, China." *Energies*, 7(5), 3339-3354.
- Charhate, S. B., Deo, M. C., and Londhe, S. N. (2009). "Genetic programming for real-time prediction of offshore wind." *Ships and Offshore Structures*, 4(1), 77-88.
- Chelton, D. B., and Freilich, M. H. (2005). "Scatterometer-based assessment of 10-m wind analyses from the operational ECMWF and NCEP numerical weather prediction models." *Monthly Weather Review*, 133(2), 409-429.

- Childs, C. 2004. “Interpolating Surfaces in ArcGis Spatial Analyst.” *ArcUser* July–September: 32–35.
- CII Karnataka Conference on Power. (2012). “Sustainable power through Renewable sources.” ([https://www.pwc.in/assets/pdfs/grid/renewable-energy/cii-report\\_-240812-sustainable-power-through-renewable-energy-updated.pdf](https://www.pwc.in/assets/pdfs/grid/renewable-energy/cii-report_-240812-sustainable-power-through-renewable-energy-updated.pdf))
- CII Karnataka. (2012). “Conference on Power 2012, Sustainable power through Renewable sources” ([https://www.pwc.in/assets/pdfs/grid/renewable-energy/cii-report\\_-240812-sustainable-power-through-renewable-energy-updated.pdf](https://www.pwc.in/assets/pdfs/grid/renewable-energy/cii-report_-240812-sustainable-power-through-renewable-energy-updated.pdf))
- CSTEP & Govt. of Karnataka. (2013). “Karnataka's Power Sector Roadmap for 2021-22” (<http://indiaenvironmentportal.org.in/files/file/KarnatakaPowerSectorRoadmapFINAL20report.pdf>)
- Damousis, I. G., Alexiadis, M. C., Theocharis, J. B., and Dokopoulos, P. S. (2004). “A fuzzy model for wind speed prediction and power generation in wind parks using spatial correlation.” *Energy Conversion, IEEE Transactions on*, 19(2), 352-361.
- Desai, P. S., Gowda, H. H., and Kasturirangan, K. (2000). “Ocean research in India: Perspective from Space.” *Current Science*, 78(3), 268-278.
- Dhanju, A., Whitaker, P., and Kempton, W. (2008). “Assessing offshore wind resources: An accessible methodology.” *Renewable Energy*, 33(1), 55-64.
- Doubrawa, P., Barthelmie, R. J., Pryor, S. C., Hasager, C. B., Badger, M., and Karagali, I. (2015). “Satellite winds as a tool for offshore wind resource assessment: The Great Lakes Wind Atlas.” *Remote Sensing of Environment*, 168, 349-359.
- Draxl, C., Clifton, A., Hodge, B. M., and McCaa, J. (2015). “The Wind Integration National Dataset (WIND) Toolkit.” *Applied Energy*, 151, 355-366.
- Dvorak, M. J., Archer, C. L., and Jacobson, M. Z. (2010). “California offshore wind energy potential.” *Renewable Energy*, 35(6), 1244-1254.
- Ebuchi, N. (2012). “Evaluation of wind vectors observed by Oceansat-2 scatterometer using statistical distributions.” *In Geoscience and Remote Sensing Symposium (IGARSS), July-2012, IEEE International*. IEEE, 2043-2046.

- Ebuchi, N. (2013). “Intercomparison of four ocean vector wind products from OceanSat-2 scatterometer.” In *Geoscience and Remote Sensing Symposium (IGARSS), July- 2013 IEEE International*, IEEE, 1254-1257.
- Ebuchi, N., Graber, H. C., & Caruso, M. J. (2002). “Evaluation of wind vectors observed by QuikSCAT/SeaWinds using ocean buoy data.” *Journal of Atmospheric and Oceanic Technology*, 19(12), 2049-2062.
- Eoport. 2015. Eoport Directory, SeaSat (Seafaring Satellite) Mission. (<https://directory.eoport.org/web/eoport/satellite-missions/s/seasat>)
- Esteban, M., and Leary, D. (2012). “Current developments and future prospects of offshore wind and ocean energy.” *Applied Energy*, 90(1), 128-136.
- Foley, A. M., Leahy, P. G., Marvuglia, A., and McKeogh, E. J. (2012). “Current methods and advances in forecasting of wind power generation.” *Renewable Energy*, 37(1), 1-8.
- Furevik, B. R., Espedal, H. A., Hamre, T., Hasager, C. B., Johannessen, O. M., Jørgensen, B. H., and Rathmann, O. (2003). “Satellite-based wind maps as guidance for siting offshore wind farms.” *Wind Engineering*, 27(5), 327-338.
- Furevik, B. R., Sempreviva, A. M., Cavaleri, L., Lefèvre, J. M., and Transerici, C. (2011). “Eight years of wind measurements from scatterometer for wind resource mapping in the Mediterranean Sea.” *Wind Energy*, 14(3), 355-372.
- Gadad, S., and Deka, P. C. (2015). “Comparison of Oceansat-2 scatterometer-to buoy- recorded winds and spatial distribution over the Arabian Sea during the monsoon period.” *International Journal of Remote Sensing*, 36(18), 4632-4651.
- Goswami, B. N., and Rajagopal, E. N. (2003). “Indian Ocean surface winds from NCMRWF analysis as compared to QuikSCAT and moored buoy winds.” *Journal of Earth System Science*, 112(1), 61-77.
- Govt. of India, Ministry of New and Renewable Energy. (2013). “National Offshore Wind Energy Policy” (<http://www.indiaenvironmentportal.org.in/files/file/draft-national-policy-for-offshore-wind.pdf>).
- Haque, A. U., Mandal, P., Kaye, M. E., Meng, J., Chang, L., and Senjyu, T. (2012). “A new strategy for predicting short-term wind speed using soft computing models.” *Renewable and sustainable energy reviews*, 16(7), 4563-4573.

- Harikumar, R., Balakrishnan Nair, T. M., Bhat, G. S., Nayak, S., Reddem, V. S., and Sheno, S. S. C. (2013). "Ship-Mounted Real-Time Surface Observational System on board Indian Vessels for Validation and Refinement of Model Forcing Fields\*." *Journal of Atmospheric and Oceanic Technology*, 30(3), 626-637.
- Hasager, C. B., Barthelmie, R. J., Christiansen, M. B., Nielsen, M., and Pryor, S. C. (2006). "Quantifying offshore wind resources from satellite wind maps: study area the North Sea." *Wind Energy*, 9(1-2), 63-74.
- Hayashi, T., Kato, M., Tagawa, K., and Hara, Y. (2006). "Study on the New Method for Investigating Offshore Wind Characteristics by Ship's Cruise." *Young*, 81000(10).
- Hsu, S. A., Meindl, E. A., and Gilhousen, D. B. (1994). "Determining the power-law wind-profile exponent under near-neutral stability conditions at sea." *Journal of Applied Meteorology*, 33(6), 757-765.
- Hunt, K., and Nason, G. (2001). "Wind speed modelling and short-term prediction using wavelets." *Wind Engineering*, 25(1), 55-61.
- Jayaram, C., Udaya Bhaskar, T. V., Swain, D., Rama Rao, E. P., Bansal, S., Dutta, D., and Rao, K. H. (2014). "Daily composite wind fields from Oceansat-2 scatterometer." *Remote Sensing Letters*, 5(3), 258-267.
- Jiang, D., Zhuang, D., Huang, Y., Wang, J., and Fu, J. (2013). Evaluating the spatio-temporal variation of China's offshore wind resources based on remotely sensed wind field data. *Renewable and Sustainable Energy Reviews*, 24, 142-148.
- Johnston, K., J. M. Ver Hoef, K. Krivoruchko, and N. Lucas. (2001). "Using Arcgis Geostatistical Analyst." Vol. 300. Redlands: Esri.
- Jung, J., and Broadwater, R. P. (2014). "Current status and future advances for wind speed and power forecasting." *Renewable and Sustainable Energy Reviews*, 31, 762-777.
- Kara, A. B., Wallcraft, A. J., and Bourassa, M. A. (2008). "Air-sea stability effects on the 10 m winds over the global ocean: Evaluations of air-sea flux algorithms." *Journal of Geophysical Research: Oceans*, 113(C4).
- Kent, E. C., (1998). "A Comparison of Ship- and Scatterometer Derived Wind Speed Data in Open Ocean and Coastal Areas." *International Journal of Remote Sensing*, 19 (17), 3361–3381. DOI: 10.1080/014311698214046.



- Kent, E. C., Berry, D. I., Prytherch, J., and Roberts, J. B. (2014). “A comparison of global marine surface-specific humidity datasets from in situ observations and atmospheric reanalysis.” *International Journal of Climatology*, 34(2), 355-376.
- Kempton, W., Archer, C. L., Dhanju, A., Garvine, R. W., and Jacobson, M. Z. (2007). “Large CO<sub>2</sub> reductions via offshore wind power matched to inherent storage in energy end-uses.” *Geophysical Research Letters*, 34(2).
- Korsbakken, E., and Furevik, B. (1998). “Wind field retrieval from SAR compared with scatterometer wind field during ERS Tandem phase.” *Earth Observation Quarterly*, (59), 23-26.
- Kota, S., Bayne, S. B., and Nimmagadda, S. (2015). “Offshore wind energy: A comparative analysis of UK, USA and India.” *Renewable and Sustainable Energy Reviews*, 41, 685-694.
- Kozai, K., Ohsawa, T., Takeyama, Y., Shimada, S., Niwa, R., Hasager, C. B., & Badger, M. (2010). “Comparison of sar wind speed retrieval algorithms for evaluating offshore wind energy resources.” *Techno-Ocean 2010: A new Era of the ocean*.
- Krohn, S., Poul-Erik Morthorst, P. K., Awerbuch, S. (2009). “The Economics of Wind Energy: A report by the European Wind Energy Association (EWEA).” ([http://www.ewea.org/fileadmin/files/library/publications/reports/Economics\\_of\\_Wind\\_Energy.pdf](http://www.ewea.org/fileadmin/files/library/publications/reports/Economics_of_Wind_Energy.pdf))
- Kumar, R. R., Kumar, B. P., Satyanarayana, A. N. V., Subrahmanyam, D. B., Rao, A. D., and Dube, S. K. (2009). “Parameterization of sea surface drag under varying sea state and its dependence on wave age.” *Natural Hazards*, 49(2), 187-197.
- Kumar, R., Chakraborty, A., Parekh, A., Sikhakolli, R., Gohil, B. S., and Kiran Kumar, A. S. (2013). “Evaluation of Oceansat-2-derived ocean surface winds using observations from global buoys and other scatterometers.” *Geoscience and Remote Sensing, IEEE Transactions on*, 51(5), 2571-2576.
- Lange, B., Højstrup, J., Larsen, S. E., and Barthelmie, R. J. (2001). “A fetch dependent model of sea surface roughness for offshore wind power utilisation.” In *Wind Energy for the new millennium. Proceedings of the European Wind Energy Conference Copenhagen 2001*. 830-833.

- Lange, B., Larsen, S., Højstrup, J., and Barthelmie, R. (2004). “Importance of thermal effects and sea surface roughness for offshore wind resource assessment.” *Journal of wind engineering and industrial aerodynamics*, 92(11), 959-988.
- Lei, M., Shiyun, L., Chuanwen, J., Hongling, L., and Yan, Z. (2009). “A review on the forecasting of wind speed and generated power.” *Renewable and Sustainable Energy Reviews*, 13(4), 915-920.
- Liu, H., Tian, H. Q., Chen, C., and Li, Y. F. (2010). “A hybrid statistical method to predict wind speed and wind power.” *Renewable Energy*, 35(8), 1857-1861.
- Luo, W., M. C. Taylor, and S. R. Parker. 2008. “A Comparison of Spatial Interpolation Methods to Estimate Continuous Wind Speed Surfaces Using Irregularly Distributed Data from England and Wales.” *International Journal of Climatology*, 28, 947–959.
- Manual, W. P. U. (2013). “Oceansat-2 Wind Product User Manual.” *Report No: SAF/OSI/CDOP2/KNMI/TEC/MA/140, Ocean and Sea Ice SAF, version 1.3*, KNMI, De Bilt, the Netherlands. ([http://projects.knmi.nl/scatterometer/publications/pdf/Oceansat2\\_Product\\_Manual.pdf](http://projects.knmi.nl/scatterometer/publications/pdf/Oceansat2_Product_Manual.pdf))
- Mathew, T., A. Chakraborty, A. Sarkar, and R. Kumar. 2012. “Comparison of Oceanic Winds Measured by Space-Borne Scatterometers and Altimeters.” *Remote Sensing Letters*, 3 (8): 715– 720. DOI: 10.1080/2150704X.2012.674226.
- MNRE. 2015. “Physical Achievements- Tentative State-wise break-up of Renewable Power target to be achieved by the year 2022.” (<http://www.mnre.gov.in/mission-and-vision-2/achievements/>)
- Mohandes, M., Rehman, S., and Rahman, S. M. (2011). “Estimation of wind speed profile using adaptive neuro-fuzzy inference system (ANFIS).” *Applied Energy*, 88(11), 4024-4032.
- Monaldo, F. M., Thompson, D. R., Pichel, W. G., and Clemente-Colón, P. (2004). “A systematic comparison of QuikSCAT and SAR ocean surface wind speeds.” *Geoscience and Remote Sensing, IEEE Transactions on*, 42(2), 283-291.
- More, A., and Deo, M. C. (2003). “Forecasting wind with neural networks.” *Marine Structures*, 16(1), 35-49.

- NCEP. 2002. “The use of QuikSCAT winds in the Ocean Prediction Center Forecast Process.” (<http://www.opc.ncep.noaa.gov/quikscat/quikscatusage.pdf>)
- Negnevitsky, M., and Potter, C. W. (2006). “Innovative short-term wind generation prediction techniques.” *In Power Systems Conference and Exposition (PSCE'06)*, October 2006, *IEEE PES*. IEEE, 60-65.
- Newman, E. L., (2007). “Pressure and Winds, GPH 111 - Introduction to Physical Geography”, Supplementary lecture materials, ([http://web.gccaz.edu/~lnewman/gph111/topic\\_units/Pressure\\_winds/pressure/pressure2.html](http://web.gccaz.edu/~lnewman/gph111/topic_units/Pressure_winds/pressure/pressure2.html))
- Oh, K. Y., Kim, J. Y., Lee, J. S., and Ryu, K. W. (2012). “Wind resource assessment around Korean Peninsula for feasibility study on 100 MW class offshore wind farm.” *Renewable Energy*, 42, 217-226.
- Pai, D. S., and Bhan, S. C. (2013). “Monsoon 2012- A Report.” Report No: Synoptic Meteorology No. 13/2013, National Climate Center, India Meteorological Department, Pune, India. ([http://www.imd.gov.in/section/nhac/dynamic/monsoon\\_report\\_2012.pdf](http://www.imd.gov.in/section/nhac/dynamic/monsoon_report_2012.pdf))
- Peng, G., Zhang, H. M., Frank, H. P., Bidlot, J. R., Higaki, M., Stevens, S., and Hankins, W. R. (2013). “Evaluation of various surface wind products with OceanSITES buoy measurements.” *Weather and Forecasting*, 28(6), 1281-1303.
- Pimenta, F., Kempton, W., and Garvine, R. (2008). “Combining meteorological stations and satellite data to evaluate the offshore wind power resource of Southeastern Brazil.” *Renewable Energy*, 33(11), 2375-2387.
- Podaac. 2014. “Discontinuation of OSCAT Data Retrieval.” ([http://podaac-www.jpl.nasa.gov/announcements/2014-04-10\\_Discontinuation\\_of\\_OSCAT\\_Data\\_Retrieval](http://podaac-www.jpl.nasa.gov/announcements/2014-04-10_Discontinuation_of_OSCAT_Data_Retrieval)).
- Potter, C., Ringrose, M., and Negnevitsky, M. (2004). “Short-term wind forecasting techniques for power generation.” *In Australasian Universities Power Engineering Conference (AUPEC, September 2004)*, 26-29.
- Ramasesha, S. K., and Chakraborty, A. (2013). Power generation using wind energy in northwest Karnataka, India. *Current Science*, 104(6), 757-761.
- Ramis, C., Romero, R., and Alonso, S. (2005). Relative humidity. *Water Encyclopedia*. ([http://www.uib.cat/depart/dfs/meteorologia/ROMU/formal/relative\\_humidity/relative\\_humidity.pdf](http://www.uib.cat/depart/dfs/meteorologia/ROMU/formal/relative_humidity/relative_humidity.pdf))

- Rani, S. I., and Gupta, M. D. (2013). “Oceansat-2 and RAMA buoy winds: A comparison.” *Journal of Earth System Science*, 122(6), 1571-1582.
- Satheesan, K., Sarkar, A., Parekh, A., Kumar, M. R., and Kuroda, Y. (2007). “Comparison of wind data from QuikSCAT and buoys in the Indian Ocean.” *International Journal of Remote Sensing*, 28(10), 2375-2382.
- Seidel, M. (2007). “Jacket substructures for the REpower 5M wind turbine.” *In European Offshore Wind Conference*, December-2007, 4-6.
- Sfetsos, A. (2002). “A novel approach for the forecasting of mean hourly wind speed time series.” *Renewable Energy*, 27(2), 163-174.
- Sheridan, B., Baker, S. D., Pearre, N. S., Firestone, J., and Kempton, W. (2012). “Calculating the offshore wind power resource: Robust assessment methods applied to the US Atlantic Coast.” *Renewable Energy*, 43, 224-233.
- Siddiqi, A. H., Khan, S., and Rehman, S. (2005). “Wind speed simulation using wavelets.” *American Journal of Applied Science*, 2(2), 557-564.
- Sideratos, G., and Hatzigryriou, N. D. (2007). “An advanced statistical method for wind power forecasting.” *Power Systems, IEEE Transactions on*, 22(1), 258-265.
- Singh, P., Parekh, A., and Attada, R. (2013). “Comparison of a simple logarithmic and equivalent neutral wind approaches for converting buoy-measured wind speed to the standard height: special emphasis to North Indian Ocean.” *Theoretical and Applied Climatology*, 111(3-4), 455-463.
- Singh, R., Kishtawal, C. M., Pal, P. K., and Joshi, P. C. (2011). “Assimilation of the multisatellite data into the WRF model for track and intensity simulation of the Indian Ocean tropical cyclones.” *Meteorology and atmospheric physics*, 111(3-4), 103-119.
- Singh, R., Kumar, P., and Pal, P. K. (2012). “Assimilation of Oceansat-2-scatterometer-derived surface winds in the weather research and forecasting model.” *Geoscience and Remote Sensing, IEEE Transactions on*, 50(4), 1015-1021.
- Sliz-Szkliniarz, B., and J. Vogt. 2011. “GIS-Based Approach for the Evaluation of Wind Energy Potential: A Case Study for the Kujawsko–Pomorskie

Voivodeship.” *Renewable and Sustainable Energy Reviews*, 15(3), 1696–1707. DOI:10.1016/j.rser.2010.11.045.

- Soman, S. S., Zareipour, H., Malik, O., & Mandal, P. (2010). “A review of wind power and wind speed forecasting methods with different time horizons.” *In North American Power Symposium (NAPS)*, IEEE, September-2010, 1-8.
- Staffell, I. (2012). “Wind turbine power curves.” Imperial College London, 2.
- Stecki, J and Altmann, J. 2000. “Surfing the wavelets.” Tutorial on wavelets, (<http://www.wavelet.org/tutorial/index.html>)
- Stephanie Bell. (2012). “Good Practice Guide No. 124- The Beginner’s Guide to Humidity Measurement.” National Physical Laboratory. ISSN 1368-6550. ([www.npl.co.uk/content/ConMediaFile/5883](http://www.npl.co.uk/content/ConMediaFile/5883)).
- Stiles, B. W., and Yueh, S. H. (2002). “Impact of rain on spaceborne Ku-band wind scatterometer data.” *Geoscience and Remote Sensing, IEEE Transactions on*, 40(9), 1973-1983.
- Stoffelen, A., and Verhoef, A. (2011). “Validation of Oceansat-2 scatterometer data.” *In the P. 59–EUMETSAT Meteorological Satellite Conference, September-2011*, 5-9.
- Subrahmanyam, D. B., & Ramachandran, R. (2003). “Wind speed dependence of air-sea exchange parameters over the Indian Ocean during INDOEX, IFP-99.” *In Annales Geophysicae*, 21(7), 1667-1679.
- Tyagi, A., and Pai, D. S. (2012). “Monsoon 2011- A Report.” Report No: Synoptic Meteorology No. 01/2012, National Climate Center, India Meteorological Department, Pune, India. ([http://www.imd.gov.in/section/nhac/dynamic/monsoon\\_report\\_2011.pdf](http://www.imd.gov.in/section/nhac/dynamic/monsoon_report_2011.pdf))
- Valsson, S., and Bharat, A. (2011). “Impact of air temperature on relative humidity-a study.” *Journal of Architecture-Time Space & People*, 38-41.
- Venkatesan, R., Shamji, V. R., Latha, G., Mathew, S., Rao, R. R., Muthiah, A., and Atmanand, M. A. (2013). “In situ ocean subsurface time-series measurements from OMNI buoy network in the Bay of Bengal.” *Current Science (Bangalore)*, 104(9), 1166-1177.

- Verburg, P., and Antenucci, J. P. (2010). "Persistent unstable atmospheric boundary layer enhances sensible and latent heat loss in a tropical great lake: Lake Tanganyika." *Journal of Geophysical Research: Atmospheres*, 115(D11).
- Yan, D., Kozai, K., Ohsawa, T., and Tsubouchi, N. (2012). "Evaluation of Offshore Wind Energy Resource in Chinese Coastal Sea Using QuikSCAT Data." *Journal of Maritime Researches*, 2(1), 69-77.
- Yao, C., Gao, X., and Yu, Y. (2013). "Wind speed forecasting by wavelet neural networks: a comparative study." *Mathematical Problems in Engineering*, 2013.
- Yun, R., Stoffelen, A., Verspeek, J., and Verhoef, A. (2012). "NWP ocean calibration of Ku-band scatterometers." In *Geoscience and Remote Sensing Symposium (IGARSS), 2012 IEEE International*, IEEE, 2055-2058.
- Zeng, J., & Qiao, W. (2012). "Short-term wind power prediction using a wavelet support vector machine." *Sustainable Energy, IEEE Transactions on*, 3(2), 255-264.
- Zheng, C. W., Li, C. Y., Pan, J., Liu, M. Y., and Xia, L. L. (2016). "An overview of global ocean wind energy resource evaluations." *Renewable and Sustainable Energy Reviews*, 53, 1240-1251.

## PUBLICATIONS

---

### INTERNATIONAL JOURNAL

**Sanjeev Gadad** and Paresh Chandra Deka. (2016). “Offshore wind power resource assessment using oceansat-2 scatterometer data at a regional scale”, *Applied Energy*, 176, 157-170. Elsevier Publications

**Sanjeev Gadad** and Paresh Chandra Deka. (2015). “Comparison of oceansat-2 scatterometer winds with buoys and spatial distribution over the Arabian Sea during the monsoon season”, *International Journal of Remote Sensing*, 36(18), 4632-4651. Taylor & Francis Publication.

**Sanjeev Gadad** and Paresh Chandra Deka. “Performance evaluation of ANFIS and Wavelet-ANFIS hybrid techniques for short-term offshore wind speed forecasting”, *Renewable Energy*, Elsevier Publication. **(Under Review)**

**Sanjeev Gadad** and Paresh Chandra Deka. “Investigation of Relative Humidity influence on ANFIS for short-term offshore wind speed forecasting in the Arabian Sea”, *IEEE Journal of Selected Topics in Applied Earth Observations and Remote Sensing (JSTARS)*, IEEE. **(Under Review)**

### INTERNATIONAL CONFERENCES

**Sanjeev Gadad** and Paresh Chandra Deka. (2014). “Performance evaluation of hybrid structured techniques for short term wind speed forecasting in Arabian sea” in Proceedings of International conference on Emerging trends in Engineering (ICETE-2014), 1, 73-78.

## RESUME

---

Name Sanjeev Gadad  
Date of Birth 06-12-1988  
Address (s/o) S. C. Gadad,  
Plot No. 27, Sector 08,  
Anjaneya Nagar, MM  
EXTN,  
Belgaum – 590016



Tel: +91-948-166-0408  
+91-973-986-7645

Email gssanjeev126@gmail.com

Qualification B.E (CIVIL)  
M.Tech (RS & GIS)

Publications International Journals: 2      Under review: 2  
International Conference: 1